

ADAPTATION OF THE ELECTROSLAG WELDING
PROCESS TO JOINING OF RAILROAD RAIL

Robert B. Turpin
A.A.S., Oregon Technical Institute, 1969
B.S. Ed., Northern Arizona University, 1975

A thesis submitted to the faculty
of the Oregon Graduate Center
in partial fulfillment of the
requirements for the degree
Master of Science
in
Materials Science and Engineering

June, 1983

The thesis "Adaptation of the Electroslag Welding Process to Joining of Railroad Rail" by Robert B. Turpin has been examined and approved by the following Examination Committee:

William E. Wood, Thesis Advisor
Professor

✓ Jack H. Devletian
Associate Professor

Nicholas G. Eror
Associate Professor

Lynwood W. Swanson
Professor

ACKNOWLEDGEMENT

I express my sincere thanks and appreciation to Dr. W. E. Wood and Dr. J. H. Devletian, who have served as my advisors during this work and whose support and encouragement have been exceptional. I also thank Drs. L. Murr, N. G. Eror, R. Rasmussen, P. Clayton, and L. Swanson for their work in planning my M.S. program and examining my thesis.

I express my thanks to S. Venkataraman and M. Scholl for their generous and valued help during this project. My sincere thanks to Ms. N. A. Fick for her assistance in preparation of this thesis.

I greatly acknowledge the sponsorship of the Southern Pacific Transportation Company and the encouragement of W. E. Thomford.

I especially express my appreciation to my wife and children for their support and understanding during this work.

TABLE OF CONTENTS

	<u>Page</u>
APPROVAL PAGE	i
ACKNOWLEDGMENT	ii
TABLE OF CONTENTS	iii
LIST OF FIGURES	v
ABSTRACT	viii
DEFINITION OF THE PROBLEM	x
1. INTRODUCTION	1
1.1. In-Plant Rail Welding	2
1.1.1. Flash-Butt Welding	2
1.1.2. Gas Pressure Welding	3
1.1.3. Friction and Inertia Welding	3
1.1.4. Summary of In-Plant Welding Processes	4
1.2. Field Rail Welding Requirements and Processes	5
1.2.1. Thermit Welding	5
1.2.2. Shielded Metal Arc Welding	6
1.2.3. Submerged-Slag Welding	7
1.2.4. Electroslag Welding	9
1.3. Electroslag Welding	11
1.3.1. Weld Initiation	12
1.3.2. Welding Power Parameters	14
1.3.3. Welding Current	17
1.3.4. Flux and Slag	17
1.3.5. Joint Spacing, Guide Tube Position and Grounding	20
1.3.6. Guide Tube Effects	22
1.3.7. Electrode Variations	23
1.3.8. Weld Position	25
2. EXPERIMENTAL PROCEDURE	26
2.1. Material	26
2.2. Equipment	27
2.3. Weld Set-up	28

	<u>Page</u>
2.4. Guide Tube Evaluation	29
2.5. Mold Evaluation	29
2.6. Weld Inspection	30
3. RESULTS	32
3.1. Equipment	32
3.2. Electroslog Rail Welding Procedure	34
3.3. Repair Procedure	37
3.4. Weld Description	37
4. DISCUSSION	38
4.1. Approach	38
4.2. Starting Block	39
4.3. Arc Starting	40
4.4. Guide Tube Design	42
4.5. Electrode Selection	44
4.6. Flux Addition	45
4.7. Mold Development	46
4.8. Weld Characterization	48
4.8.1. Fusion and HAZ Patterns	49
4.8.2. Form-factor	49
4.8.3. Hardness Data	50
4.8.4. Weld Quality	50
4.9. Repair Conditions	52
5. CONCLUSIONS AND RECOMMENDATIONS	53
5.1. Conclusions	53
5.2. Recommendations	54
REFERENCES	56
FIGURES	59
APPENDICES	114
I. Glossary of Rail Steel Terminology	114
II. Chemical Analysis of Rail Steels	116
III. Sulfur Printing Procedure	117
IV. Dye-Penetrant Inspection Procedure	119
V. Conversion Table	121
BIOGRAPHICAL NOTE	122

LIST OF FIGURES

	<u>Page</u>
1. American Railway Engineering Association recommended rail section dimensions for 136 pound per yard rail (1971)	60
2. Sulfur Print of Transverse and Longitudinal Sections of a Thermit Rail Weld	61
3. Enclosed arc welding enclosure block assembly	62
4. Submerged-slag rail welding sequence	63
5. Schematic representation of consumable guide electrosag welding	64
6. Schematic representation of conventional electrosag welding	65
7. Consumable guide plate electrode used by V. I. Svetlopolyan-skii for welding type R43 tram rail	66
8. Electrode movement pattern used by Kopetman and Mukanaev in conventional electrosag welding of crane rail	67
9. Schematic representation of the consumable guide electrosag welding process equipment	68
10. Slag bath current path variations	69
11. Voltage and base metal dilution relationship	70
12. High voltage penetration pattern that results in slag entrapment as voltage fluctuates, proposed by Solari, et al. . . .	71
13. Experimentally determined parabolic relationship between welding current and electrode velocity	72
14. Effect of current on the weld pool geometry	73
15. Effect of voltage on the weld pool geometry	74
16. Effect of the slag bath electrical conductivity on the weld pool	75
17. Effect of ground location and electrode position on electro-slag weld penetration	76
18. Calculated and actual penetration shapes with variations in guide tube arrangement by L. P. Eregin	77

	<u>Page</u>
19. Extreme conditions resulting from electrode wire spacing variations in a two electrode system	78
20. Effect of non-vertical electrosag welding on weld pool shape by Jones, et al.	79
21. Schematic illustration of the consumable guide electrosag welding system used in this investigation	80
22. Schematic illustration of the electrode feeder and rail positioning	81
23. Macrosectioning diagram for rail welds	82
24. Sulfur print of transverse and longitudinal ESRW sections . .	83
25. X-Y electrode positioners with the electrode feeder, conduit, and electrode spools	84
26. Schematic of mold components	85
27. Schematic sectional view of the weld starting block	86
28. Final guide tube design	87
29. Guide tube position relative to the rail and mold cavity profile	88
30. Cross sectional area relationship of the weld metal, weld joint, and guide tube	89
31. Completed electrosag rail weld ready for service	90
32. Initial copper side shoe design	91
33. Fusion pattern at the rail base from electrosag weld #3 . .	92
34. Starting block design with preliminary insert and insulation patterns	93
35. Ceramic starting block insulation before (a) and after (b) welding	94
36. Improper penetration and weld shape (cavity) in the weld beneath the rail base as a result of gas entrapment	95
37. Initial guide tube design	96

	<u>Page</u>
38. Guide tube influence on slag bath formation	97
39. Initial guide tube specifically designed to improve slag bath formation	98
40. Mold and weld set-up for evaluation of the guide tube influence upon weld starting	99
41. Uniform 1/2 inch thick guide tube design	100
42. Welding power control comparison by strip chart recordings for solid (E70-S-3) vs. tubular electrode wire (E70T-G)	101
43. Weld reinforcement notching due to over cooling of the slag bath	102
44. Typical ESRW fusion and heat affected zone patterns through the longitudinal rail and weld center section	103
45. Typical thermit weld fusion and heat affected zone patterns through the longitudinal rail and weld center section (38) .	104
46. Hardness traverse locations through the longitudinal center section of ESRW	105
47. Hardness traverse plot of the weld metal ("A" Figure 46) from an ESRW	106
48. Variation of carbon content in an ESRW using E70S-3 electrode wire (as in Figure 46)	107
49. Hardness traverse plots from Band c of Figure 46	108
50. Hardness traverse of a typical thermit weld	109
51. Transverse and longitudinal sections of an ESRW made with ER90S-B3 electrode wire	110
52. Macrosection of a typical thermit weld	111
53. HAZ cracks in ESRW resulting from excessive weld speeds . . .	112
54. ESRW Rail base undercut repair used in this investigation . .	113

ABSTRACT

Adaptation of the Electroslog Welding Process
to Joining of Railroad RailRobert Byron Turpin, M.S.
Oregon Graduate Center, 1983Supervising Professors:
William E. Wood and Jack H. Devletian

For more than fifty years, the use of continuous welded rail has been increasing in American rail track systems. Field welding for repair and maintenance purposes has largely been limited to use of the thermit process. During this same time period, the train car tonnage and speeds have come to exceed the mechanical property limits of the thermit process, which had a relatively high failure rate even during the early years. This investigation entailed adaptation of the consumable guide electroslog welding (E.S.W.-C.G.) process as an alternative for field welding of 136 pound per yard carbon steel rail. The electroslog process was selected for this application because of the sound weld deposits normally produced with the high deposition single-pass welds and its potential for portability through use of an engine-driven generator power source.

The weld sensitive rail chemistry and complex geometry posed a very unusual application for E.S.W., which is normally applied to structural steel plates of uniform thickness. The high E.S.W. heat input and slow cooling rate, however, proved to be advantageous for producing acceptable properties in the weld heat affected zone, and electroslog welded rail

sections are presently being observed in track to determine their actual degree of acceptability.

The success of the E.S.W. application for rail welding (E.S.R.W.) was largely a result of the development of (1) a multi-section copper mold assembly, (2) a unique weld starting method, (3) a plate guide tube that accommodates two electrode wires and regionally affects slag bath heating, and (4) a welding procedure that provides a uniform depth of fusion over the length of the weld joint.

DEFINITION OF THE PROBLEM

Of the welding methods applied to joining railroad rail, only the thermit process has been practical for field maintenance and repair situations. However, greater rail strength requirements to accommodate increased tonnage and train speeds have outdated the mechanical property and quality levels of thermit welds. The objective of this project was to adapt the consumable guide electroslog process with its sound single pass vertical welds, as an alternate field rail welding process.

Major process and procedural variations were required to meet production standards and to compensate for the complex geometry of the rail. To meet practical production standards, the run-in and run-out, normally removed after completion of the weld, had to be modified in order that it be retained or more easily removed. A mold had to be developed that allowed free vertical movement of the slag and weld pool, sufficient guide tube clearance, and compensation for rail shape discontinuities. Procedurally, the changes in rail width from 6 inches at the base to 3/4 inch at the web and to 3 inches at the head required compensation for changes in slag depth and depth of fusion without increasing the welding operator involvement.

1. INTRODUCTION

Continuous welded railroad rail, first used over fifty years ago, has demonstrated significant economic and service improvements over otherwise bolted rail joints. Welded rail not only eliminates frequent maintenance of bolted joint components, it eliminates damage to ties, fasteners, ballast, rolling stock and freight caused by wheel impact on flexible bolted joints. Welded rail has resulted in 15 to 50 percent increased track life and reduction of track maintenance costs by \$198 to \$1,200 per mile per year according to 1975 statistics.¹ Between 1929 and 1975, average freight car capacity has increased from 45 to 74 tons, with loads reaching 120 tons under acceptable conditions.² Continuous welded rail (CWR) is a necessity for the faster and heavier trains and most new rail installations are with CWR. Rail networks in the United States are gradually and systematically converting to the welded rail system.

A survey report in 1975 by D. Hauser,¹ entitled "Methods for Joining of Rail", pointed out that "presently available rail welding and laying facilities limit the conversion of bolted track to CWR to about 6,000 miles per year." When shape and chemistry are considered, the primary difficulty in welding railroad rail is obvious, Figure 1 and Appendix II. The rail shape prohibits use of common welding processes because of high labor cost and skill level requirements. The thermally sensitive rail chemistry further complicates rail joining procedures.³

1.1. In-Plant Rail Welding

Rail welding processes can be generally categorized as "in-plant" or "field welding processes." In-plant methods produce the highest quality welds and decidedly the highest production volume. In-plant welding is normally used for joining 39 foot sections of new or reclaimed rail into 1/4-mile ribbon rail sections that are transported to the rail site for installation. Flash welding and gas pressure welding are the most universally accepted in-plant processes.

These methods produce a high volume of good quality welds, but development of alternative techniques like friction welding are also of interest to the railroad industry because of additional energy and cost saving potential.

1.1.1. Flash-Butt Welding. Flash-butt welding is accomplished in an automatic two-step procedure while the rail sections are positioned in a fixture that provides axial movement of one or both rails. Pre-heating is the first step, and involves butting and separating the mated rail ends repeatedly. During each brief contact, a current of 20,000 to 100,000 amps at 5 to 10 volts is passed through the joint. Each contact and separation creates an arc flash that melts the surface and flashes away any rough points on the rail ends. The cycle is repeated up to 20 times, or until the interface temperature reaches 1,750 to 2,000°F.

The second step involves a final flash under controlled acceleration and contact that causes melting of the rail ends and subsequent expulsion of molten metal and contaminants in an upsetting fashion. Continued

pressure of up to 60 tons is applied until a minimum upset of 0.5 inches and refusal is reached. Welding power is then terminated and the pressure is maintained for a 10 second cooling period. Welds that typically possess 98% of the base metal strength are produced in 3 to 5 minutes.^{1,4,5}

1.1.2. Gas Pressure Welding. Gas pressure welding is similar to flash-butt welding in that heat and pressure are combined to produce joining, but it is actually a solid state process involving diffusion and deformation at the joint interface to produce coalescence rather than a melting of the components. In the weld procedure, rail ends are butted together under pressures of 3,000 to 20,000 pounds and multiple oxyacetylene flames are used to heat a two-inch long area at the joint. As the rail temperature reaches 2,000°F, upsetting begins. As 2,500°F is reached, each rail will have moved 3/8 inch to complete upsetting and joining. With this gas pressure welding method, fluid metal flow is not present in the upset to assist elimination of contaminants as with flash-butt welding, and as a result, weld integrity is more dependent upon proper joint preparation. Total weld time ranges from 5 to 8 minutes, depending upon the rail size, and welds at 93% of the base metal strength are typical.^{1,5}

1.1.3. Friction and Inertia Welding. Friction and inertia welding of rail are only in the research stage, but both hold promise for increased use because of the short welding time, narrow heat affected zone, and low energy requirement (about one-tenth of that for flash welding).¹

Both processes are performed by spinning a steel disc between the rail ends while axial pressure of up to 15 tons is gradually applied through the rails. The heat generated is controlled by regulating the speed of the rotating disc and the axial force on the rails. As the metal interface is heated to the desired temperature, it softens, disc rotation is stopped, and axial forging pressure is applied.

The primary difference between the two processes is that a braking system is applied to stop the disc in friction welding, while in inertia welding, kinetic energy of a rotating flywheel is used to spin the disc and rotation stops as the kinetic energy is expended.

1.1.4. Summary of In-Plant Welding Processes. Flash and gas pressure welding produce welds that are 92% to 98% as strong as the parent metal.² All four previously described processes resulted in production rates that exceeded 80 welds per day in the field. These processes all require complete unspiking and removal of the rail sections for each weld joint and result in significant disruption of rail service. The equipment for rail handling, welding, and rail finishing which involves shearing and grinding of residual weld material must be mounted on specially designed rail cars. An in-track flash welding unit used in the United States costs approximately \$500,000, according to Hauser's 1975 survey on rail joining methods.¹ Although these systems are quite efficient for major track upgrading or new installations, they are not practical for routine repair and maintenance.

1.2. Field Rail Welding Requirements and Processes

A viable field rail welding process should produce high integrity welds with minimum disruption of track installation and road service. To meet this objective, the process must be portable, inexpensive, be available for routine repair and maintenance, and require only limited operator skill.

Presently, the predominant field welding method used in the United States is the thermit^{*} process. Most countries use the thermit process to some extent, but references indicate increasing interest and varying degrees of success with enclosed arc, submerged-slag and electrosag welding.

1.2.1. Thermit Welding. There are many variations of the thermit process, but most use the following procedure: With rail ends aligned and spaced 1/2 to 1-1/4 inches apart (depending upon the rail size), a pre-formed sand mold is placed around the rail joint. The rail ends are oxy-fuel preheated to between 950 and 1,000°F through the opening at the top of the mold. After preheating, a specially designed crucible containing iron oxide, granulated aluminum and alloying elements is placed over the mold cavity and the contents are ignited. In a few seconds, the resulting exothermic chemical reaction produces a molten steel and slag pool in excess of 3,500°F. The crucible melt is then tapped into the mold cavity to fuse with the preheated rail ends.

^{*}Thermit--a group of processes which uses heat from exothermic reactions to perform welding and other operations.

Thermite--the generic name given to reactions between metal oxides and reducing agents. (Welding Handbook, Vol. I, 7th ed.)

The mold is left in position for at least five minutes after the weld is cast to reduce the cooling rate and improve weld properties. The mold is then removed and the sprue and risers trimmed prior to final finishing by grinding.

The thermit process has a propensity for severe entrapment of non-metallic inclusions and evolved gasses in the fusion zone, Figure 2.⁶ Thermit welding was restricted to emergency applications in the Russian rail network after 1977, when extensive weld testing indicated only 70% of the rail strength was achieved in the typical weld. The Japanese National Railway has limited thermit welding to a "first-aid" treatment of damaged rail, but because of process speed and mobility, various investigations have been undertaken to improve weld quality.³

1.2.2. Shielded Metal Arc Welding. Shielded metal arc has very limited use for rail joining in the United States, but a variation called "enclosed arc welding" is widely used in Europe and Japan. The process normally requires use of 3/16 inch or larger E-8018 and E-8036 electrodes to fill the 3/4 inch space between rail ends. The rail ends are preheated to 500°C and a removable copper or permanent steel plate is placed beneath the rail base to support the first weld passes. The first weld passes are made with E-8018 electrodes and are started on tabs at each edge of the rail base to prevent arc impingement on the copper backing plate. Slag removal after each pass with the E-8018 electrode is required to avoid entrapment in successive welds. When the weld has progressed to the rail web, the starting tabs are removed and the first of

four levels of weld enclosure blocks are placed over the rail joint, Figure 3.

The remainder of the weld is made with E-8036 electrodes without slag removal between passes. The E-8036 slag has a very low melting point and low viscosity, which allows excess slag removal between each enclosure block and the rail surface. Upon weld completion, slag is removed and the rail head contour is ground. When steel backing plates are used, post-weld removal by a portable milling rig is necessary.⁷

Enclosed arc welding normally requires a 45-55 minute arc time, depending upon the rail size, and post-weld heat treatment of $680^{\circ}\text{C} \pm 30^{\circ}$ for ten minutes followed by a cooling period of 40 minutes. Full-scale testing of weld sections have repeatedly demonstrated weld properties equal to the rail. Equipment costs are low and the enclosure blocks are reusable. However, the total weld time requires 2-1/2 to 3 hours and relies heavily upon operator skill.³

1.2.3. Submerged-Slag Welding. Japanese National Railroad (JNR) observations have determined that fusion welding of rail in the field was too dependent upon operator skill. To overcome operator skill dependency, the JNR developed an automatic process that combines submerged-arc and electroslog welding, known as submerged slag welding.⁵ The submerged-arc process is applied until the weld has progressed to the rail web where the transition to electroslog takes place for the remainder of the weld, Figure 4.

The submerged-arc process utilizes a continuous electrode wire system in which the arc for welding is completely covered (submerged) by a

granular flux. The first weld passes are supported and formed by a copper backing placed beneath the rail joint. The backing is lined with solid flux to prevent copper pickup from the eroding action of the arc. The submerged-arc phase normally requires three passes at 800 to 1000 amps, depending upon the rail spacing. After each pass, the slag and unfused flux must be removed from the weld joint by chipping and wire brushing.

When the submerged-arc phase is completed, the welding nozzle is fitted with a consumable guide tube for electroslog welding. A water-cooled copper mold is placed around the rail joint containing the molten metal and slag of the continuous deposit electroslog process. This electroslog process is identical to the tubular consumable guide electroslog process described later as an independent joining method (section 1.2.4.).

Total weld time is normally 30 minutes for each submerged-slag rail weld. In 1971, a special rail car was constructed by the JNR to make field welds using the submerged-slag process, and only favorable results have been reported regarding process efficiency and weld integrity.³ Characteristics of electroslog welding that can affect submerged-slag weld quality include frequent defects at weld initiation and the requirement for a process stabilization period to establish uniform fusion. Presently, there is no indication that submerged-slag welding of rails has been accepted as a standard field welding method.

1.2.4. Electroslag Welding. Electroslag welding (ESW) has been reportedly used for on-site joining of crane rails in the Soviet Union for the past fifteen years.⁸ There are no publications to verify its successful use for railroad rail joining, but electroslag joining has repeatedly been attempted by Australian, Canadian, and Soviet groups.^{9,10}

Electroslag welding is typically applied to plate material in excess of 3/4 inch in thickness as in ship and bridge construction, and utilizes a single pass in the vertical position.¹¹⁻¹⁵ The process produces coalescence of metals with a molten slag bath that melts the filler metal and the surfaces of the members being welded. The process is initiated by an arc that melts a predetermined quantity of flux and forms a 1-1/2 inch nominal slag bath depth. As the slag bath is formed, the arc is extinguished and the conductive molten slag is maintained in excess of 3,800°F by resistance to current passing through the slag.

The slag bath and molten metal are contained in the weld joint by molds made from copper, ceramic, or other suitable material depending upon the application, Figure 5. Water cooling is often applied to protect the mold and to accelerate cooling rates. The shape of the weld reinforcement is determined by relief provided in the molds.

Arc initiation and slag bath development is normally confined to a starting block (run-in) that extends 3 to 4 inches below the weld members, and the last 3 or 4 inches of weld performed in run-out blocks above the weld members. Both are removed upon weld completion to insure uniform ingress and egress of the fusion pattern and to eliminate defects inherent with weld initiation and termination.

Electroslag welding can deposit up to 45 pounds of weld per hour with a single electrode, and multiple electrodes can be used for high deposition in thicker weldments. Oscillating the electrode improves the thermal distribution and allows further increases in weld thickness to be achieved for a given number of electrodes. A detailed description of consumable guide electroslag welding and its applications will be presented in section 1.3.

There are two major variations in the electroslag process, known as the consumable guide method and the conventional or non-consumable guide method. The consumable guide method uses a 1/2 inch or 5/8 inch tubular guide to position the electrode at the center of the weld joint and provide welding power to the electrode for the duration of the weld. The guide tube melts just above or at the surface of the slag bath and becomes part of the weld deposit; thus, the name consumable guide tube.

The conventional electroslag process uses a curved electrode guide or snorkel that extends over the edge of the mold to direct the electrode into the slag bath, Figure 6. An appropriate electrode stickout distance is maintained to protect the snorkel from the heat of the slag bath, and a plate crawler or special fixture is used to raise the snorkel and mold as the weld progresses.

V. I. Svetlopolyanskii⁹ at Volgograd Institute of Municipal Transport Engineers reported welding of tram rails using a plate electrode, which is a variation of the tubular consumable guide. The plate guide tube design was similar to the one used for crane rail welding by L. N. Kopetman⁸ and Kn. Mukanaev, who also developed a conventional electroslag

procedure for crane rail, Figures 7 and 8. In the conventional application, the proximity of the two curved guides was adjusted to the mold contour as the weld entered the rail web.

1.3. Electroslag Welding

Standard welding procedures with the consumable guide electroslag process only requires periodic flux additions, cooling shoe movement, and minor amperage and voltage adjustments to maintain superficially acceptable weld conditions. The weld metal pool and subsequent solidified weld are never visible because of the slag bath position, and a clear view of the slag bath is restricted by the weld members and cooling shoes during most of the weld. As a result, diligence on behalf of the operator is required to prevent excessive variation in welding conditions, particularly where quality control is limited to post-weld visual examination.

To properly adapt and utilize ESW for other than plate welding, it is essential to understand the effects of amperage, voltage, wire feed rate, slag pool conditions, and guide tube position, as well as the thermal effects attributable to the base metal and mold characteristics. In addition to in-process variables, it is important to be cognizant of process options, including guide tube oscillation, type and number of guide tubes, joint spacing, and flux chemistry.

In heavy section plate welding, ESW has an approximate ten-fold production rate advantage over other processes, but it has been limited to applications where impact strength or transverse tensile requirements

are minimal. Low strength characteristics inherent to a large weld pool with a slow solidification rate are also attributable to the wide range of weld parameters that produce visually acceptable welds.¹⁶

Several groups have studied the effects of process variables in efforts to improve weld properties.¹⁷⁻³⁴ Among the most comprehensive of these investigations is one by S. Venkataraman,¹⁷ entitled "Effects of Process Variables and Microstructure on the Properties of Electroslag Weldments". He presented the effects of in-process variables upon weld morphology as well as those of guide tube design innovations and low frequency weld pool vibration. A significant result of Venkataraman's investigation was development of an ESW procedure that produces weld metal properties equivalent to the 2 inch thick ANSI/ASTM A588 steel base metal.

1.3.1. Weld Initiation. While not an arc welding process, the ESW slag bath is initiated by establishing an open arc between the electrode wire and a weld run-in tab. Power settings for weld initiation are normally 45 volts and 500 amperes for the commonly used 3/32 inch diameter electrode. During this arc initiation period, flux is gradually added in a premeasured amount to produce a 1-1/2 inch deep slag pool in approximately one minute. As soon as the slag bath is established with stable amperage and voltage readings, the power setting should be adjusted to meet the requirements of the specific welding situation.

Two common practices are employed to improve arc starting:

- (1) the electrode should have a sharply pointed end to improve contact with the starting plate.

- (2) a ball of clean steel wool may be placed between the electrode and the arc initiation surface.

A less common but more dependable procedure is to pour molten slag into the weld joint as the power is initiated.¹⁴

When proper starting procedures are not followed, stubbing may occur. This results when the electrode makes contact with the starting surface without arcing. Electrode stubbing often causes deflection of the guide tube and subsequent short-circuiting between the guide tube and the base metal. This condition normally requires partial disassembly and re-adjustment of the weld set-up before successful weld initiation can be made. Excessive voltage or insufficient amperage setting may result in a similar situation, since the resulting excessive arc length will cause fusion of the electrode with the end of the guide tube. With a multiple electrode system, occurrence of burnback on one electrode is not as harmful in that the remaining electrode will establish the slag bath. Then, as the obstructed guide tube is melted by the advancing slag, electrode feed resumes.

To initiate an E.S.W. multiple electrode weld, each electrode must be started separately. As soon as the arc is initiated with the first electrode, a proportional amount of the premeasured flux is added. As the slag bath forms under the adjacent electrode, the second electrode feeder is engaged and the allotted flux added. This procedure is repeated for all successive electrodes until the slag bath is fully established.

1.3.2. Welding Power Parameters. Electroslag welding requires a remotely controlled constant voltage power supply, electrode wire feeder, and guide tube positioning fixture as shown in Figure 9. These components and controls are essentially the same as used for gas metal arc, submerged arc, and other continuous electrode welding processes. With this continuous electrode process, the current and electrode metal transfer is restricted to a narrow plasma column between the electrode and weld puddle. With ESW, welding power and electrode (+ guide tube) metal transfer takes place within the much larger area of a conductive slag bath; yet, the effect of power variations are equally as sensitive.

To state that voltage determines arc length and amperage determines electrode feed speed as with other constant voltage continuous electrode processes would be a gross oversimplification of their effects. Assuming an ohmic ($E = IR$) model, the relationship of amperage and voltage can be described. Jones et al.¹⁹ have proposed that for a particular slag depth and composition, the deposition rate, depth of fusion, and solidification pattern are controlled by the current and voltage. Assuming that current follows the path of least resistance, there are three possible modes of current transfer through the slag bath as shown in Figure 10.

A high voltage and low amperage results in short electrode extension into the slag bath and limits the current path to the area between the electrode surface and the plates being welded. This generates the majority of heat at the top of the slag bath and results in thermal losses through radiation and subsequent reduction in depth of fusion.

The other extreme, low voltage at proportionately high amperage, results in electrode extension nearly to the bottom of the slag bath. This enhances current flow between the end of the electrode and the weld metal pool while reducing current flow between the electrode surface and plate edges. Furthermore, concentration of heat at the center of the weld pool reduces penetration at the plate edges and may even lead to lack of fusion.

Moderate voltage and amperage conditions provide electrode extension such that a current flow balance is established between the electrode, both plate edges, and the weld pool. This condition produces a fusion pattern that provides complete fusion with both weld members and the most efficient use of energy.

Voltage variation has the greatest effect on heat input and depth of fusion, and should be carefully controlled since it directly influences dilution and microstructure. For example, a 3 volt increase at 500 amperes produces a gain of 1500 watts in welding power. Two inch steel plates welded with various guide tube designs and joint spacing exhibit a 10% increase in base metal dilution with only a 3 volt increase, Figure 11.⁹ Since voltage is the major determinant of fusion depth, it has a greater effect on electrode position during welding than was described in the fixed slag depth model of Figure 10. If a constant volume of slag was maintained during welding, an adjustment in voltage would change the slag depth and consequently the electrode/slag contact area, which compounds the effect of the voltage change.

It is important to avoid any voltage fluctuation, but it is particularly important at high voltage conditions. Solari et al.²⁰ have shown that welding at high voltage produces a penetration pattern as shown in Figure 12. A sudden drop in voltage will cause slag entrapment beneath the overhanging base metal as the subsequent reduction in depth of fusion occurs.

The effect of current can be considered by fixing the voltage and adjusting the wire feed rate. Since an increase in current increases the energy input per unit surface area of weld, it might be expected that deeper penetration and greater heat affected zone width would result. It has been shown that the opposite occurs; since an increase in current requires an increase in electrode feed rate, the weld pool velocity is increased and the energy input per unit of weld surface area decreases.^{17,21} More simply stated, increased weld velocity decreases the time that the molten flux is in contact with any given point on the weld surface.

A less significant factor in energy input is the current and electrode feed-rate relationship since it is not linear, but rather that current is proportional to the square root of the electrode feed rate, Figure 13.²⁰⁻²² The net effect of current change at a constant voltage is that increased current increases weld pool depth and deposition rate. R. W. Frost et al.²¹ reported that an increase in the current at a constant voltage reduced the depth of fusion and under extreme conditions resulted in lack of side wall fusion.

Venkataraman and other investigators have used the weld form factor, which is the width to depth ratio of the weld pool, to aid in determining

the effects of parameter variations.^{17,19-21,23} The weld pool shape, and hence the form factor, are identified by measurement of solute dumping lines that are revealed by macroetching the longitudinal vertical center section of the weld. The effects of current variation at a constant voltage, voltage variation at constant current, and slag bath conductivity are schematically depicted by the solute bands, Figures 14-16.

1.3.3. Welding Current. The single electrode consumable guide method of electroslog welding normally uses direct current electrode positive welding power. With three or more electrodes, D.C. welding power creates a magnetic field that often results in excessive slag pool turbulence and a preferential fusion pattern to one weld member. However, when alternating current is used for one or all of the electrodes, a more balanced penetration pattern is obtained.

1.3.4. Flux and Slag. Chemical electroslog flux properties vary greatly and even from lot to lot by the same manufacturer. Variations in electrical resistance between fluxes have an effect on the weld pool similar to voltage variation, Figure 14. The electrical resistance of the flux directly influences slag bath temperature, thus affecting weld penetration. High resistance restricts current flow and results in a cold slag bath. Low slag resistance allows excessive current flow and creates slag overheating. The flux composition should minimize resistance variations as the slag temperature changes, or accurate power control will be difficult. Flux composition should also be matched to alloys in order to prevent undesirable removal of elements through fluxing

action. Improper flux chemistry may not only affect alloy transfer, but it may change the electrical resistance of the slag bath as element concentrations change.

In addition to resistivity, slag viscosity is important. The slag must be fluid enough to prevent entrapment or restrict weld pool flow, but viscous enough to prevent excessive leaking around the cooling shoes. Fluxes containing calcium fluoride are often used for starting the weld because of increased slag fluidity that accelerates transition from the arc to the slag mode. Therefore, to assure consistent reproducible results, careful consideration of flux chemistry and properties must be taken into account.

Maintaining the proper slag depth is essential to production of sound welds. An excessively deep slag bath reduces thermal efficiency because of the increased volume of slag to be heated and the increased contact with the weld members.²² Under this condition, the weld pool becomes deeper and narrower, which can result in hot-cracking at the weld center.²³ On the other hand, a shallow slag bath results in large scale fluctuation in amperage and voltage, violent slag action, and in extreme conditions, arcing across the top of the slag pool. When the slag depth is reduced, depth of fusion is reduced and surface contaminants that are normally removed may remain in the weld. Microcracking at grain boundaries in the weld center has also been associated with low slag depth.²⁴

A slag layer is deposited between the cooling shoe and the weld surface that results in a constant depletion of the slag bath. Thus,

properly controlled flux additions are necessary to maintain the slag depth at approximately 1-1/2 inches to avoid the aforementioned problems.

A common method for monitoring slag depth is to quickly plunge a probe (usually a piece of electrode) to the bottom of the weld pool, then withdraw it for examination, much like the oil dipstick in an automobile engine. Frequently, slag depth is monitored by the operator's sensitivity to the sound of the arc and observation of the slag bath turbulence.²⁵ With either monitoring method, the flux must be added intermittently and subjectively as to the proper volume. Limited success in constant slag bath maintenance has been achieved through use of a flux coated guide tube that resembles a shielded metal arc electrode, but this allows little tolerance for variations in welding conditions.

Venkataraman¹⁷ has shown that the slag level can be accurately produced and maintained by monitoring the welding current with an oscilloscope or chart recorder. Proper slag depth produced a stable amperage trace, but as the slag depth decreased to one inch, intermittent spikes of medium amplitude were observed. A proportional increase in frequency and amplitude of the amperage trace occurred as the slag depth decreased to 1/2 inch where severe arcing began. In addition to monitoring the effects of slag depletion, he was able to determine that random bulk flux addition can be detrimental to weld stability by changing the slag temperature and resistance. An example of the inefficiency of random flux addition was the occasional presence of unmelted flux in the slag coating of the completed weld.

For a given weld geometry, the rate of slag depletion was determined and a flux metering device was adapted to provide continuous flux addition at that same rate. The result was a constant slag depth that allowed more accurate control of welding parameters. By continuing to monitor the current, it was found that minor adjustments in the flux feeder could compensate for unintentional slag losses and joint geometry variations. When proper slag depth and power settings were established at the weld initiation, stability provided by continuous metered flux additions largely eliminated the need for additional adjustments during the remainder of the weld.

1.3.5. Joint Spacing, Guide Tube Position and Grounding. Joint spacing for consumable guide electroslag welding ranges from 1 to 1-3/4 inches and is determined by three general factors. The primary performance consideration is to provide sufficient guide tube clearance from the cooling shoes and weld members. The remaining factors are more difficult to determine and involve the dilution of the weld metal, depth of fusion, and the distortion based upon the overall weld geometry.

Welds have been made with joint spacing as narrow as 3/4 inch using standard 1/2 inch guide tubes. Narrower joint spacing increases the welding speed because of the reduction of area, but increased arcing and slag turbulence also occur because of the reduced guide tube clearance. Extra care must be taken to insulate and center the guide tube in narrower weld joints. If the guide tube makes contact with a weld member, it will cause short circuiting, which usually fuses the guide tube to the member and terminates the weld.

Venkataraman¹⁷ has shown that by decreasing the joint spacing with all other parameters constant, the depth of fusion (thus, base metal dilution) will increase linearly with minimal effect upon the form factor. If a specific composition of the weld deposit is required, the dilution must be considered.

An advantage of the electroslog process is the low rate of distortion that occurs during welding. The uniform axial distortion that does take place is easily compensated for by progressively increasing the joint spacing (.015 inch per foot of weld).¹¹

The location of the guide tube in the weld joint has a significant effect upon the symmetry of the weld fusion pattern. The intensity of heat generated near the electrode can be up to an order of magnitude greater than the heat near the slag-base metal interface and will result in greater heating and depth of fusion in the plate closest to the electrode.²⁶ The location of the ground attachment has an effect similar to guide tube positioning in that if only one plate is grounded, a preferential current path may be established. This will result in a greater heating of the grounded member. The results of variations in guide tube position and grounding are shown in Figure 17.¹⁷ Since the weld width is determined by voltage conditions, there is minimal effect upon weld size and grain pattern when guide tube or ground positions are varied. However, to avoid asymmetry in the weld fusion pattern, even to the extent of incomplete fusion at one side, the guide tube must be straight and centered in the weld joint, and both weld members must be grounded.

1.3.6. Guide Tube Effects. The main function of the guide tube is to deliver the electrode to the proper location in the slag bath. It provides electrical contact as close to the slag as possible and thus avoids excessive resistance heating of the electrode wire. The standard guide tube is made from cold-drawn low carbon steel in 1/2 or 5/8 inch outside diameter and 1/8 inch inside diameter. The end of the guide tube is normally in contact with the top of the slag bath but occasionally melts off above the surface or extends slightly beneath the slag surface. Since the guide tube is used to provide electrical contact for the electrode, it is also a source for electrical conductivity to the slag bath when the two are in contact. It is generally recognized that the guide tube carries approximately 35 to 40% of the power to the slag bath, with the remainder being carried by the electrode wire. By using a guide tube with greater cross section and different shape, higher current settings may be used, and the slag bath thermal patterns altered to concentrate or distribute heat as desired.^{17,27,28} Enhanced guide tube geometry is a more effective method of heat distribution than guide tube oscillation because it limits the occasional arcing and slag entrapment that can occur with oscillation.

Venkataraman¹⁷ fabricated a "winged guide tube" by welding two 1/4 inch steel strips of appropriate width to a 1/4 inch tube. The winged guide tube was used to weld 2 inch steel plates with 3/4 inch joint spacing at twice the amperage used with the standard guide tube. This resulted in a 66% reduction in weld time, and a 50% reduction in specific heat input.

1.3.7. Electrode Variations. Solid uncoated 3/32 inch diameter electrodes are normally used for electroslog welding. Copper coated electrodes used with gas metal arc and submerged metal arc are not recommended for the ESW of consumable guide process since the copper coating tends to build up in the heated guide tube and interfere with the electrode feed. Electrodes of less than 3/32 inch diameter are too flexible to be pushed through the guide tube and require excessive feed rates to meet higher current requirements. Larger electrode diameters have little advantage over the 3/32 inch electrode and are more difficult to feed through the guide tube because of deflection from the electrode cast.

Electrode wire cast is a problem recognized in other continuous electrode process and is remedied by the use of a wire straightening roll where the electrode enters the drive roles of the feeder. In the ESW process, cast removal is especially important since the wire is not visible in the slag bath, and its adverse effect will be unnoticed until the weld is completed. Wire cast causes the electrode to curve to one side as it exits the guide tube and has the same effect as moving the guide tube to one side as discussed earlier. To maintain symmetry within the slag bath and, thus, within the fusion pattern, the electrode stickout must be as straight as possible for one inch beyond the end of the guide tube.^{17,26} Careful adjustment of the wire straightener is required during the weld setup while the electrode is visible.

Multiple electrodes can be used as the material thickness exceeds the capability of a single electrode. When multiple electrodes are required, a power source is recommended for each electrode. The power

sources must be paralleled with a common control so that all electrodes and power sources function as a unit. The guide tubes must be bridged or a specially designed plate guide may be used, but welding control will be unstable if the guide tubes are not rigidly positioned to act as a single guide tube.

The distance between electrodes has a significant effect upon the shape of the weld pool and "maximum" depth of fusion into the weld members. Eregin²⁹ has developed a method for calculating the shape of penetration for multiple electrode electroslog welding. Figure 18 shows a comparison of calculated and actual penetration shapes and demonstrates the penetration pattern resulting from variations in the number of and distance between electrodes.

Patchett³⁰ has shown the extreme conditions for electrode spacing on a two electrode system in Figure 19. He has proposed that a practical balance in electrode spacing be one-half the plate thickness and electrode-to-shoe distance be one-quarter of the plate thickness, up to a maximum plate thickness of about 125mm.

Strip electrodes, also known as ribbon or plate electrodes, have been used with varying degrees of success by several investigators.³¹⁻³⁴ Delawari et al.³¹ have shown that the strip electrode system has a melting rate 30% greater than the wire system. It has also been shown that the use of a properly positioned strip electrode, as wide as the weld joint and combined with a low conductivity flux, will increase weld velocity and reduce base metal dilution, undercut, and heat input.

1.3.8. Weld Position. The ESW process is normally performed in a vertical orientation.¹⁴ This allows a more precise control of the large weld pool as well as the guide tube positioning. Paton²³ has placed a limit on weld axis inclination at 10 to 15 degrees from vertical.

Jones et al.¹⁹ has shown that the significant difference between vertical and non-vertical welds is that the fusion zone exhibits a skewed cross section, although the initial cavity was circular in cross section. Figure 20 contains a schematic representation of a 45 degree electroslog weld made by filling the 1 inch inside diameter of a 3-1/8 inch O.D. steel tube. Preferential radiation preheating of the upper weld surface was the major cause of penetration and H.A.Z. anisotropy. Mathematical models have been established to study the slag bath and radiant heating, but according to Jones, none are sufficient for a system composed of more than one surface, or when surfaces are at different temperatures.¹⁹

Jones also determined that non-vertical electroslog welds are quite sensitive to welding parameters, and that resulting non-uniformity of thermal patterns in small angle welds is much more sensitive to parameter values than in large angle welds. Welds were made at angles of up to 60 degrees with satisfactory penetration by maintaining tight control of amperage and voltage.

2. EXPERIMENTAL PROCEDURE

2.1. Material

Southern Pacific Transportation Company provided randomly selected sections of rail steel in order to reflect the range of geometric tolerances encountered in actual service. Each section complied with American Railway Engineering Association and American Society for Testing and Materials (AREA/ASTM) specifications for 136 pound per yard rail. Rails were cut to 18 inch lengths and used for all of the developmental welds. Two 5-foot sections of 136 pound per yard chromium molybdenum rail were supplied for full-scale testing at the conclusion of the initial project. The AREA/ASTM rail chemistry specifications and chemistry of rail supplied by Southern Pacific Transportation Company are shown in Table I.

The same commercial fused flux was used for all welds in this project. PF-201 flux (Hobart Bros., Inc.) was used for the major portion of the slag bath, and PF-203 was used for weld starting as recommended by the manufacturer. Flux chemistry is proprietary, but both fluxes are described by the manufacturer as "neutral".

Three variations of 3/32 inch diameter electrode were used during process development. One electrode was the AWS E70S-3, an uncoated carbon steel electrode commonly used with ESW plate welding; second, an AWS E70T-G electrode with powdered steel core and without copper coating;^{*} and thirdly, a copper coated AWS ER90S-B3 alloyed electrode with 2-1/4Cr-1Mo.^{**}

^{*} Metal-cor 6, Airco Welding Products, Clermont Terrace, Union, New Jersey
^{**} AS-521, Acco/Page, Bowling Green, Kentucky

2.2. Equipment

A commercially available electroslog system was used for this project as shown in Figure 21.* Two 750 ampere, 100% duty cycle constant voltage rectifier power sources were paralleled to provide undiminishing weld power as high as 1500 amperes and 58 volts. The system was equipped with a dual electrode drive unit including the torch, guide tube clamping assemblies, and electrode spool mounts. This assembly was attached to an x-y positioning fixture. The fixture was designed to clamp directly over the weld joint on material up to 3-1/4 inches thick. It was equipped with an optional electrode oscillating unit that was variable in travel speed, distance, and directional change dwell time.

A remote control panel provided common control and monitoring over both power sources. The voltage was controlled by a single variable transformer and voltmeter on the remote panel. The amperage was controlled by a single variable transformer labeled wire feed speed control, but an ammeter for each power source was provided. The remaining items on the remote panel included the weld start-stop switch, wire feed direction switch, a manual electrode feed switch labeled "inch control", and a section with oscillator speed control and off/auto/manual selection switch.

A strip chart recorder was used to record the amperage and voltage during all welds and a digital voltmeter was added to the system to provide more accurate monitoring and control. A jet-Line electrode feedrate meter was incorporated to monitor the electrode feed in inches per minute.

* Porta-slag, Hobart Brothers Co., Troy, Ohio

The chart recorder was used on selected welds to verify the relationship of electrode velocity to other variables, but the feedrate was noted by the operator for all other welds. A metered flux feeding device as described in Venkataraman's¹⁷ work was used to add the flux at the weld start until the desired slag depth had been established.

2.3. Weld Set-Up

In each weld set-up, the rails were placed on a solid base and one section was securely clamped to maintain a reference. Rail sections were matched gage side to gage side, and the joint spacing was evaluated over the range of 5/8 to 1-1/4 inches. The nominal joint spacing was established at the rail base, and a 1/16 inch per lineal foot incline (crown) was set on each rail to increase the joint spacing at the rail head, Figure 22.

The electrode feeder was then attached to the secured rail section and the guide tube positioned symmetrically in the joint. When joint spacing or guide tube flexibility created possible contact with the rail ends, commercial ring-shaped guide tube insulators were wedged between the guide tube and rail ends.*

The basic mold components, consisting of the starting block, mold shoes, and runout, were positioned around the weld joint as symmetrically as possible. Guide tube clearance with the mold members was carefully checked during each set-up to avoid contact or arcing during the weld.

*Hobart Portaslag Insulators, Part #S5 17100-54

Poor fit-up between the mold and rail surfaces was remedied by performing additional shaping of the mold or by filling gaps with refractory cement.

2.4. Guide Tube Evaluation

Guide tube designs were developed based on results of preceding welds, starting with the 1/4-inch plate design described in section 4.4. Each design was evaluated subjectively by the operator during welding. The efficiency of slag bath formation, freedom of electrode movement, controllability of welding amperage, and stability of position in the weld joint were observed. Heat distribution between the guide tube and slag bath was determined by examination of the completed weld for uniformity of fusion and slag covering.

2.5. Mold Evaluation

Mold materials, including OFHC copper, graphite, bonded refractory and casting sand were evaluated by visual examination following application in a basic rail weld. Mold material erosion or gross contamination of the weld metal were unacceptable. Examination was also conducted for mold material outgassing, adhesion to the slag layer, and arc impingement, but these conditions were not considered crucial enough to disqualify the material without further testing.

An important consideration in the mold cavity design was the ease of post weld mold removal. For expendable molds, the material merely had to be easily removed for weld inspection. For reusable molds, the material had to part from the weld without damage to either surface.

2.6. Weld Inspection

Visual examination of the weld was directed to undercutting, overlapping, weld cracking, and lack of fusion as well as the conditions specifically listed in sections 2.4 and 2.5. When visual examination of the weld indicated a defect-free product, or if more detail was required than observable by surface examination, the weld and heat affected zone of the rail were sectioned as shown in Figure 23. Each section was surface ground under a steady coolant flow to an 8 G finish on the S-22 microfinish comparator.* After removing grinding residue, the sections were etched with a 10% nitric acid/methanol solution until the grain structure was clearly visible. Etching was stopped by successive tap water and ethanol rinses followed by hot air drying. Sectioning allowed examination for piping porosity, slag inclusion, hot cracking, and lack of fusion.

For a more quantitative analysis, welds were sectioned to measure form-factor, depth of fusion, and the heat affected zone area. Surface and weld cross sectional analysis were combined with the amperage/voltage traces and electrode feed-rate, to aid in determining procedural modifications.

Even though sulfur printing is normally intended for identifying sulfid concentrations, it was also used in this investigation to enhance form-factor and fusion boundary identification as shown in Figure 24. Sulfur prints were taken from weld sections prepared in the same manner as for etching. The sulfur printing procedure is described in section 2

*GAR Precision Products Inc., Microfinish Comparator, Stanford, CT.

of the Appendix. All samples were numbered, coated with a transparent protective finish, and stored for further analysis.

3. RESULTS

3.1. Equipment

The final equipment required for consumable guide electrosag rail welding (ESRW) included two constant voltage 750 ampere 100% duty cycle power sources, a common control unit as described in section 2.2, and a dual electrode feeder and spool mount. The electrode feeder was attached to an x-y positioner which was clamped to the head of the rail as shown in Figure 25. The mounts for the sixty pound electrode coils were separated from the electrode feeder, and six foot flexible conduits were used to guide the electrode between the two units. The wire feed meter and flux metering device were incorporated with the electrode feeder over the weld joint.

Five pieces of OFHC copper were cast to form the mold set. These components are identified in Figure 26 as a starting block, two water cooled side shoes, and a two-piece runout block. The starting block dimensions are 2 x 6 x 8-5/8 inches with a 7/8 x 2 x 7-3/8 inch weld starting recess centrally on the top surface. Five vent slots 1/4 x 1/4 inch were milled from both sides of the 7-3/8 inch weld starting recess, parallel with the rail bottom and extending to the edge of the starting block. The vent slots were spaced on 1-1/4 inch centers with the middle slot centered on the block. Commercially available 1/4-inch weld backing ceramic (primarily magnesium silicate), was cut as required and used to line the weld starting recess. A 6-inch long insert fabricated from one 1/4 x 1 inch strap and two 0.059 x 0.6 inch strips of SAE/AISI 1010 steel,

was placed on top of the ceramic and formed to provide electrical contact with the rail base, Figure 27.

Shoes were formed to fit the gage and opposite sides of the rail and marked accordingly. Each shoe was $6\frac{5}{8}$ inches high and extends from the bottom of the rail to $\frac{5}{8}$ inch below the top of the rail head. Two $\frac{7}{16}$ inch water passages were drilled through each shoe parallel to the rail head and are attached to a 13-gallon recirculating water cooler by $\frac{1}{4}$ inch hose.

The runout block was cast in one piece with a groove across the bottom that is contoured to match the top of the rail head. The groove positions the $2 \times 6 \times 8\frac{5}{8}$ inch block in alignment with the side shoes and the runout passage over the weld joint. The runout passage has $1\frac{3}{4} \times 3\frac{1}{4}$ inches with a one inch radius on the edges where the weld enters from the rail head. The block was cut into two equal parts transverse to the rail and through the center of the run-out passage.

The guide tube was fabricated from commercial $\frac{1}{2}$ inch electrosag guide tube stock and $\frac{1}{2}$ inch SAE/AISI 1010 steel plate, Figure 28.* Approximately $\frac{3}{4}$ inch of electrode stickout was provided by recessing the commercial guide tube $\frac{1}{2}$ inch from the end of the fabricated guide tube. When the rail guide tube was positioned in the weld joint, $\frac{3}{8}$ inch clearance remained between it and each rail end, and $\frac{1}{4}$ inch minimum clearance with each side shoe. The relative positions of the guide tube, rail profile, and mold cavity are shown in Figure 29. Weld area calculations starting at the bottom of the rail base were performed by

* Hobart type 48 Porta-slag guide $\frac{1}{2}$ inch (13mm) O.D., $\frac{1}{8}$ inch (3mm) I.D.

sectioning a weld horizontally at 1/4-inch intervals and measuring the section surfaces. A plot of the guide tube, weld joint, and weld metal cross sectional areas are shown in Figure 30.

3.2. Electroslog Rail Welding Procedure

1. The rail sections are to be aligned and spaced 1-1/4 inches apart with a 1/16 inch incline (crown) per foot of rail. The rail ends should be cut perpendicular to the running surface and clean.
2. Place the starting block with the insulation and insert symmetrically beneath the rail joint, insuring that the starting insert has positive contact with the rail base.
3. The guide tube is attached to the electrode feeder and one electrode is extended 1/2 inch beyond the end of one tube. The other electrode is positioned approximately ten inches short of the end of the second tube. Each electrode end must be cut to produce a sharp point (electrode type specified to match rail chemistry).
4. Attach the positive welding cable (DCEP) and the guide tube to the electrode feeder, then clamp the feeder to the head of the rail. The guide tube must be positioned symmetrically in the weld joint and have two insulators placed over the end to provide a 0.15 inch minimum spacing between the guide tube and starting insert.
5. Securely clamp one ground lead to each rail base, approximately ten inches from the weld joint.

6. Both side shoes are then clamped in position on their respective sides of the rail while insuring that the guide tube has proper clearance and the mold cavity is formed symmetrically over the weld joint.
7. With the same precautions as in step 6, place both runout block halves in position.
8. Check the fit-up of all mold components relative to each other and the surface of the rail. Seal any areas at the outer edges that fail to make contact by applying a small quantity of suitable insulating cement.*
9. Preheat the starting block and rail base to between 450° and 600°F with an approved oxyafuel torch.
10. Start the weld at 31 volts and 1100 amperes. As the arc is established with the second electrode, the primary consideration is to maintain 31 volts and 50 inches per minute electrode feedrate. As the slag bath contacts the bottom of the guide tube, amperage will automatically increase to approximately 1800 amperes and then gradually decline as the larger base of the guide tube is consumed. As the amperage declines, gradually increase the electrode feedrate to stabilize 1100 amperes and maintain that amperage for the remainder of the weld.
11. Steadily add 100 grams of PF203 starting flux through the top of the mold cavity as the arc is started so that it is completely deposited within 10 seconds. The automatic flux feeder must start at the same time as the arc,

* For this investigation, Keen No. 1 Plus, Keen Corporation, Vienna, WV 26105

and at the rate of 180 grams per minute deposit 450 grams of PF201 running flux. The flux addition and total slag volume should be achieved within 2-1/3 minutes of the weld start.

12. Start water circulation through the side shoes 2-1/2 to 3 minutes after starting the weld, and continue water cooling for five minutes after the shoes have been removed from the completed weld.
13. When the top of the slag bath has reached the top of the runout block, terminate the weld.
14. Within 10 seconds of terminating the weld power, separate one side of the runout block and drain the molten slag into a suitable receptacle. Then remove the hot runout blocks.
15. As quickly as possible after removing the runout blocks, remove the weld runout with a hot chisel or other suitable device.
16. Remove the side shoes and starting block, chip the slag from all weld surfaces, and visually inspect the weld and heat affected zone.
17. Grind the weld area at the head of the rail using the same procedure and equipment as specified in the General Rules Regulations and Practices manual pertaining to thermit welding (Appendix section 3).

3.3. Repair Procedure

In the event that undercut or underfill conditions exist at the edge of the weld, remove all slag and contaminants in preparation for filling the defect with the shielded metal arc process. A 1/8 inch AWS E8018 electrode is required for use on ESRW standard carbon rail applications. The repair weld must be made before the defective area cools to below 450°F. The repair weld profile must be minimized and formed to blend with the electroslog weld to rail surface transition. All shielded arc welds must be made from the edge of the rail base toward the rail web and terminate in the electroslog weld metal. No shielded arc weld will be made in the downward inclination or shall it terminate on rail steel.

3.4. Weld Description

The weld produced by following the procedure in section 3.2 was completed in an average of 19-1/2 minutes and deposited 15 pounds of weld metal. The slag bath depth at the rail base was a minimum 3/4 inch and increased to 1-1/2 inches by the time it reached the top of the runout.

The weld starting deposit extends 5/8 inch beneath the rail base and is 1-3/4 inches from the fusion boundry of one rail base to the other. The weld reinforcement extends 3/8 inch beyond each side of the rail base and gradually tapers to the lower edge of the rail head where it is ground to match the head contour. An example of the final weld after slag removal and finish grinding is shown in Figure 31.

4. DISCUSSION

4.1. Approach

Adaptation of ESW to rail joining was complex since many, if not all the process variables are interrelated and have a substantial influence that prohibits quantitative analysis of individual variable influences. For example, the starting block size and composition were determined by the joint spacing, electrode position, guide tube size, arc starting method, and time required to establish the slag bath. In turn, joint spacing was dependent upon how successfully the slag bath was established prior to passing through the rail base, and how much dilution of the rail steel could be tolerated metallurgically, as well as the thermal effect of the varying rail cross section upon the slag temperature.

Little or no information was available concerning high quality weld starts, rapid establishment of the slag bath, welding of joints with varying cross section, or irregular guide tube and weld reinforcement patterns. As a result, the objective of the first welds involved evaluation of a guide tube design based upon the one shown in Figure 7.^{8,9} This joint spacing, power setting and flux addition were determined by electroslog recommendations for a four inch plate weld using two electrodes and a steel starting sump. Solid copper shoes that allowed a 3/8 inch guide tube clearance were used on the sides of the rail, as seen in Figure 32.

Results of the first welds indicated that the guide tube had potential for producing an acceptable rail weld, but that modifications would

be required to improve mold cooling and the fusion pattern at the rail base, Figure 33. From this point, the development of the starting method, guide tube, mold, and welding procedure were approached synergistically, with each weld reflecting changes in conditions derived from the preceding effort.

4.2. Starting Block

Post weld removal and heat flow were the two major considerations involved in developing the starting block. An insulating layer placed between an electrically conductive consumable starting insert and the supporting block met both of these requirements, Figure 34. Insulating materials were selected and tested based upon their expected tolerance to high temperatures and chemical compatibility with the slag and weld pool. Graphite plates, high temperature refractory, fused fluxes, and magnesium silicate ceramic tiles were tested. With the exception of one magnesium silicate ceramic, conditions of outgassing, excessive melting, and weld metal contamination were sufficient to disqualify each material without further evaluation.

The magnesium silicate ceramic that provided satisfactory results was a proprietary weld backing ceramic, and the exact composition is unavailable. Additional advantages to the ceramic insulation are that it melts on the weld contact surface to provide a compatible slag coating on the weld start, and the remainder of the ceramic forms a smooth, rounded contour under the weight of the weld deposit, Figure 35.

The starting block was designed to provide electrical contact with the rail for arc starting and maintain it until the slag bath reached the rail base, Figure 35a. As shown in this figure, the arc starting plate, 1/4-inch thick low carbon steel, prevented arc impingement and severe erosion of the insulation layer, Figure 35b. The .060 inch steel side pieces provided good electrical contact with the rail base while extracting a minimum of the weld energy for melting.

As the fusion pattern at the rail base was optimized, the presence of cavities (bubble-like defects) persisted at the fusion boundary near the rail base center, Figure 36. In some cases, the cavity was limited to the run-in material while in others, it extended as much as 3/8 inch into the weld fusion boundary. These cavities were caused by gas entrapment beneath the rail base as the slag bath advanced. Five vent slots 1/4 inch square were milled into the top of the starting block to allow sufficient ventilation but avoid slag loss, Figure 27.

The number and spacing of vent slots was determined by examining welds for cavitation after a single slot had been milled in the center of the block. One slot reduced the cavity size by more than 50%. Two additional vent slots of the same size were added to each side of the original on 3/4 and 1 inch centers. Subsequent welds have produced complete fusion along both sides of the weld joint.

4.3. Arc Starting

The conventional arc starting method with steel wool was dependable for starting a single electrode. In dual electrode applications, however,

one electrode would often "burn back" and fuse to the end of the guide tube, or fail to arc (stubbing), which resulted in shorting. The maintenance of an electrode stickout distance of between $3/4$ and 1 inch was essential to eliminate these starting problems. Methods tested to improve arc starting included the use of a high frequency device (normally used for furnace arc starting),* guide tube oscillation, amperage and voltage variations, powdered metal addition, and delaying the start of the second electrode for various periods of time. The high frequency unit and the electrode oscillation methods were of little value. The powdered metal worked well, particularly aluminum powder or filings, but is not advisable because of potential weld contamination.

Staggering the electrode wire positions prior to the weld start was the most dependable procedure for arc starting. One electrode is positioned approximately $1/4$ inch from the starting insert, and the second is withdrawn 10 to 12 inches into the guide tube. This method allows the second electrode to enter a partially ionized zone where the molten slag is forming. In addition, the second electrode will enter the weld zone at a velocity of approximately 65 inches per minute rather than 100 inches per minute as with simultaneous arc strikes. Stubbing occurred in each instance when the electrodes were not cut to provide sharply pointed ends for arc starting. Electrode pointing is a standard practice for continuous electrode processes when the electrode is $1/16$ inch or greater in diameter.

* Airco Mod. HF 20-1, Output unavailable

4.4. Guide Tube Design

The first guide tubes were designed to deliver the electrode to an area of the joint that corresponded with the recommendations for multiple electrode spacing in plate welds, Figure 19. A 1/4-inch AISI/SAE 1010 steel plate was used to position the electrodes and provide sufficient guide tube current carrying capability, Figure 37. Variations of this design worked well after the slag bath was established, but were ineffective in providing complete fusion across the base of the rail. It was noted that on welds where the plate guide member had earlier and greater contact with the flux, that the slag bath was established more uniformly and with less violent arcing. A guide tube similar to the one in Figure 37 was positioned so the plate was 1/8 inch above the arc starting surface, and the arc was established with one electrode to observe the effect of the plate, Figure 38. The arc transferred from the electrode to the plate corner instantly, and traversed the plate edge to produce an arc zone the full width of the plate within 3 seconds.

A second generation guide tube was developed that established the slag bath more quickly and provided better fusion over the rail base, Figure 39. This was accomplished by adding a standard 3/4 inch structural angle steel piece to the bottom of the guide tube described in Figure 37, and filling the angle cavity with flux. The design was studied by using a special mold set and welding only the base of the rails. This allowed clear observation of a single electrode start and the effect of the larger triangular section during slag bath formation, Figure 40. The slag bath was established over the entire weld starting

area within 20 seconds, and it was apparent that the larger guide tube area was providing significant improvement in heating of the slag bath.

Eight welds were made with variations of the second generation guide tube, and the presence of unmelted flux at the weld start was completely eliminated. Still, fusion at both sides of the rail base was not satisfactory. It was also evident that fabrication requirements were too complex for economical application. Analysis of the guide tube development thus far revealed that the most significant change had been in the increased volume of the guide plate rather than just its width or thickness. Increased guide tube volume allowed more constant contact between the guide tube and slag bath, which improved thermal distribution. The previous guide tube designs melted off above or just at the top of the slag bath, and caused amperage fluctuations.

The third generation guide tube design consisted of two straight sections of 1/2-inch commercial guide tube divided by 1/2-inch SAE/AISI 1010 steel plate, Figure 41. Triangular pieces of 1/2-inch plate (wings) were added to each side of the lower guide tube to match the width of the rail base. The increased guide tube width provided complete fusion at both outer edges of the rail base.

The final guide tube design is shown in Figure 28. The 1/2 x 1-3/4 inch slot was centered in the guide tube base to improve amperage control during the first three minutes of welding. Without the slot, the added guide tube area resulted in uncontrollable excessive amperage (over 1800 amperes), which tripped thermal safety switches in the machines. The double bevel that reduces the guide tube thickness to 1/8 inch at the

base also helped provide better amperage control. Any rapid change in guide tube area resulted in radical amperage fluctuation and excessive slag bath turbulence.

Closer spacing of the electrodes at the head of the rail would simplify weld set-up, but a 3 inch guide tube width at the rail head was necessary to control the penetration pattern. The guide tube carries approximately 40% of the weld energy to the slag bath while the balance is concentrated where the electrode wires enter. By separating the electrodes with the guide tube plate, the weld energy and, thus, excessive penetration, was reduced at the 3/4-inch rail web. The same consideration improved the fusion pattern at the sides of the rail head by concentrating the electrode wire energy near the water cooled area of the side shoes.

4.5. Electrode Selection

Electrodes with copper coatings were only used when uncoated products were not available. When used with the first two generations of guide tube (with the curved tubing), the copper coating caused erratic electrode feeding and, in some cases, terminated the weld. With the final guide tube design, the copper coating caused no problem as long as the guide tube was properly aligned in the clamping fixture.

Comparison was made between the plain carbon AWS E70S-3, which is the traditional electrode for welding structural carbon steel, and AWS E70T-G, which is a proprietary^{*} tubular electrode with powdered steel

^{*} Airco, Metal-Cor 6

in the core. Both electrodes were 3/32 inch diameter and uncoated. Under identical welding conditions, the tubular wire provided more dependable arc starting and power control, as shown by the voltage amperage traces in Figure 42. More stable power control reduced slag bath turbulence and less frequency of arcing between the guide tube and rail ends. The E70S-3 electrode was satisfactory for developmental applications, and is more commonly used for ESW; hence, it was used for the majority of welds.

The alloy electrode recommended in the welding procedure (section 3.2) meets requirements for AWS A5.28/ER90S-B3 and had a copper coating. The as-welded electrode chemistry provided by the manufacturer was: .07-.12%C, 2.25-2.75%Cr, .025%S, .45-.60%Si, .40-.70%Mn, .90-1.10%Mo, and .025%Ph. According to work done by M. Scholl,³⁷ the ER90S-B3 electrode produced a bainitic microstructure throughout the entire weld deposit. The hardness at the top of the rail ranged from 33 HRC at the fusion line to 25 HRC at the weld center. This range complies well with the A.R.E.A. specification of 24 HRC minimum for 136 pound per yard carbon rail steel, Table I.

4.6. Flux Addition

The use of one hundred grams of starting flux was required for rapid establishment of the slag bath. Starting flux has a lower viscosity than running flux and accelerates distribution of the molten slag bath, electrical contact, and solid flux addition during the early stages of slag bath formation.

When the total 550 grams of flux had been added, the slag bath was approximately $3/4$ inch deep at the rail base where the joint area was 10 square inches. As the weld progressed to the rail head, the slag was $1-1/4$ inches deep in a 4.8 square inch area. Approximately $2-1/4$ cubic inches of slag was lost to the slag coating formed between the weld metal and the mold surface. Flux additions of less than 450 grams resulted in poor power stability and lack of fusion at the rail base, while additions exceeding 630 grams caused excessive penetration at the rail web and head. A larger volume of flux was avoided during weld starting to minimize the loss of heat to slag bath formation that could otherwise be directed to melting of the rail base.

Flux addition rates described in step 11 of the welding procedure should be followed closely. When starting flux was not added simultaneously with running flux, weld porosity and excessive melting of the insulating material occurred. If the flux was added too quickly, it did not melt efficiently and was deposited with the slag layer on the surface of the weld. Surface deposits of unmelted flux may become severe enough to prevent establishment of sufficient slag depth. Uneven or excessive flux additions also had the effect of cooling the surface of the slag bath and reducing radiant preheating of the rail base.

4.7. Mold Development

Materials evaluated for mold design included solid OFHC copper, graphite, bonded refractory, and casting sand. Each material had been used successfully by other investigators and in practice for various

degrees of containment or backing in other high deposition welding processes. Each material was evaluated by forming mold components in the shape of the preliminary design and making welds under otherwise uniform conditions. The large mold surface area in contact with the slag bath, and the slow travel speed caused excessive heating and erosion of all the materials except copper. Refractory and zirconium casting sand are both used with high temperature castings and would have been economically suited for an expendable mold design. Both materials, however, were severely eroded causing contamination of the weld metal. Graphite demonstrated only minor erosion under the arc starting area and near the rail head, but fractured extensively when removed from the weld. With the copper mold, minor erosion occurred at the top of the side shoes because of overheating. This was eliminated by addition of water cooling in that area.

The size and angle of the mold cavity and weld reinforcement just above the base of the rail was critical in prevention of slag entrapment and notching of the weld metal as shown in Figure 43. This notch formation was not due to guide tube heat distribution, but due to the sudden cooling effect as the weld progressed from the preheated starting block into the larger side shoes that were near ambient temperature. Both problems were eliminated by delaying the water circulation for 2-1/2 to 3 minutes after the weld start, which in effect provided preheating of the side shoes prior to slag contact.

Similarly, areas with sudden profile changes, including the weld to base metal interface, required radius formations sufficient to minimize

stress riser and notch effects in the finished weld. Intimate contact at right angle intersections of the cooling shoes and the rail allowed the rail steel to melt beyond the mold cavity. As the rail steel melted, a small amount was always displaced by slag which resulted in an undercutting effect similar to that resulting from excessive voltage, Figure 12. A larger radius or spacing at the shoe/rail steel intersection reduced the cooling rate of the slag and allowed the heavier molten steel to displace all but a thin layer of solid slag at the shoe surface. A major consideration in mold cavity design was to provide 1/4-inch minimum clearance between the guide tube and mold surface. Therefore, as the guide tube designs were changed, the mold cavity was modified accordingly.

The final mold cavity pattern was partially determined by postweld examination of the cavity surface for arc pitting and areas that had obstructed mold removal. As these conditions were corrected, effort was also made to produce a symmetrical overall pattern that resulted in greater guide tube clearance than was actually required.

Because of continual mold modification and variations in weld procedures, it was not possible to determine the life expectancy of a copper mold set. However, one set of shoes was used for over 30 welds without excessive wear.

4.8. Weld Characterization

The electroslog rail weld condition and appearance are generally described in section 3.4. A more detailed description of the weld and heat affected zone is best achieved by comparison to the thermit process.

4.8.1. Fusion and HAZ Patterns. Typical fusion and heat affected zone patterns through the longitudinal rail and weld center section are shown in Figure 44. The width of the fusion zone averages 1-3/4 inches at the bottom of the rail and increases to 2-1/2 inches at the top of the rail head. The heat affected zone is proportional to the fusion zone, and averages 3/4 inch, except at the rail base where it increases to 1-1/4 inches because of preheating. Figure 45 shows a comparable section of a thermit rail weld made with a 1 inch joint spacing and 5 minute preheat. The thermit fusion zone averages 1-7/16 inches over the length of the weld, and the heat affected zone ranges from 7/8 inch at the rail base to 1-1/4 inches at the head.³⁸

4.8.2. Form-factor. A longitudinal section at the center of the rail and weld are shown in Figure 46. The weld was made with E70S-3 filler metal, which enhances the solute dumping lines and more clearly demonstrates the form-factor produced by the final welding procedure. Even though solute bands are present in the alloy weld, they are not well defined for photographic purposes.

The solute dumping lines and darker regions of the weld metal in Figure 46 clearly show carbon concentrations that vary with the volume of rail steel dilution. As the slag bath enters the runout mold, the rail steel dilution is eliminated and the shading of the weld metal in area "A" is changed accordingly. The results of the vertical weld center hardness traverse ("A" from Figure 46) are shown in Figure 47, and the carbon analysis results from the same region of an identical weld are shown in Figure 48. Both hardness and carbon content peaks are located

at a distance equal to the weld pool depth below the rail base and head. The form-factor in Figure 46 is typical of ESRW and ranges from 5.45 at the top of the rail base to 2.33 at the rail head.

4.8.3. Hardness Data. Hardness traverse plots through the heat affected zone of the rail head (traverse B) and base (traverse C) are shown in Figure 49. The peak hardness in the heat affected zone of the ESRW is 33 HRC compared with 34 HRC in the typical thermit weld.³⁸ Weld metal hardness analysis are not included since the high heat input of ESRW makes the weld hardness more dependent upon electrode chemistry than welding procedure. Surface decarburization of the new rail steel used for this project was approximately 1/32 inch deep, which prevented valid Rockwell hardness data from the rail rolling surface. Detailed weld metal hardness and other mechanical property data from the weld and heat affected zone have been reported elsewhere.³³

The range of heat affected zone hardness for the ESRW was 22-33 HRC. A hardness traverse for a typical thermit weld is shown in Figure 50 and has a range of 22-34 HRC.³³ These values relate to the American Railway Engineering Association Specification (part 2, 1979) that requires a minimum Brinell Hardness of 248 (24 HRC).

4.8.4. Weld Quality. Transverse and longitudinal vertical sections of an ESRW made with ER90S-B3 alloy, including the runout, are shown in Figure 51. Conspicuous absence of voids or gross inclusions in either weld section exemplifies one of the major advantages of ESRW, and the pipe and very small slag inclusions present in the runout are completely

eliminated by removal of the runout during the normal welding procedure. The transverse thermit weld section in Figure 52 exhibits typical inclusion and porosity conditions. The uniform grain structure of the thermit weld is in sharp contrast to the directional and non-uniform microstructure of ESW. The weld metal deposition rate that produced this contrast also accounts for the difference in weld quality. The thermit weld metal is rapidly poured into the preheated mold and solidifies at an accelerating rate from all surfaces, causing entrapment of gases and other impurities. ESRW metal is deposited over a slowly solidifying vertical front, which allows time for gases and oxides to partition to the lighter slag, and finally the runout for removal during weld finishing.

Rapid deposition ESW plate welding studies have shown that high quality welds can be produced while decreasing weld time by as much as 60%.^{17,34} These studies have evaluated combinations of reduced joint spacing, use of modified plate guide tube or strip electrodes, and increased amperage and electrode feed rates. With exception of the strip electrode, variations of these methods were used with ESRW. Welding time was reduced to 14-1/2 minutes while retaining the high quality of the "weld metal". However, welds made in less than sixteen minutes resulted in heat affected zone hot cracking within 2 to 4 grain widths of the fusion boundary, Figure 53. Sulfur prints in Figure 22 show the sulfur concentration in a transverse rail section and a longitudinal section of a weld. Chemical analysis of these rail sections revealed compositions by weight percent of .73C, .043S, .033P, and .93Mn.

4.9. Repair Conditions

Prior to improvement of the electrode straightener and use of the modified insulator to aid guide tube positioning, undercut occurred at the top of the rail base in approximately 20% of the welds. In most cases, the undercut was limited to one area and was no more than 1/8 inch deep and 3/8 inch wide. The repair procedure in section 3.3 was developed to allow full-scale testing of these welds without unnecessary delay to other areas of ESRW development. An example of undercutting and the repair weld is shown in Figure 54. The shielded metal arc weld produced a pearlitic microstructure in the weld metal and merely refined the heat affected zone pearlite in both the rail steel and ESW, ER90S-B3 weld metal. The repair weld had Rockwell C hardness values of 20 in the weld metal, 29 in the rail steel HAZ and 28 in the ESRW steel heat affected zone. The repair procedure is easily performed and could foreseeably be applied to ESRW applications where rail conditions prohibit proper mold positioning or use on mis-matched rails.

5. CONCLUSIONS AND RECOMMENDATIONS

5.1. Conclusions

1. With the development of a multi-section copper mold assembly, a composite weld starting block, and a dual electrode plate guide tube, standard 136 pound per yard carbon steel railroad rail has been successfully welded utilizing the consumable guide electroslog process.
2. The size of the weld starting area has been significantly reduced by using a ceramic backed thin steel insert as a consumable portion of the starting block. The depth of the starting area was reduced further by locating the end of the plate guide tube $1/8$ to $1/4$ inch from the starting insert, which improved heat distribution during early slag bath formation.
3. Arc initiation dependability for the dual electrode system has been significantly improved by providing a $3/4$ to 1 inch electrode wire stickout for each electrode and delay of initiation for the second electrode. The second electrode thus enters a partially formed slag bath at a lower velocity than it would during a simultaneous start.
4. A plate guide tube can be used to improve heat distribution over the slag bath. Where required, it may be designed to increase or reduce thermal concentrations in specific regions of a weld. A major requirement for effective use of the guide tube in this manner is to provide a sufficient guide tube volume to maintain contact with the slag bath surface.

5.2. Recommendations

It is anticipated that prior to service implementation of ESRW, the following investigations and improvements will be made.

1. The starting insert and insulation geometry will be improved and formed as a single part or as a trough with separate end pieces.
2. The guide tube design will be simplified for fabrication purposes and to improve welding power stability.
3. The guide tube clamping fixture on the electrode feeder will be designed to allow rapid positioning of the guide tube after preheating the rail ends and starting block.
4. Use of solid copper side shoes rather than the water cooled design should be investigated to improve process portability.
5. Use of a single thin strip electrode rather than the dual wire electrode should be investigated. It is anticipated that a single strip electrode would improve heat distribution, weld starting, and simplicity of the guide tube design. In addition, a single weld length electrode role, along with a premeasured flux packet and guide tube, could be provided more easily for each weld.
6. Use of constant current welding power sources should be investigated. This system would vary the electrode (wire or strip) feed rate while maintaining a constant current and varying voltage for a more precise control of weld deposition and regional heating. This system may also be more compatible with automatic controls.
7. In the event that the constant current power source does not perform as expected, a sensing system or programmed control should be developed for use with the more sensitive constant voltage power sources in present use.

8. By using engine driven generators for welding power sources, ESRW can be applied as a portable welding process. Two generators rated at 700 amperes and 100% duty cycle would provide adequate welding power for the process as it is presently designed.

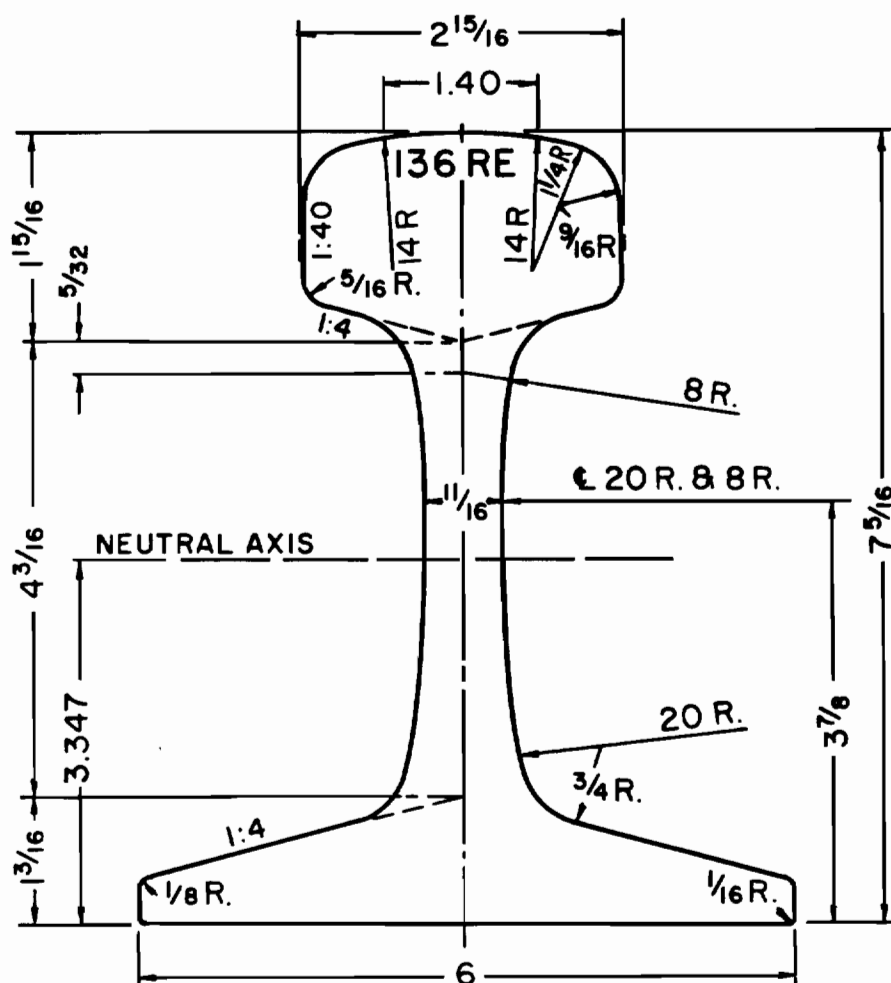
REFERENCES

1. D. Hauser, "Methods for Joining of Rails: Survey Report", Battelle-Columbus Laboratories, December 1975.
2. D. H. Stone and R. K. Steele, "The Effect of Mechanical Properties Upon the Performance of Railroad Rails", Rail Steels--Developments, Processing and Use, ed. by D. H. Stone and G. G. Knupp, ASTM, 1978, p. 21.
3. AREA Manual, American Railway Engineering Association, Chicago, IL, Chapter 4, pp. 4-2-6.7 through 4-2-6.9.
4. M. J. Vines, "The Flash Butt Welding of High Strength Rail", Heavy Haul Railway Conference Proceedings, 18-22, September 1978, Session 411, Paper H.6.
5. H. Oishibashi, "Rail Welding Methods", Quarterly Reports, RTRI, V. 15, No. 2, 1974, p. 69.
6. R. F. Beck, "U.S.-U.S.S.R. Track and Rail Metallurgy Information Exchange", U.S. Department of Transportation, 1977, FRA/ORD-77/19.
7. J. A. N. Clevers and J. W. A. Stemerding, "Enclosed Welding of Vertical Grooves", Welding Journal, March 1960, pp. 223-228.
8. L. N. Kopetman and K. H. Mukanaev, "Electroslag Welding of Crane Rail", Svar. Proiz., No. 5, 1967, pp. 32-34.
9. V. I. Svetlopolyanskii, "The Semi-Automatic ESW of Rails", Avt. Svarka, No. 3, 1966, p. 53.
10. N. E. Govozhaninov, "The Bath Welding of Crane Rail", Svar. Proizv., 1965, No. 9, p. 35.
11. E. Sudasch, "Welding Design & Fabrication", Sept. 1971, Vol. 44, 9, pp. 58-60.
12. B. D. Lawrence, "Electroslag Welding Curved and Tapered Cross-Sections", Welding Journal, April 1973, pp. 240-246.
13. K. E. Dorsch, J. E. Norcross, and C. C. Gage, Welding Journal, Nov. 1973, Vol. 52, 11, pp. 710-716.
14. Welding Handbook, AWS, Vol. 2, 7th ed., 1978, pp. 225-247.
15. R. R. Irving, "Electroslag Welds Face New Challenge", Iron Age, April 26, 1973, pp. 66-67.

16. J. D. Culp, "Electroslag Weldments: Performance and Needed Research", Michigan Department of State Highways & Transportation, Lansing, MI, Sept. 1977.
17. Srivathsan Venkataraman, "Effect of Process Variables and Microstructure on the Properties of Electroslag Weldments", Ph.D. Dissertation, Oregon Graduate Center, Beaverton, OR, 1981.
18. Hobart Technical Center, "Porta-Slag Welding", Hobart Brothers Co., Troy, OH, 1970.
19. J. E. Jones, D. L. Olson and G. P. Martins, "Metallurgical and Thermal Characteristics of Non-Vertical Electroslag Welds", Welding Journal, September 1980, Vol. 59, 9, p. 245-s.
20. M. Solari and H. Biloni, "The Effect of Wire Feed Speed on the Structure in Electroslag Welding of Low Carbon Steel", Welding Journal, September 1977, Vol. 56, 9, p. 274-s.
21. R. H. Frost, G. R. Edwards, and M. D. Rheinlander, "A Constitutive Equation for the Critical Energy Input During Electroslag Welding", Welding Journal, January 1981, Vol. 60, 1, p. 1-s.
22. A. L. Liby and D. L. Olson, "Metallurgical Aspects of Electroslag Welding in Review", Quarterly of the Colorado School of Mines, 1974, 1.
23. B. E. Paton, "Electroslag Welding", 2nd ed., AWS, New York, NY, 1962.
24. E. E. Banks and J. Ritchie, "Australian Welding Journal, Jan/Feb 1975, p. 7.
25. K. E. Dorsch, J. E. Norcross and C. C. Gage, "Unusual Electroslag Welding Applications", Welding Journal, November 1973, Vol. 52, 11, p. 710.
26. T. Debroy, J. Szekely and T. W. Eager, "Heat Generation Patterns and Temperature Profiles in ESW", Massachusetts Institute of Technology, Cambridge, MA, March 1978.
27. G. I. Estratov, Welding Prod., 1979, 6, p. 43.
28. M. V. Nolan, Founding, Welding, Production Eng. J., April 1970, p. 14.
29. L. P. Eregin, "Calculation of the Parameters of the Shape of Penetration in Electroslag Welding with a Consumable Guide", Svar. Proiv., 1974, No. 4, pp. 27-29.

30. B. M. Patchett, "Vertical Welding Efficiently with the Consumable Guide Electroslag Process", SME Tech. Paper, Dearborn, MI, 1974, pp. 1-14.
31. A. H. Dilawari, T. W. Eager, and J. Szekely, "An Analysis of Heat and Fluid Flow Phenomena in Electroslag Welding", Welding Journal, 1978, Vol. 57, 1, p. 24-s.
32. K. Watanabe, I. Sejima, S. Kokura, G. Taki and H. Miyake, "Advanced Welding Technology, Tokyo, Japan Welding Society, 1975, p. 513.
33. Y. Asai and U. Nakamura, "Electroslag Welding of Steel Slabs with Plate Electrodes", Proceedings 2nd International Symposium of Japan Welding Society, Osaka, 25-27 August 1975, Vol. II, Paper 2-4-(5), pp. 525-530.
34. Y. Ito, "Narrow Gap Electro-slag Welding Process", 2nd International Symposium of the Japan Welding Society, Osaka, 25-27 August 1975.
35. G. L. Kehl, "Metallographic Laboratory Practice", 3rd ed., McGraw-Hill, New York, NY, 1949.
36. H. C. Campbell, Welding Research Council Bulletin No. 154, September 1970.
37. M. Scholl, "Alloying of Electroslag Welded Railroad Rail", Masters Thesis, Oregon Graduate Center, Beaverton, OR, 1982.
38. G. H. Geiger, "Metallurgical Evaluation of Thermit-type Railroad Rail Welds", University of Arizona, 1979.
39. G. E. Linnert, Welding Metallurgy, Vol. 2, 3rd ed., AWS, New York, NY.

F I G U R E S



	Area Sq In	Percent
Head	4.86	36.4
Web	3.62	27.1
Base	4.87	36.5
TOTAL	13.35	100.0

Calculated weight, lb per yd.--136.2

Figure 1. AMERICAN RAILWAY ENGINEERING ASSOCIATION RECOMMENDED RAIL SECTION DIMENSIONS FOR 136 POUND PER YARD RAIL (1971).

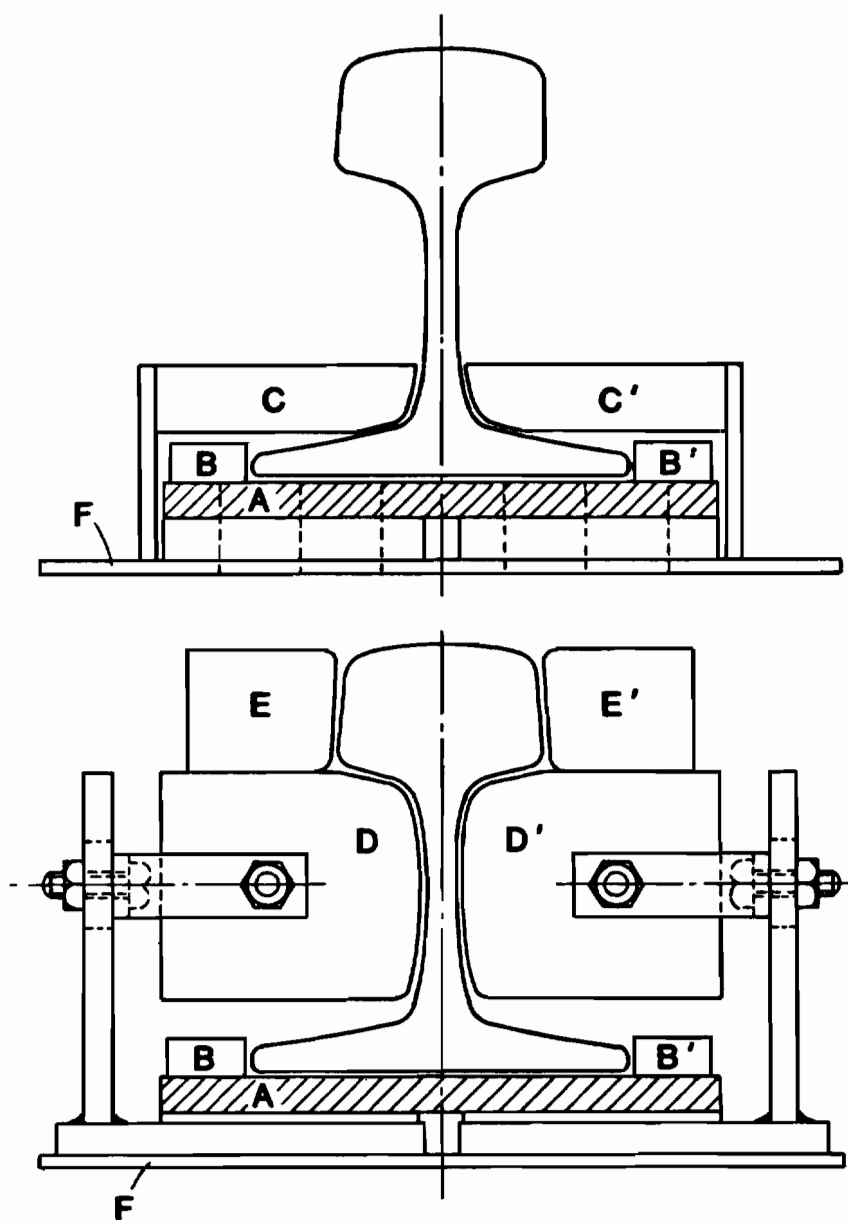


Figure 3. ENCLOSED ARC WELDING ENCLOSURE BLOCK ASSEMBLY.

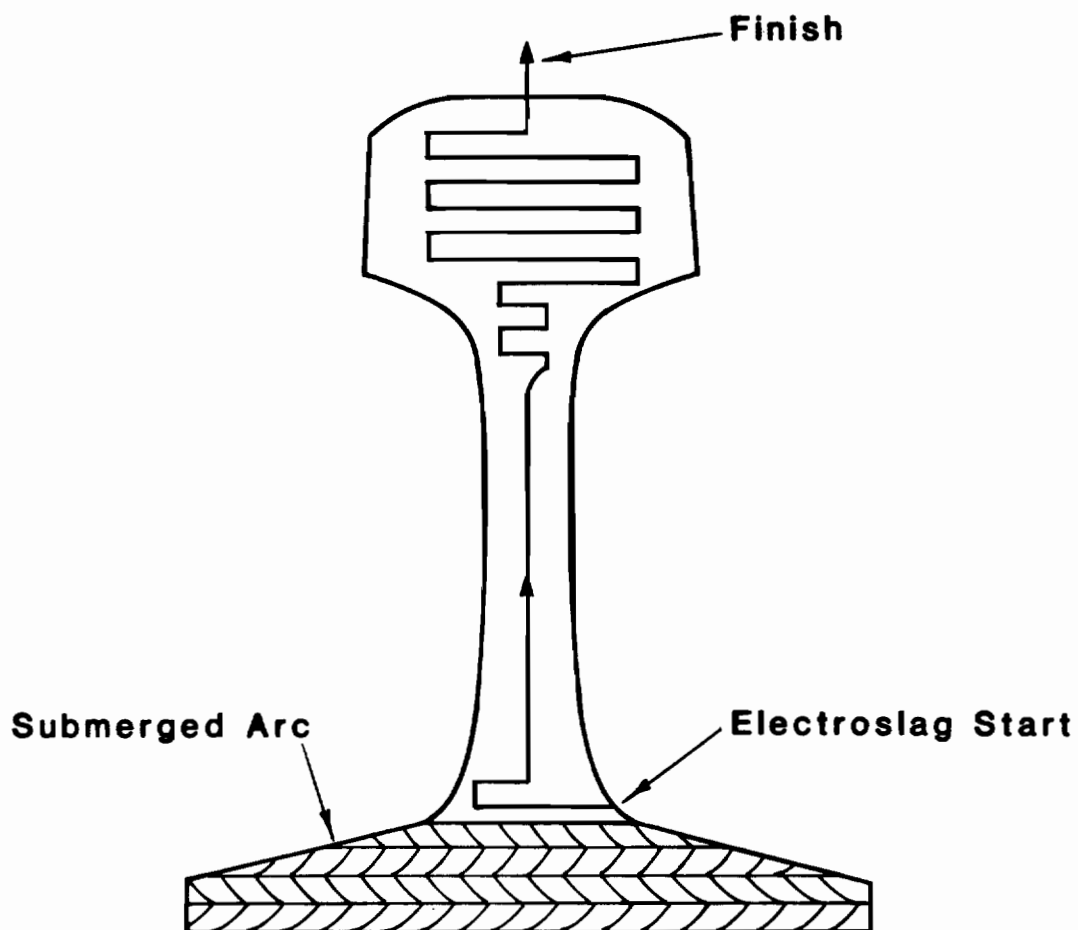


Figure 4. SUBMERGED-SLAG RAIL WELDING SEQUENCE.

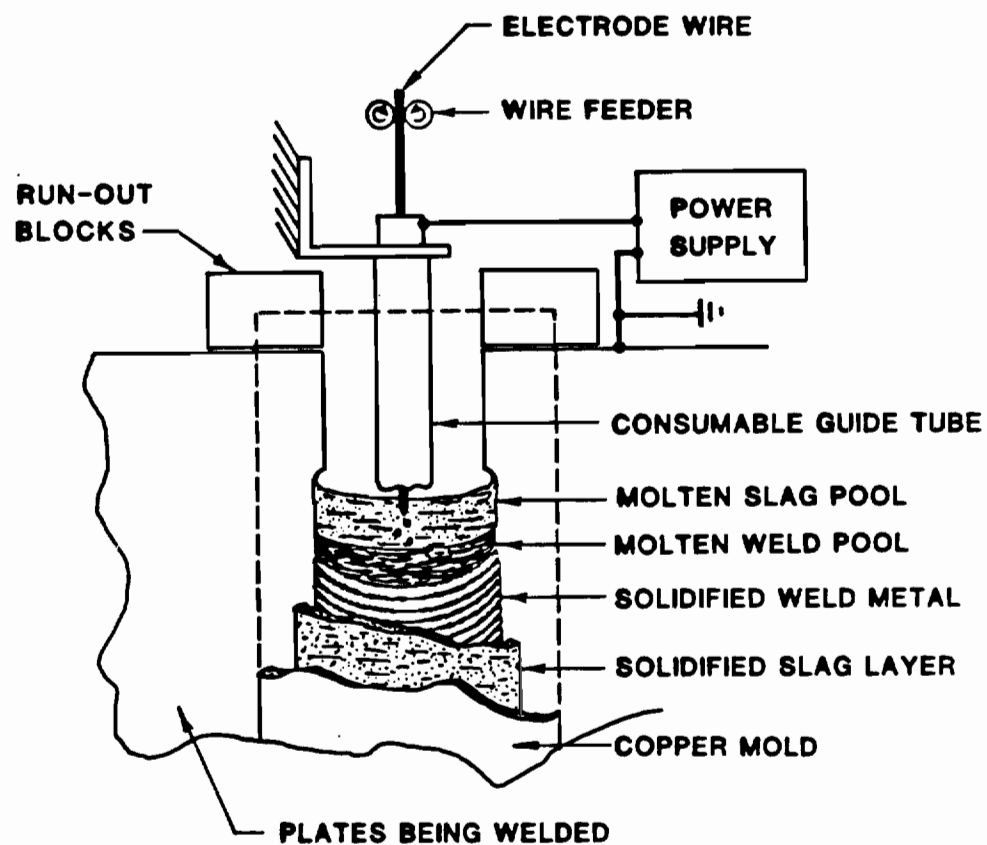


Figure 5. SCHEMATIC REPRESENTATION OF CONSUMABLE GUIDE ELECTROSLAG WELDING.

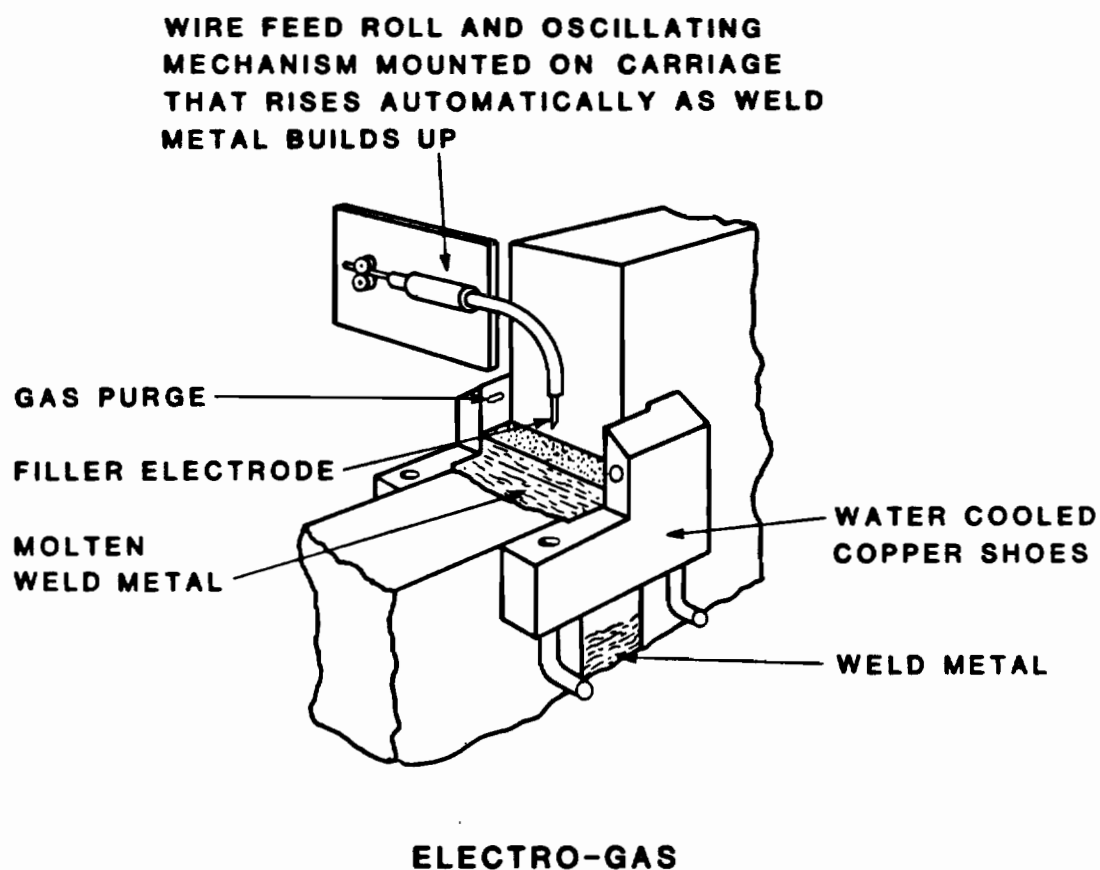


Figure 6. SCHEMATIC REPRESENTATION OF CONVENTIONAL ELECTROSLAG WELDING.

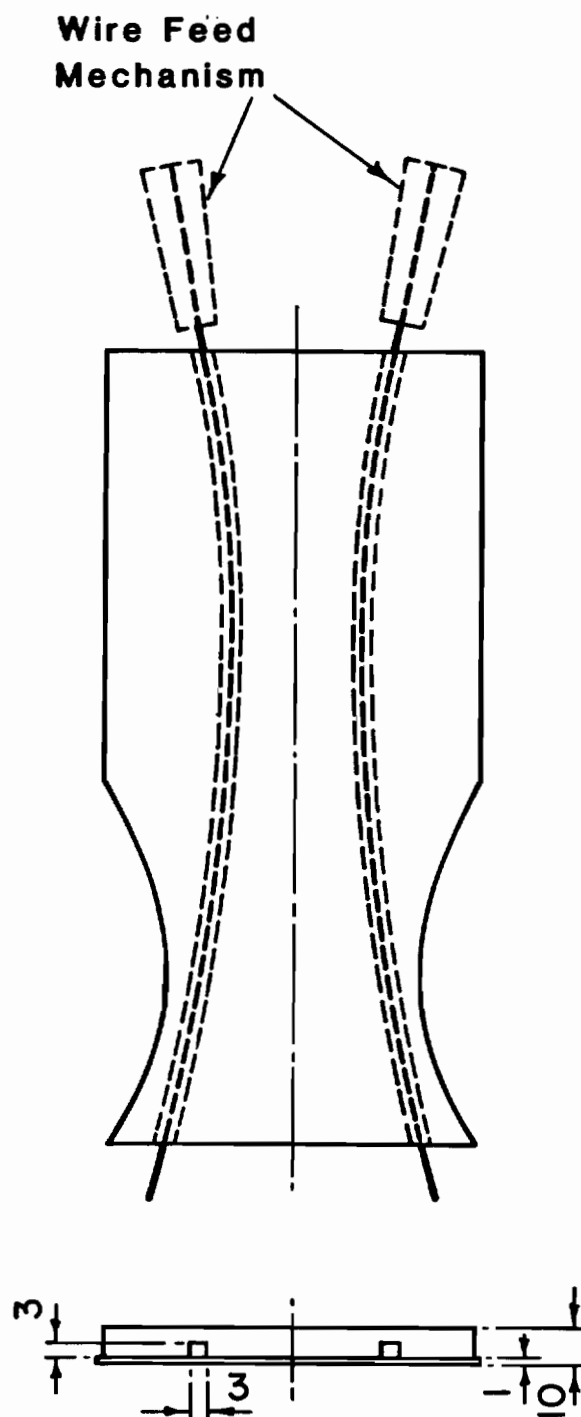


Figure 7. CONSUMABLE GUIDE PLATE ELECTRODE USED BY V. I. SVETLOPOLYANSKII FOR WELDING TYPE R43 TRAM RAIL.

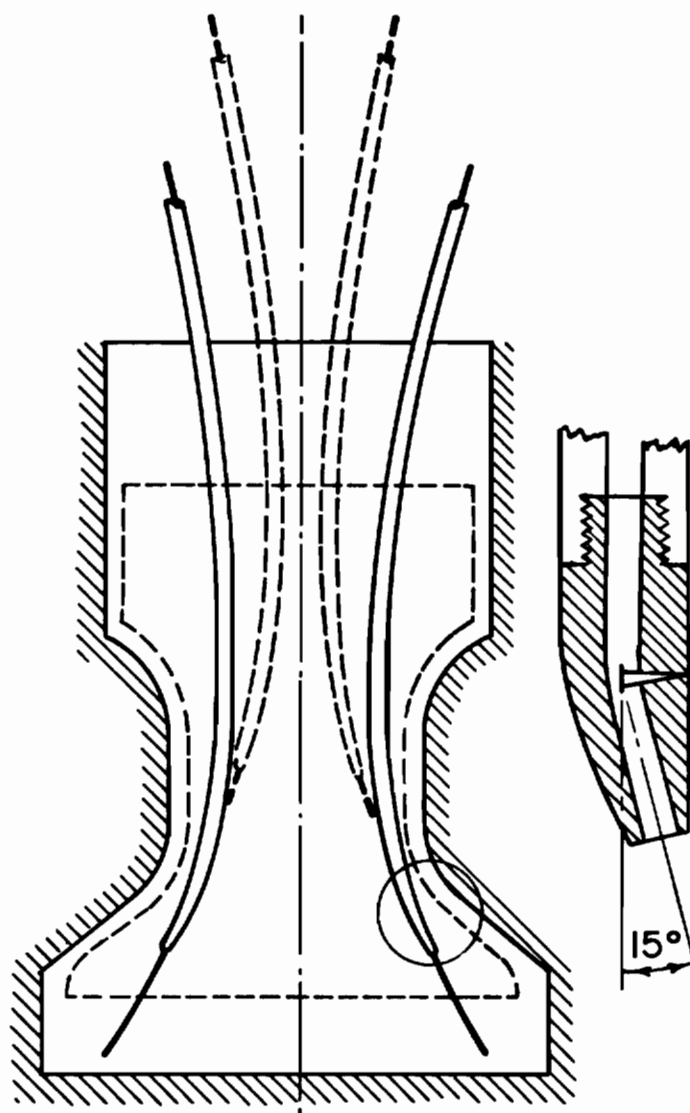


Figure 8. ELECTRODE MOVEMENT PATTERN USED BY KOPETMAN AND MUKANAEV IN CONVENTIONAL ELECTROSLAG WELDING OF CRANE RAIL.

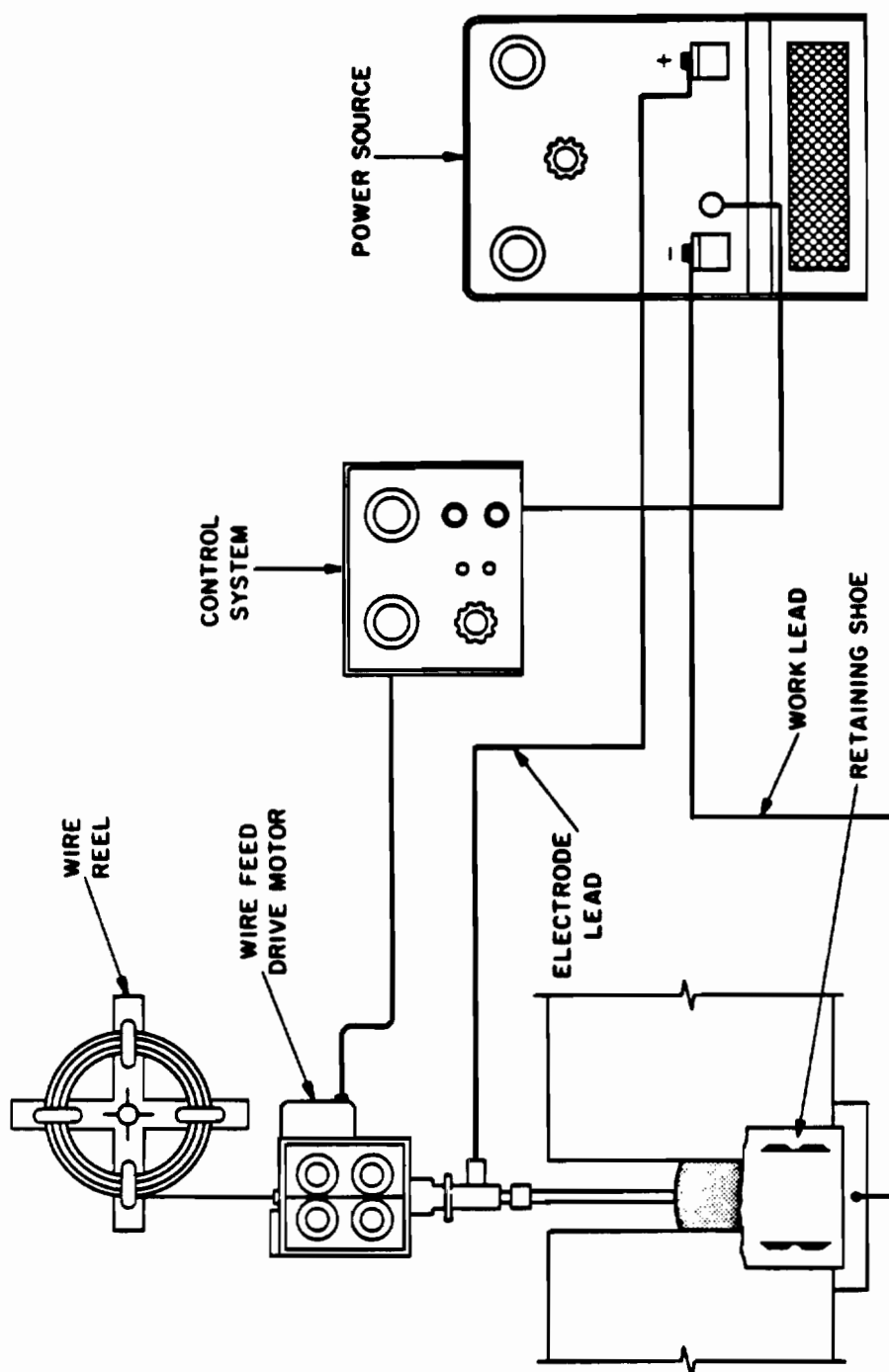
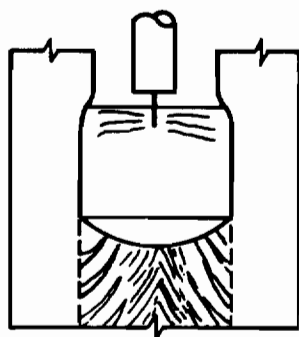
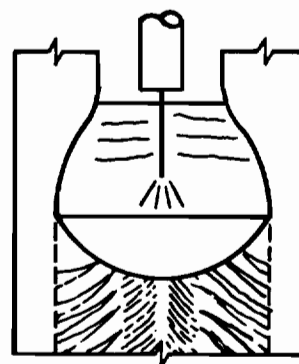


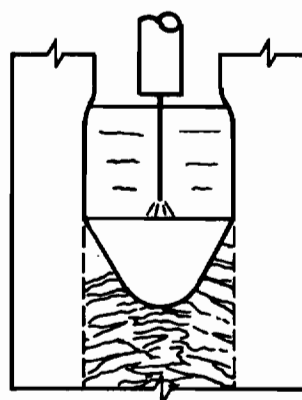
Figure 9. SCHEMATIC REPRESENTATION OF THE CONSUMABLE GUIDE ELECTROSLAG WELDING PROCESS EQUIPMENT.



**High Voltage
Low Current**

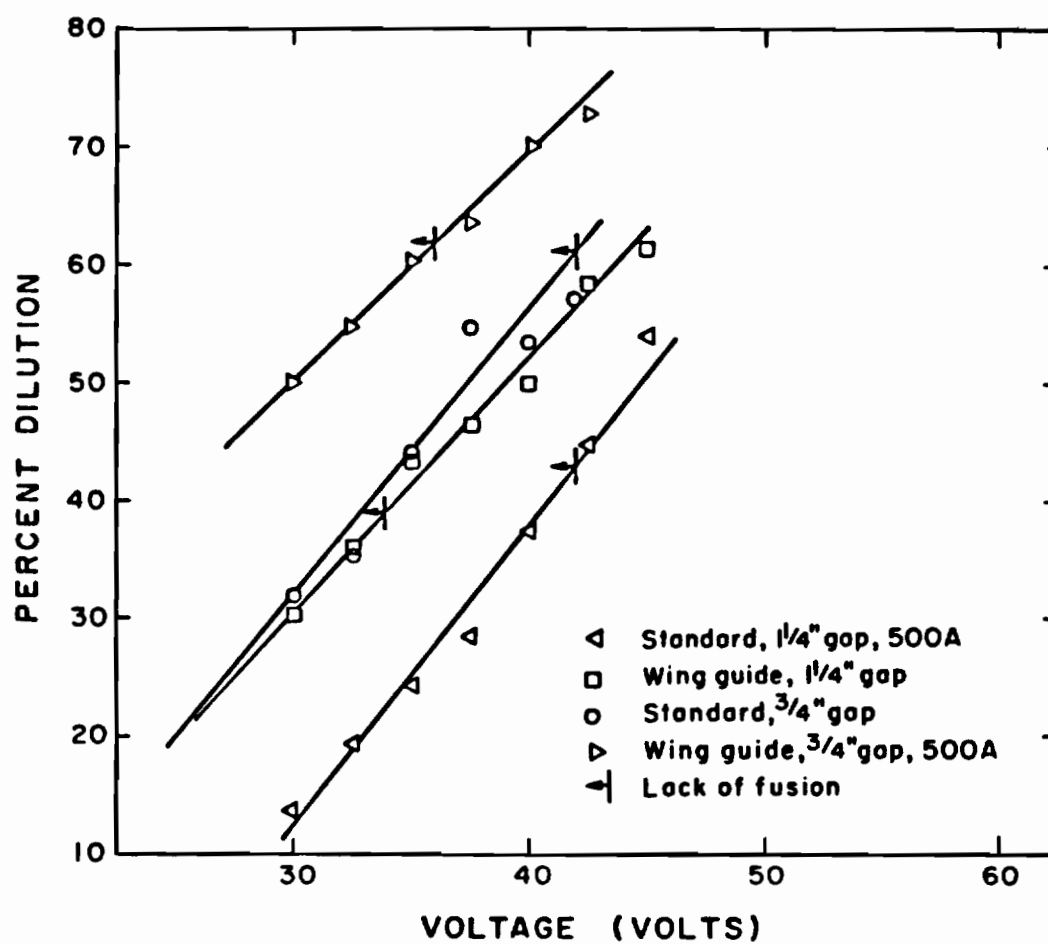


**Moderate Voltage
Moderate Current**



**Low Voltage
High Current**

Figure 10. SLAG BATH CURRENT PATH VARIATIONS.



Relation between voltage and base metal dilution

Figure 11. VOLTAGE AND BASE METAL DILUTION RELATIONSHIP.

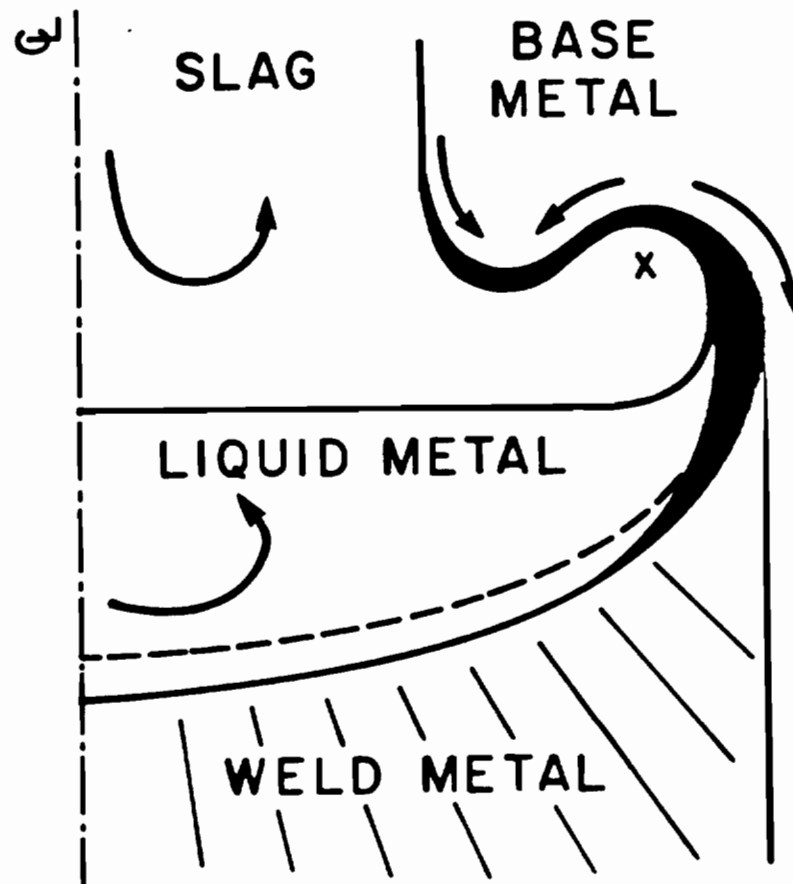


Figure 12. HIGH VOLTAGE PENETRATION PATTERN THAT RESULTS IN SLAG ENTRAPMENT AS VOLTAGE FLUCTUATES, PROPOSED BY SOLARI, ET AL.

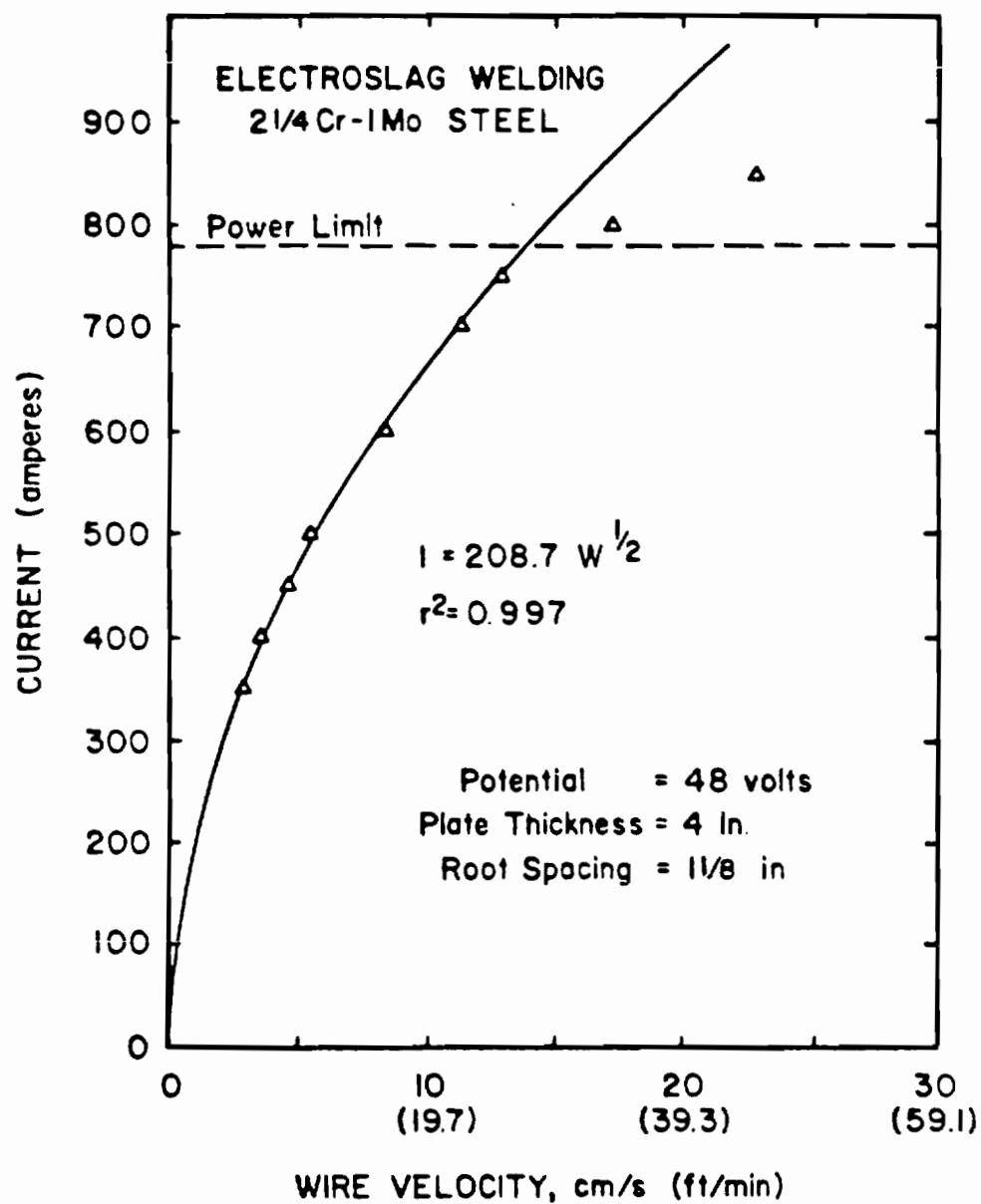


Figure 13. EXPERIMENTALLY DETERMINED PARABOLIC RELATIONSHIP BETWEEN WELDING CURRENT AND ELECTRODE VELOCITY.

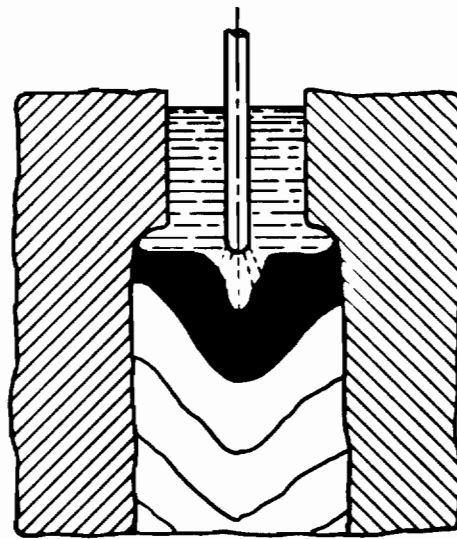
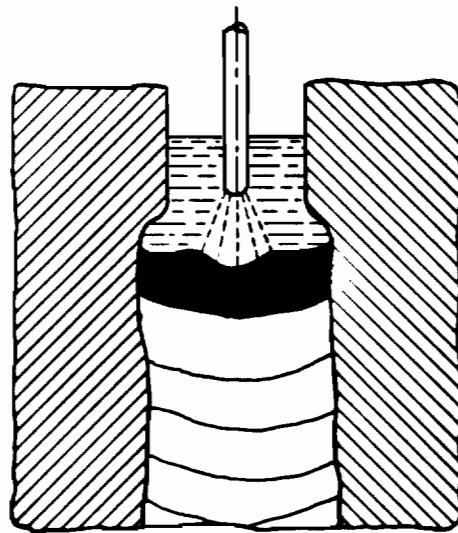
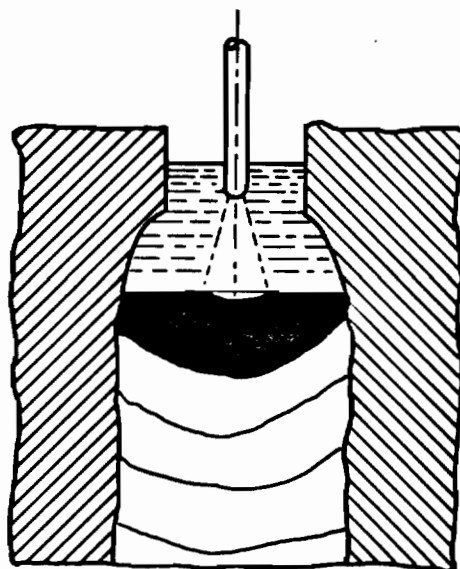
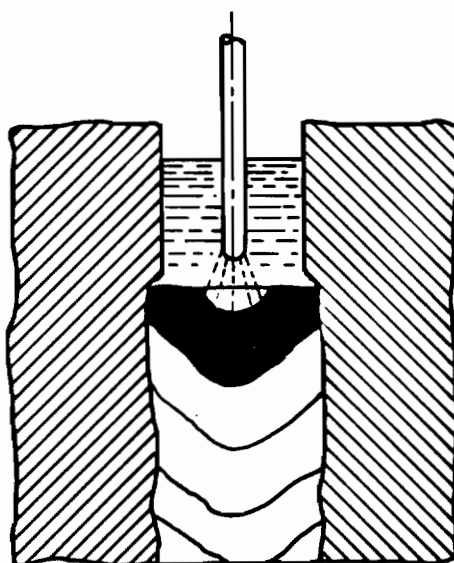
**HIGH CURRENT****LOW CURRENT**

Figure 14. EFFECT OF CURRENT ON THE WELD POOL GEOMETRY.

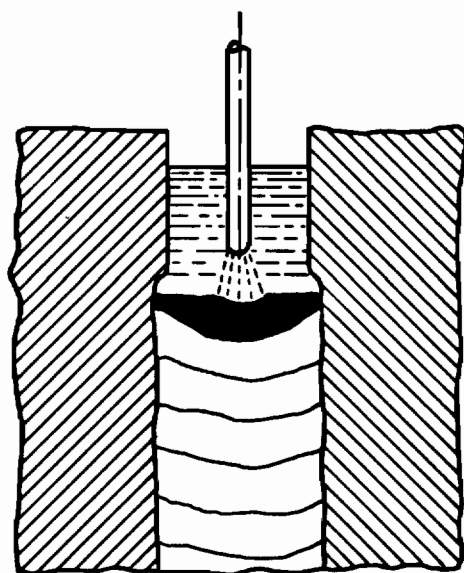


HIGH VOLTAGE

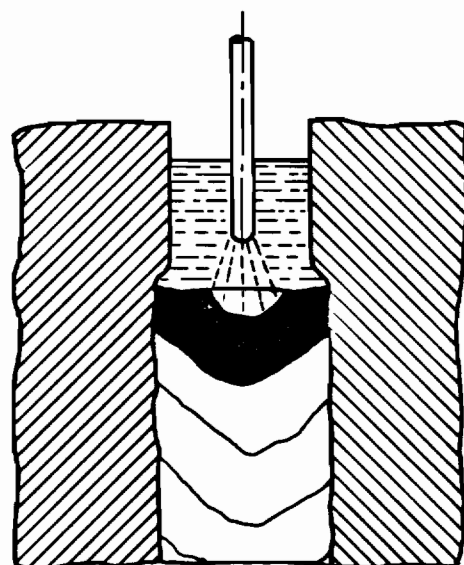


LOW VOLTAGE

Figure 15. EFFECT OF VOLTAGE ON THE WELD POOL GEOMETRY.

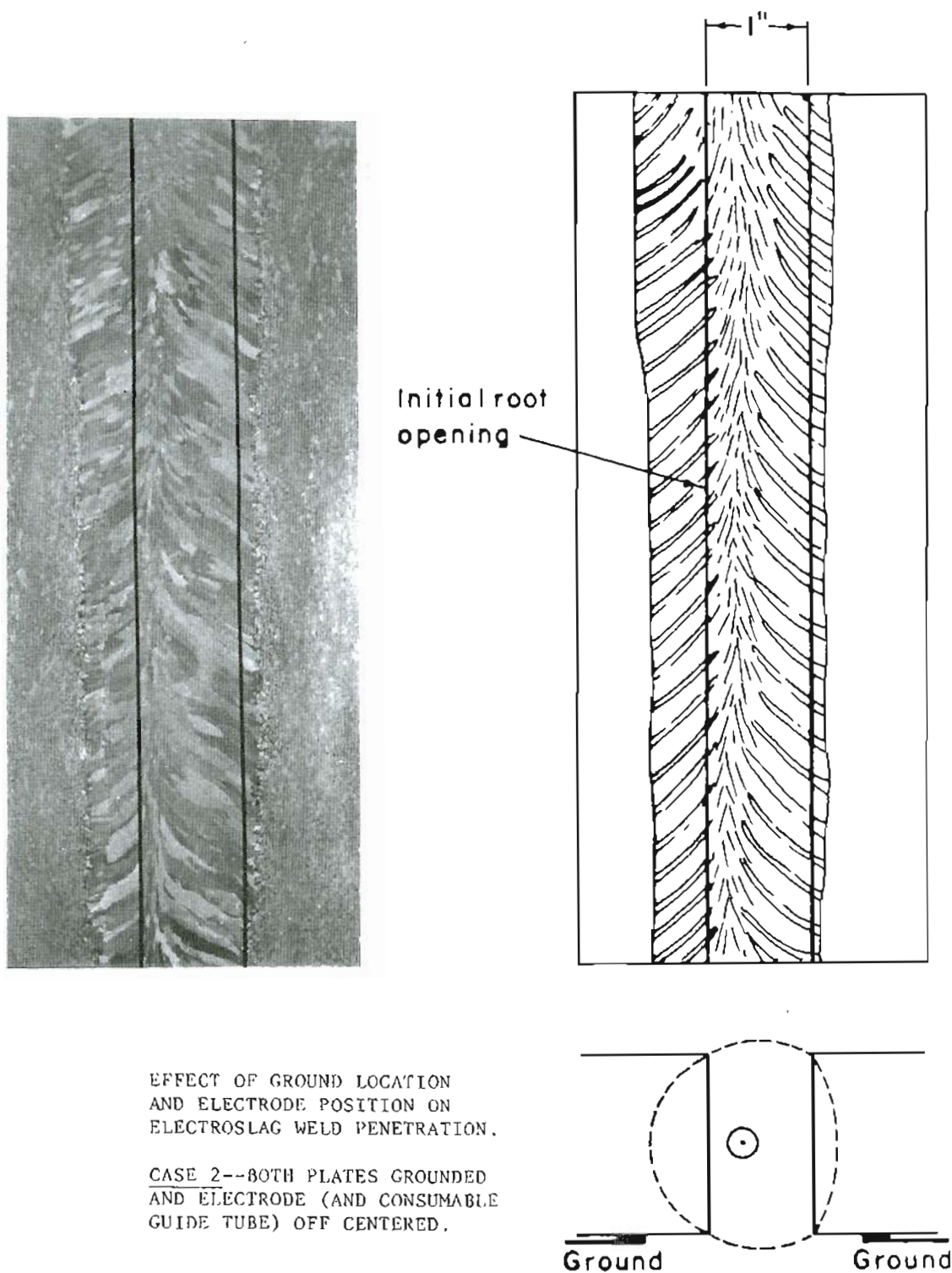


LOW RESISTANCE



HIGH RESISTANCE

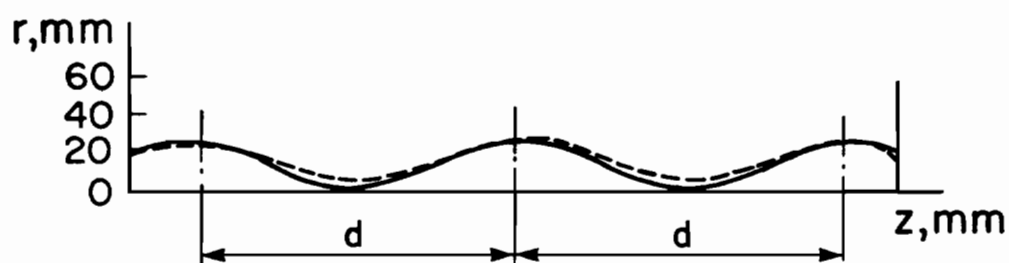
Figure 16. EFFECT OF THE SLAG BATH ELECTRICAL CONDUCTIVITY ON THE WELD POOL.



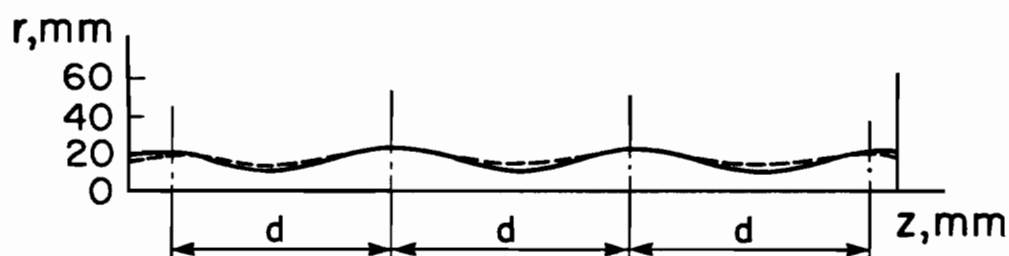
EFFECT OF GROUND LOCATION
AND ELECTRODE POSITION ON
ELECTROSLAG WELD PENETRATION.

CASE 2--BOTH PLATES GROUNDED
AND ELECTRODE (AND CONSUMABLE
GUIDE TUBE) OFF CENTERED.

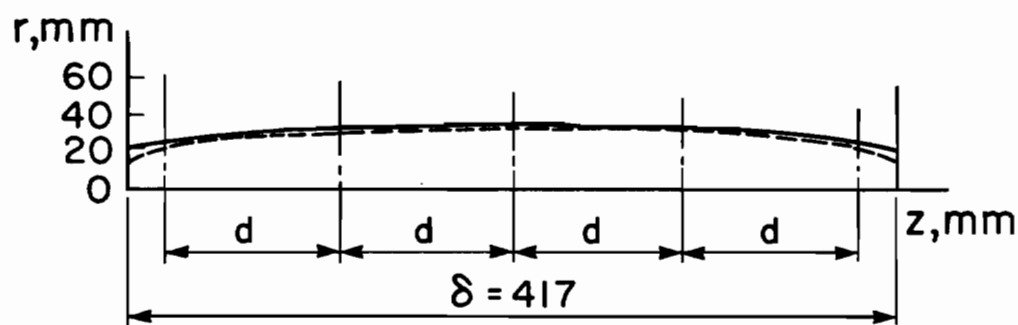
Figure 17. EFFECT OF GROUND LOCATION AND ELECTRODE POSITION ON ELECTROSLAG WELD PENETRATION.



(a)

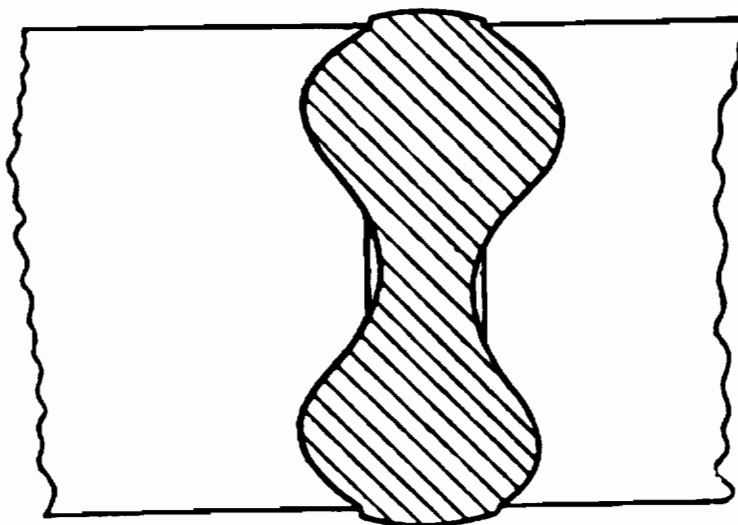


(b)

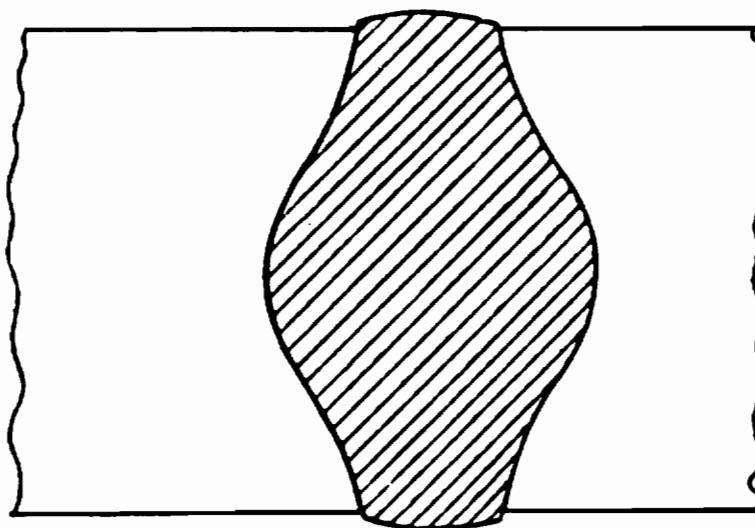


(c)

Figure 18. CALCULATED AND ACTUAL PENETRATION SHAPES WITH VARIATIONS IN GUIDE TUBE ARRANGEMENT BY L. P. EREGIN.



**EXCESSIVE SPACING
BETWEEN THE ELECTRODES**



**ELECTRODES SPACED
TOO NEAR THE CENTER**

Figure 19. EXTREME CONDITIONS RESULTING FROM ELECTRODE WIRE SPACING VARIATIONS IN A TWO ELECTRODE SYSTEM.

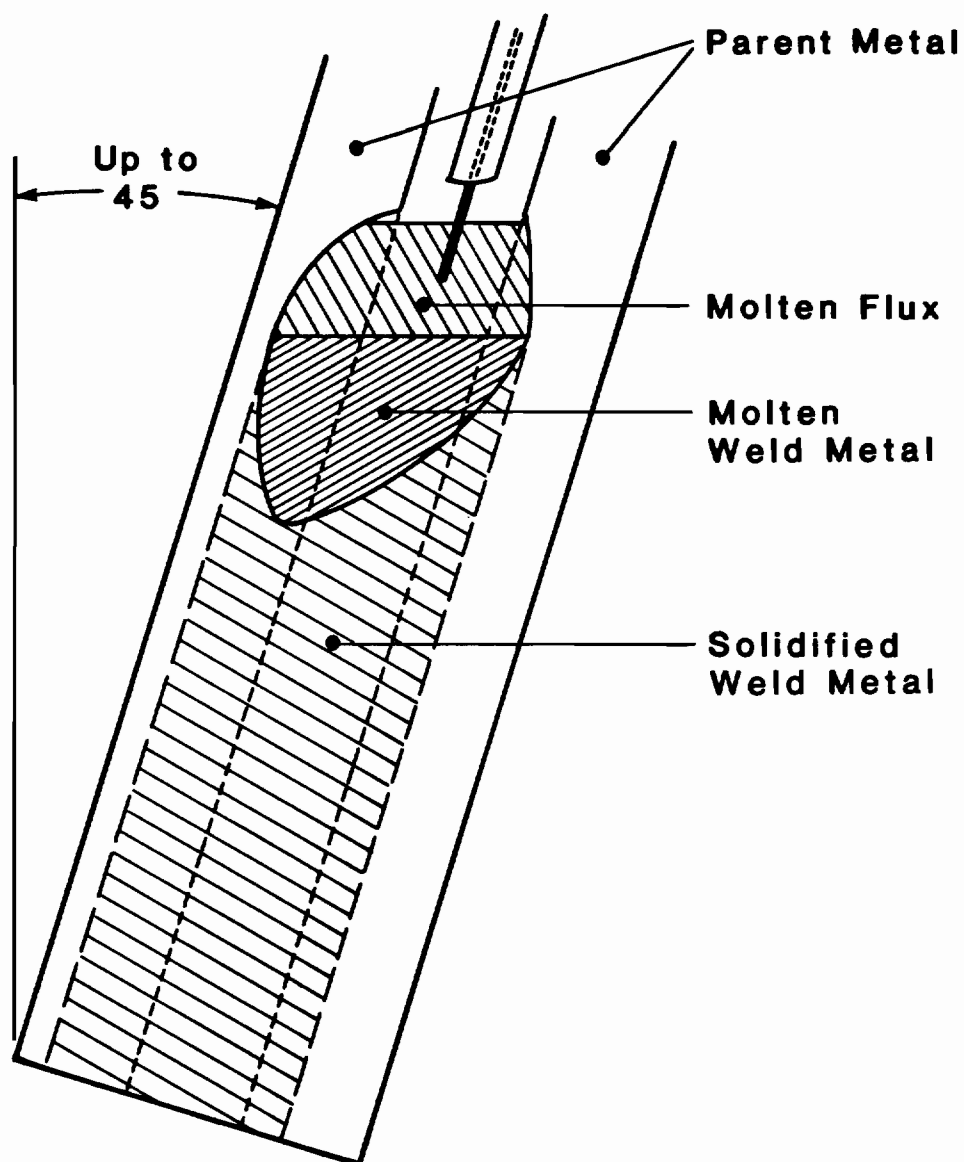


Figure 20. EFFECT OF NON-VERTICAL ELECTROSLAG WELDING ON WELD POOL SHAPE BY JONES, ET AL.

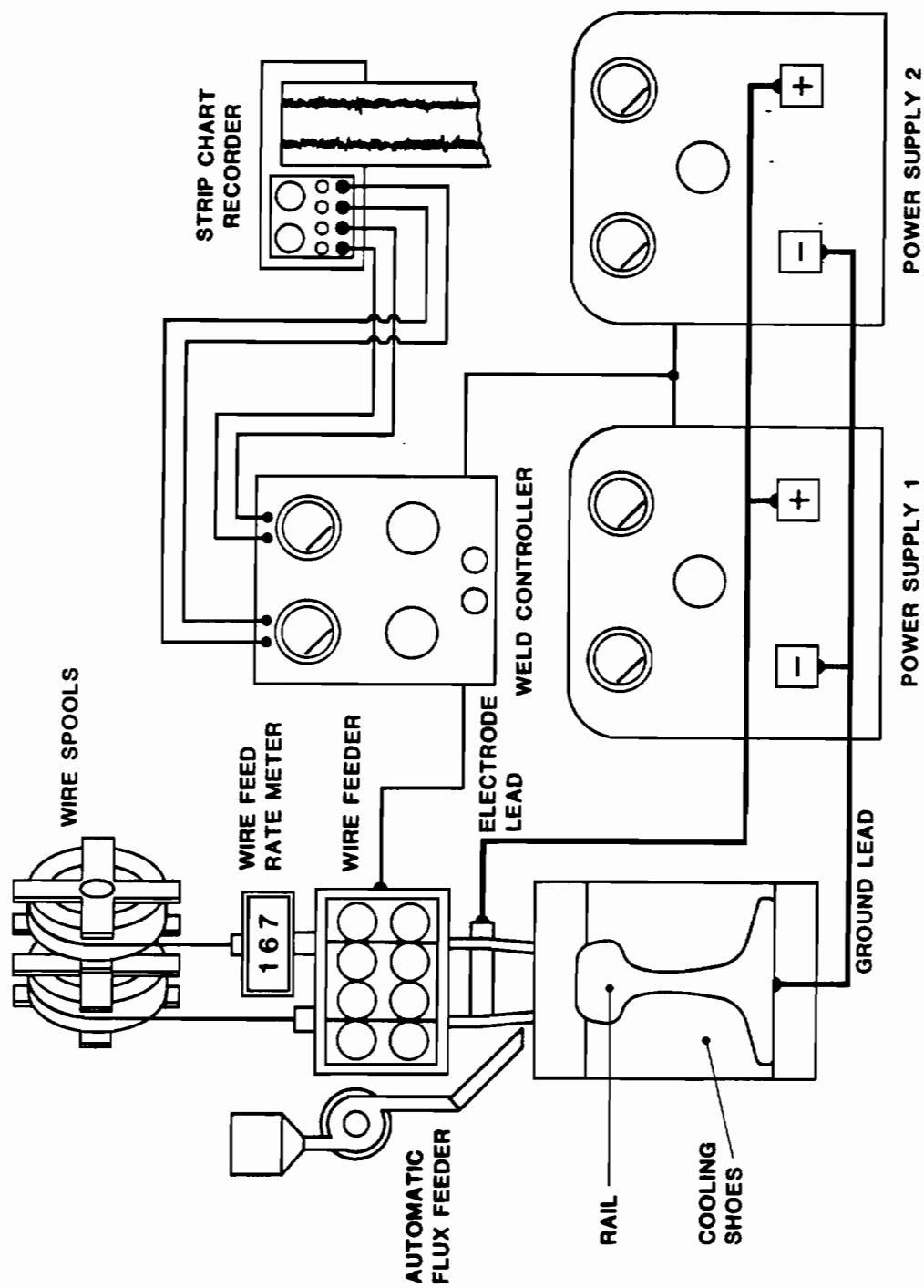


Figure 21. SCHEMATIC ILLUSTRATION OF THE CONSUMABLE GUIDE ELECTROSLAG WELDING SYSTEM USED IN THIS INVESTIGATION.

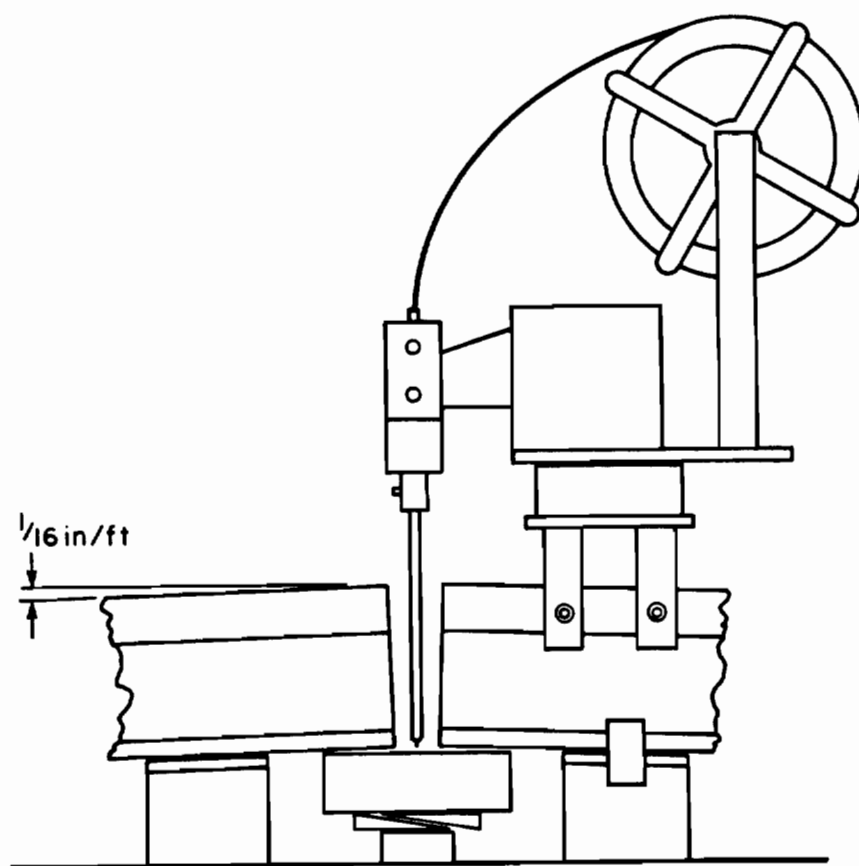


Figure 22. SCHEMATIC ILLUSTRATION OF THE ELECTRODE FEEDER AND RAIL POSITIONING.

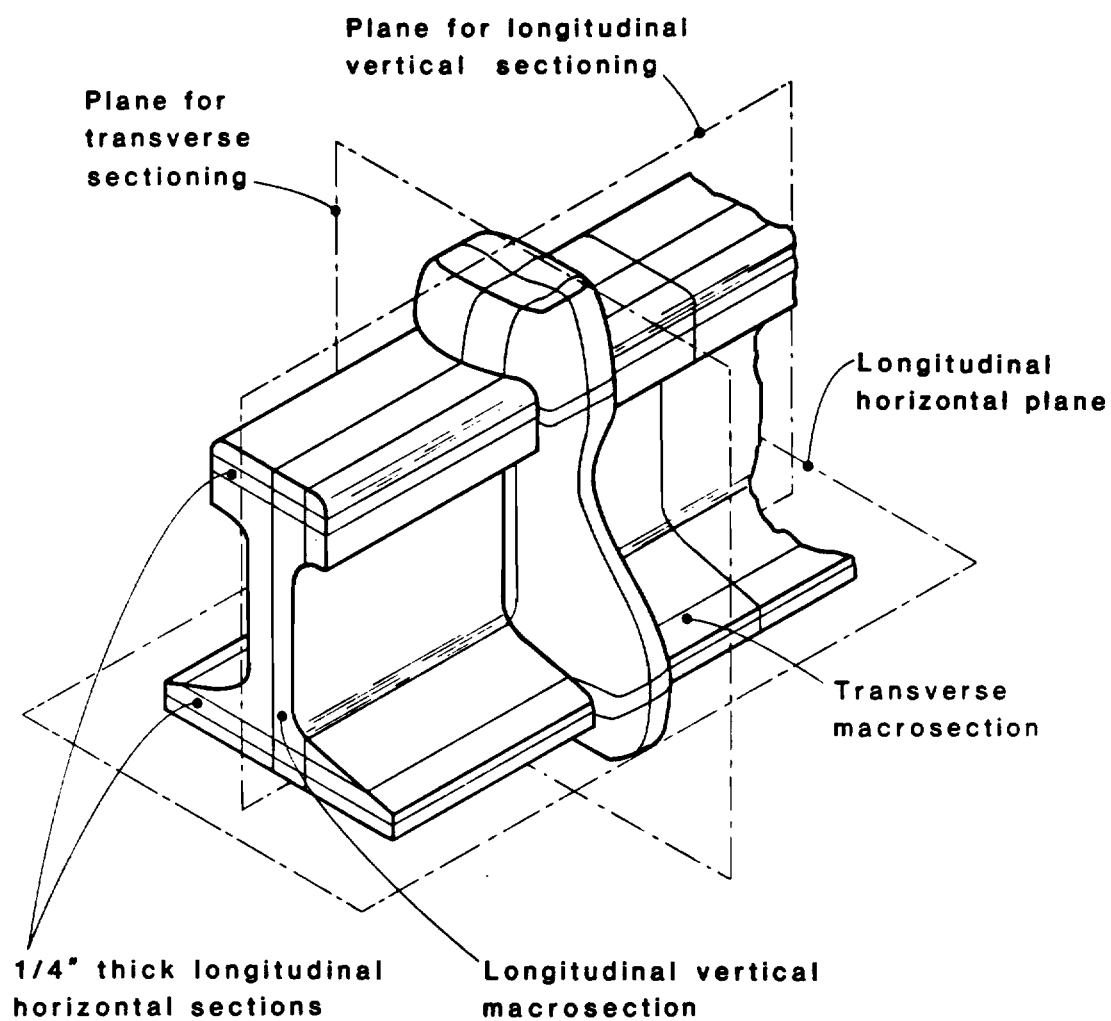


Figure 23. MACROSECTIONING DIAGRAM FOR RAIL WELDS.

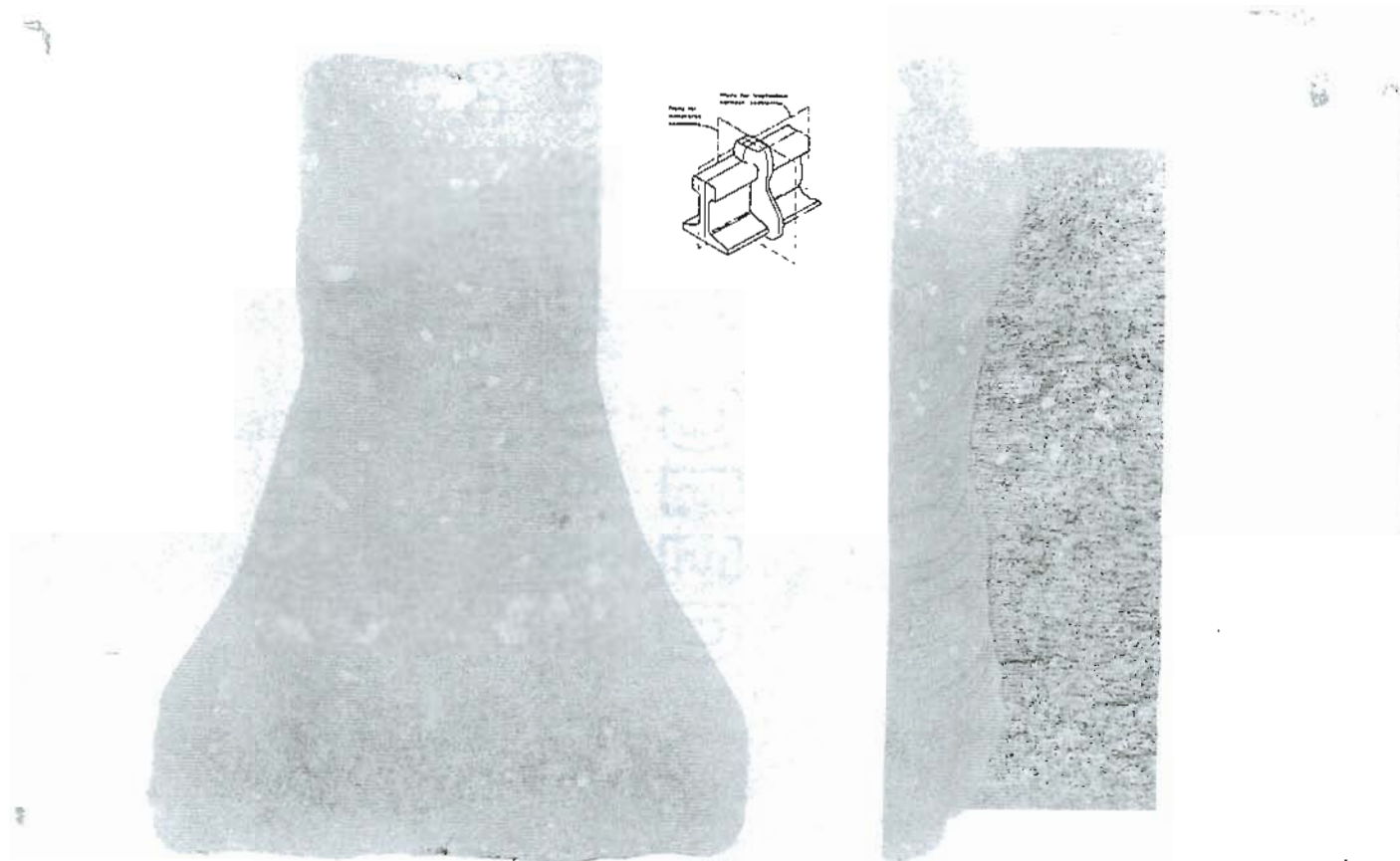


Figure 24. SULFUR PRINT OF TRANSVERSE AND LONGITUDINAL ESRW SECTIONS.

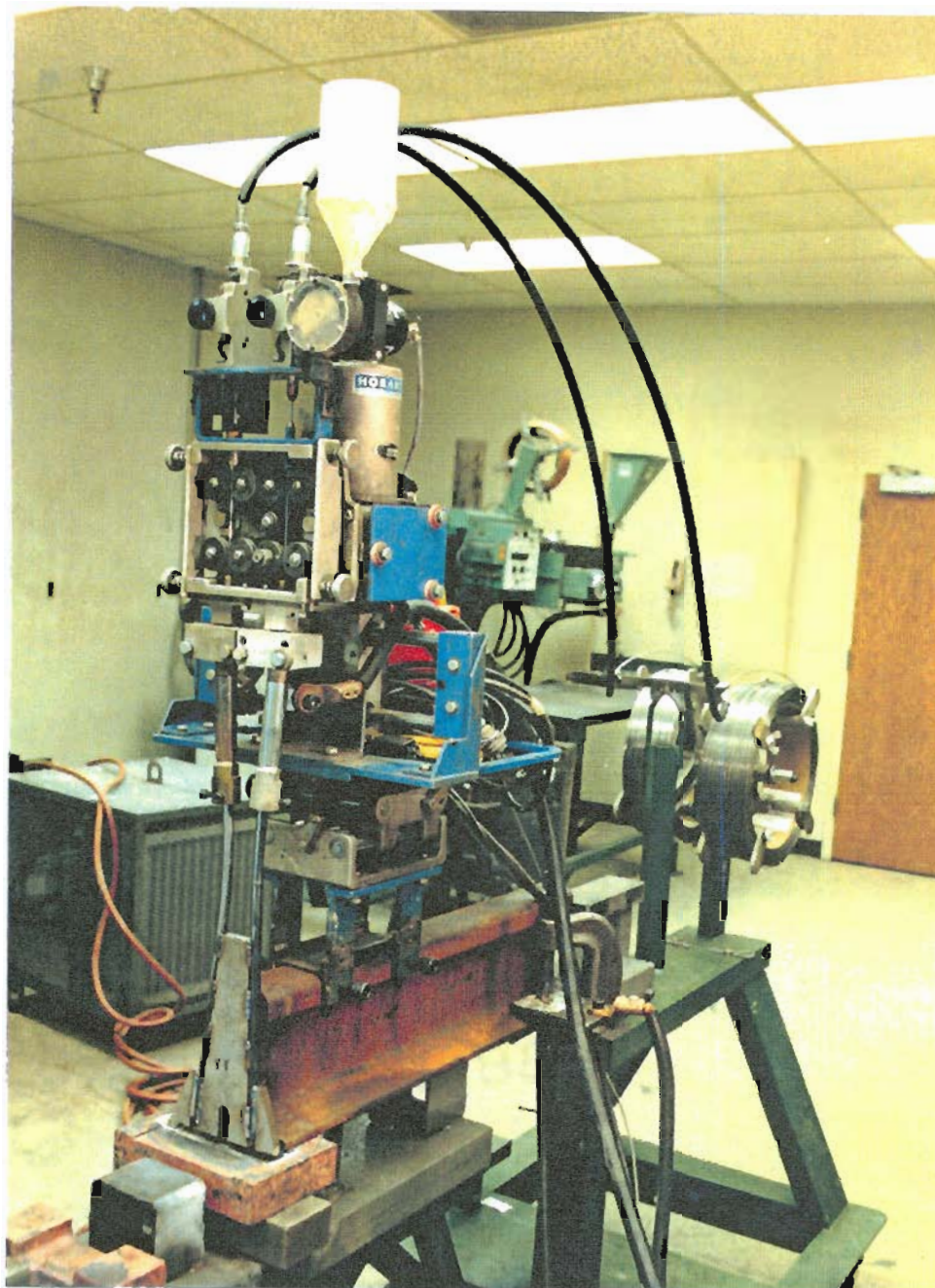


Figure 25. X-Y ELECTRODE POSITIONERS WITH THE ELECTRODE FEEDER, CONDUIT, AND ELECTRODE SPOOLS.

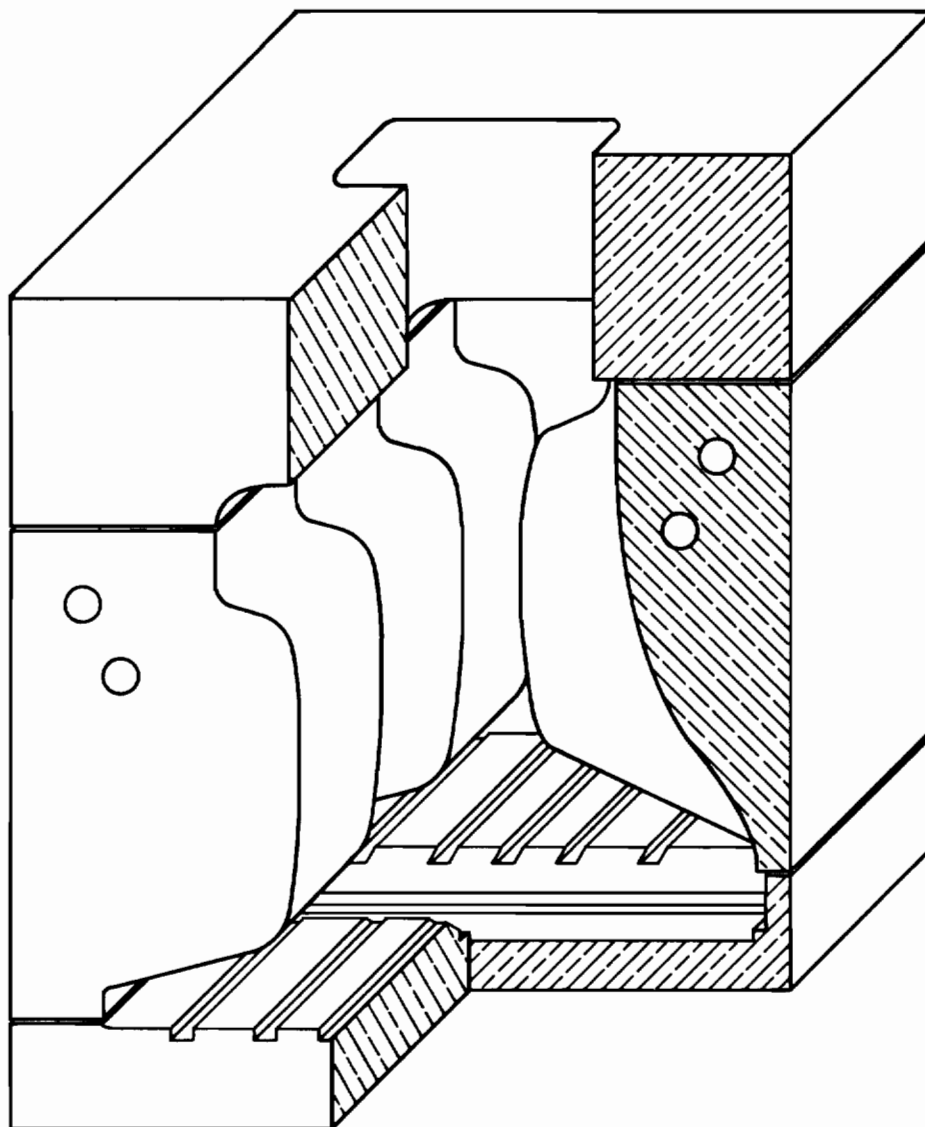


Figure 26. SCHEMATIC OF MOLD COMPONENTS.

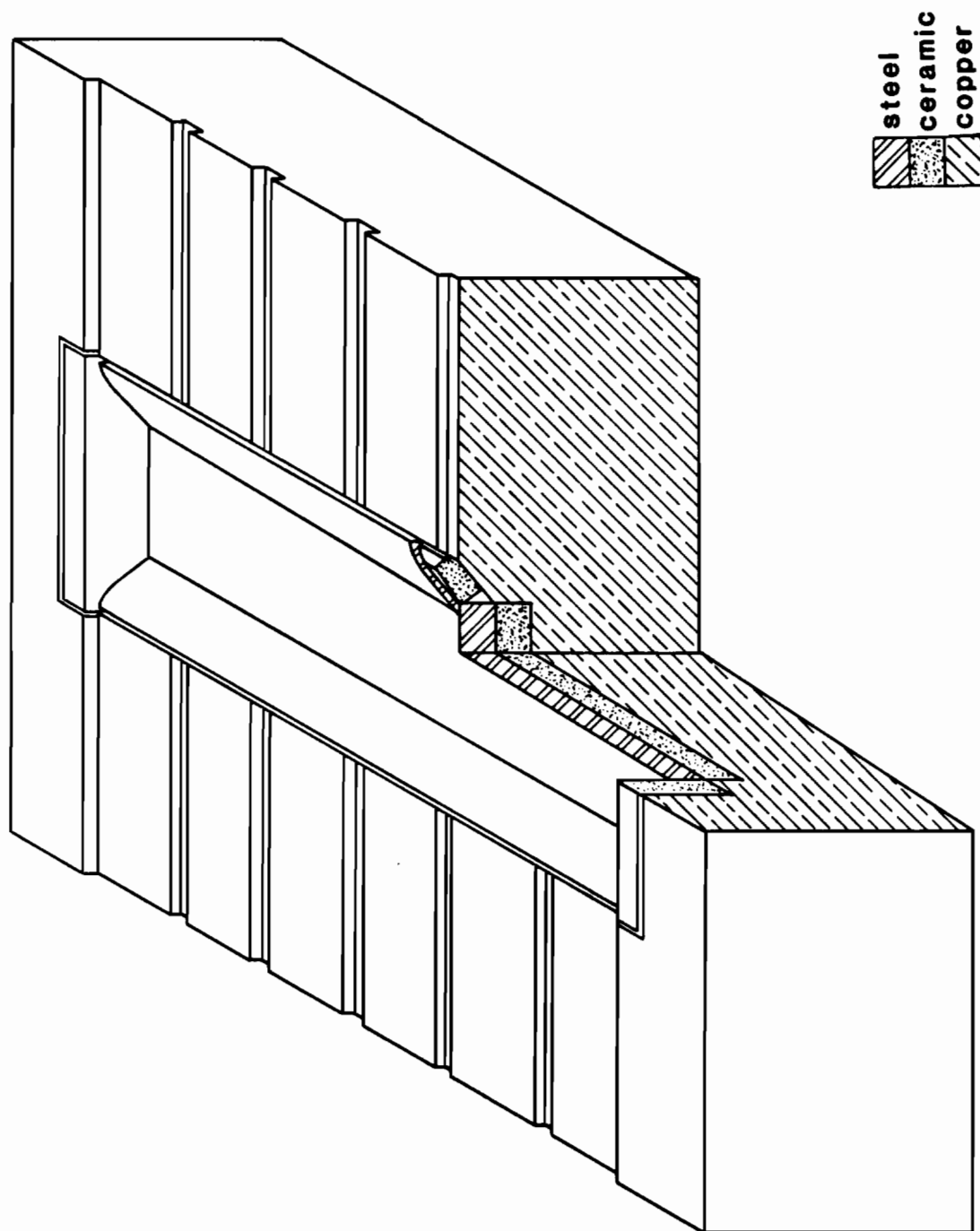


Figure 27. SCHEMATIC SECTIONAL VIEW OF THE WELD STARTING BLOCK.

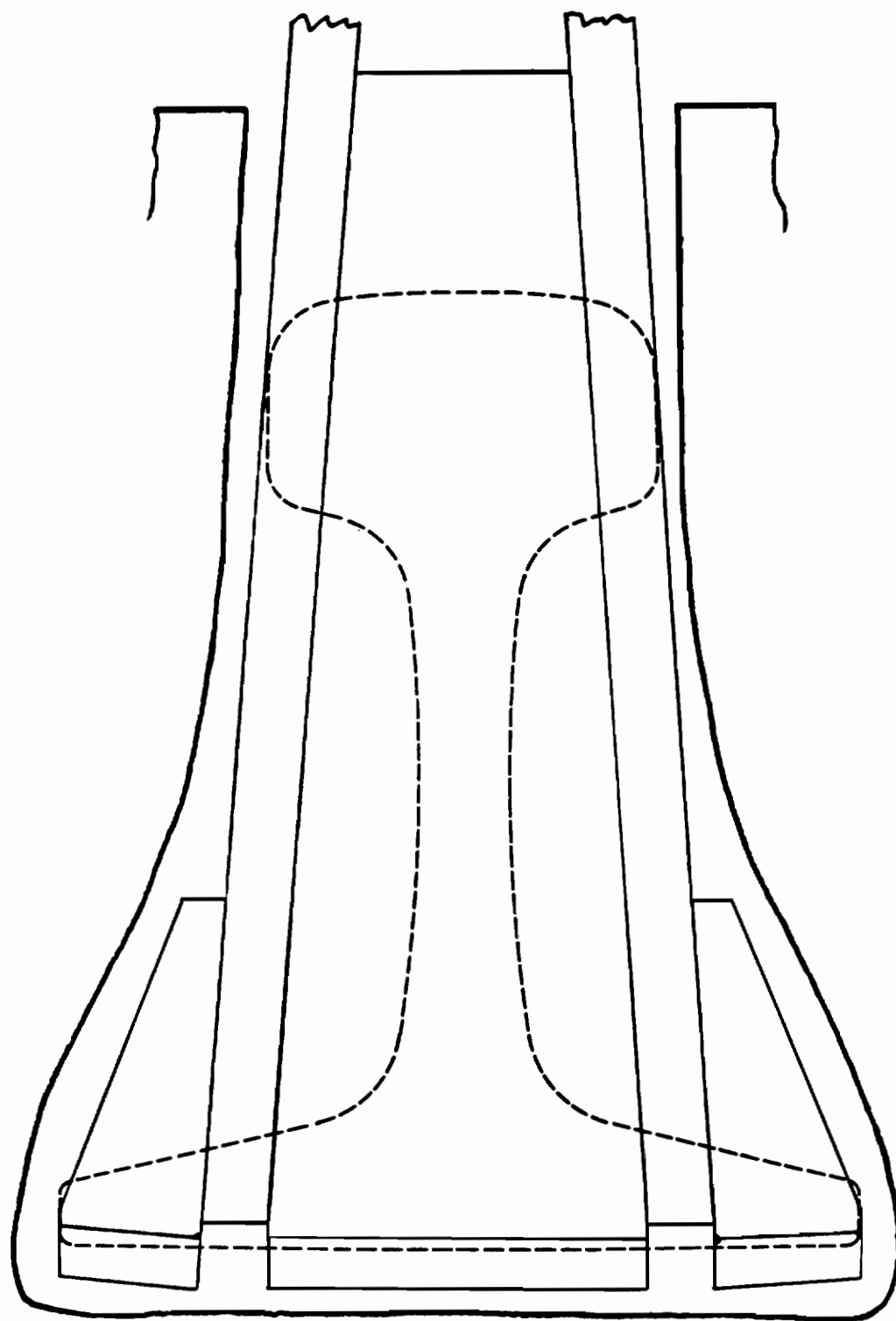


Figure 29. GUIDE TUBE POSITION RELATIVE TO THE RAIL AND MOLD CAVITY PROFILE.

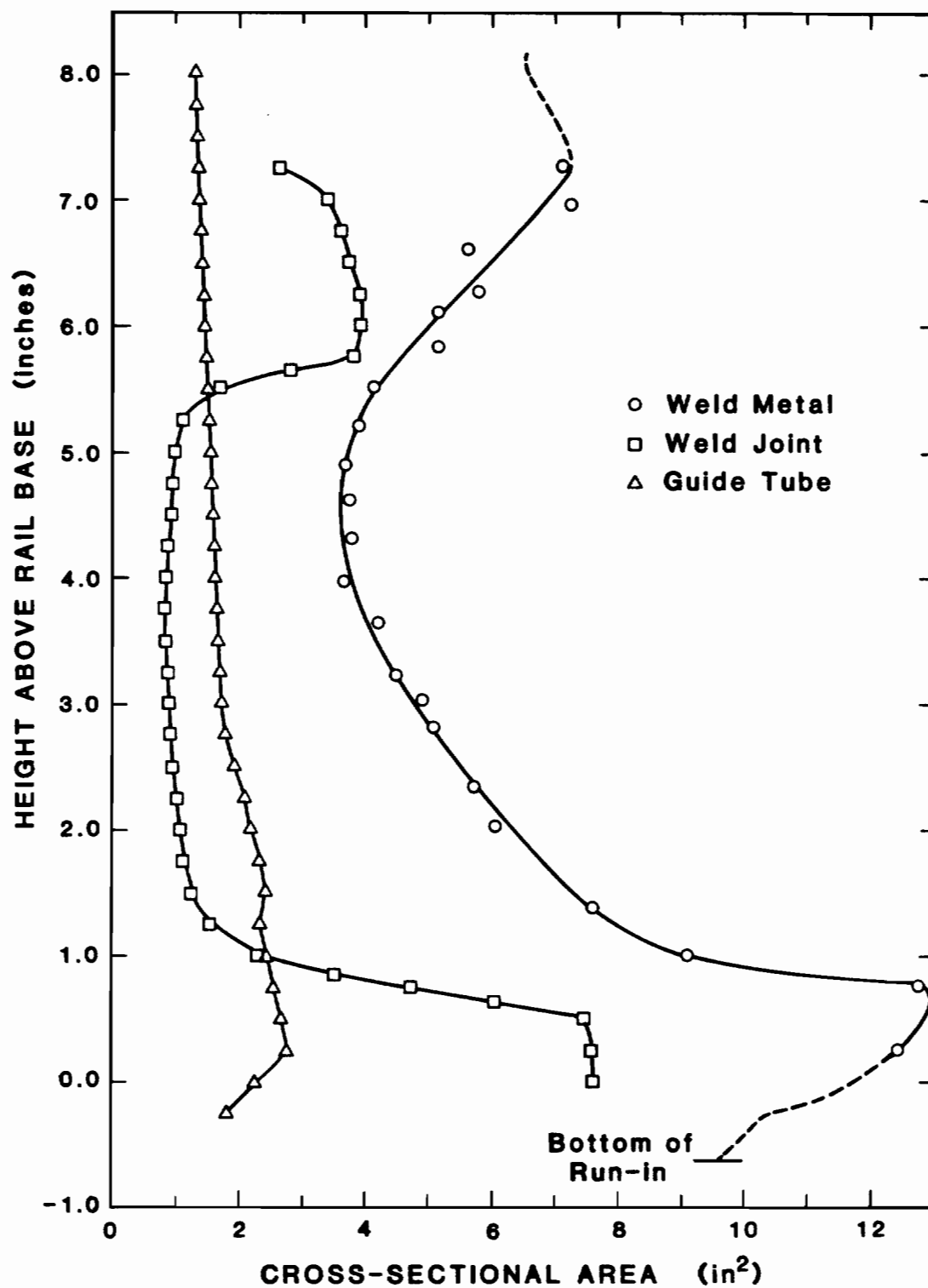


Figure 30. CROSS SECTIONAL AREA RELATIONSHIP OF THE WELD METAL, WELD JOINT, AND GUIDE TUBE.



Figure 31. COMPLETED ELECTROSLAG RAIL WELD READY FOR SERVICE.

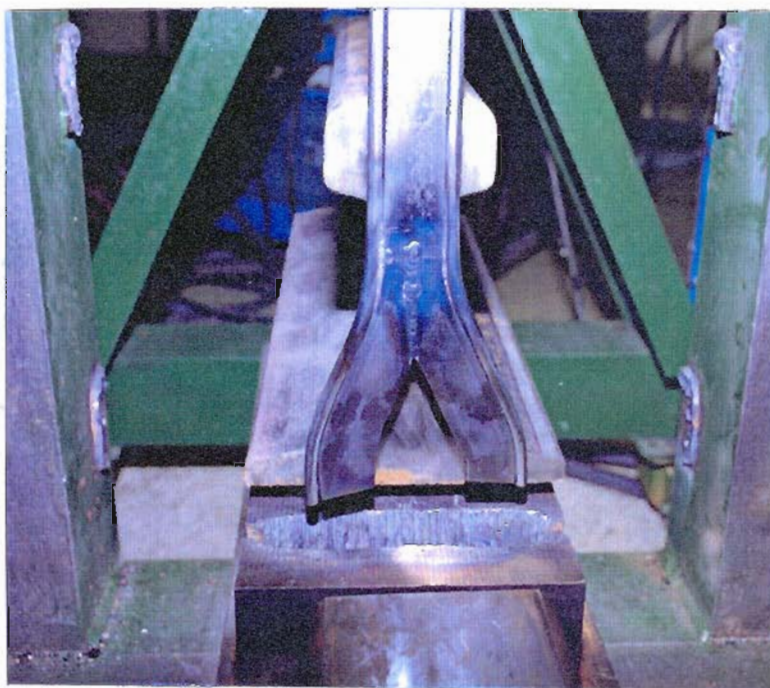
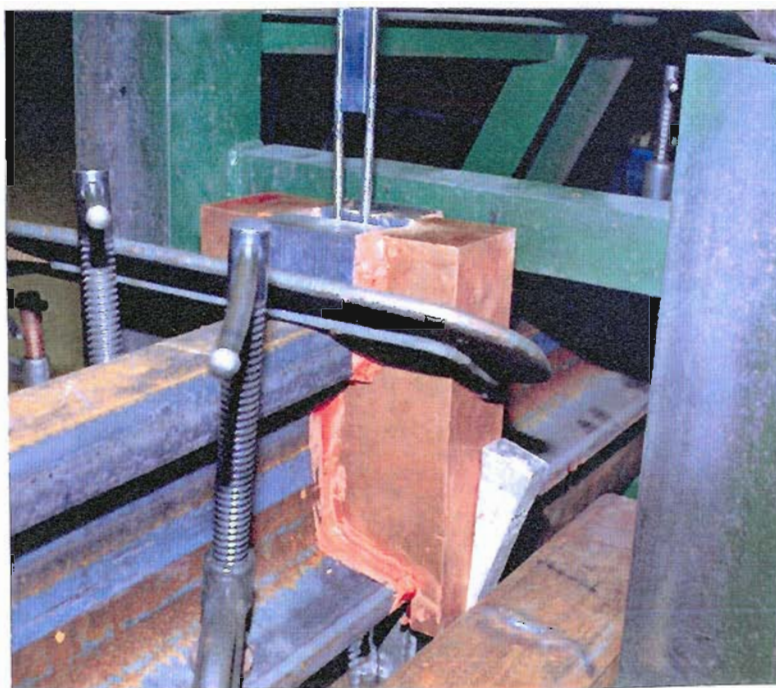


Figure 32. INITIAL COPPER SIDE SHOE DESIGN.

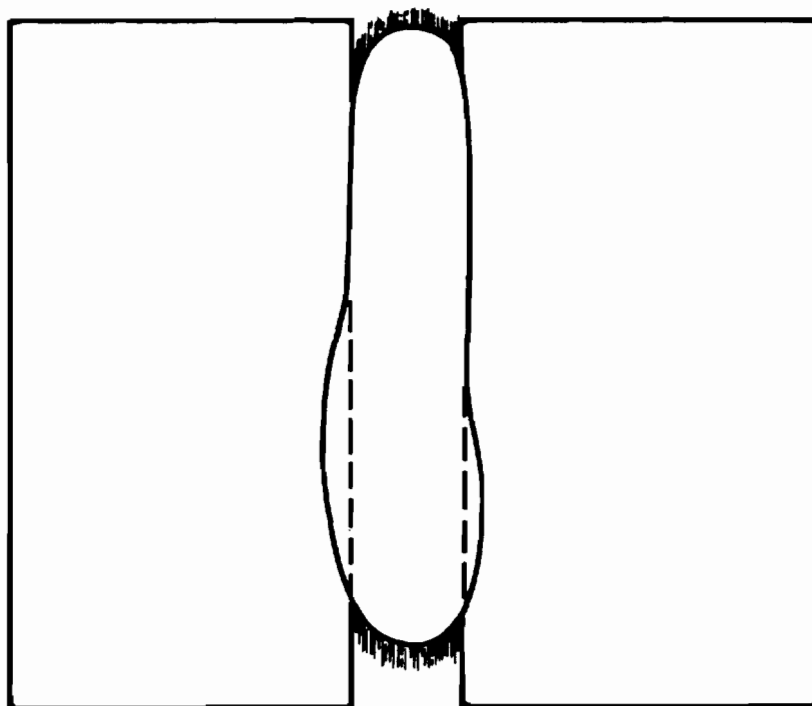


Figure 33. FUSION PATTERN AT THE RAIL BASE FROM ELECTROSLAG WELD #3.

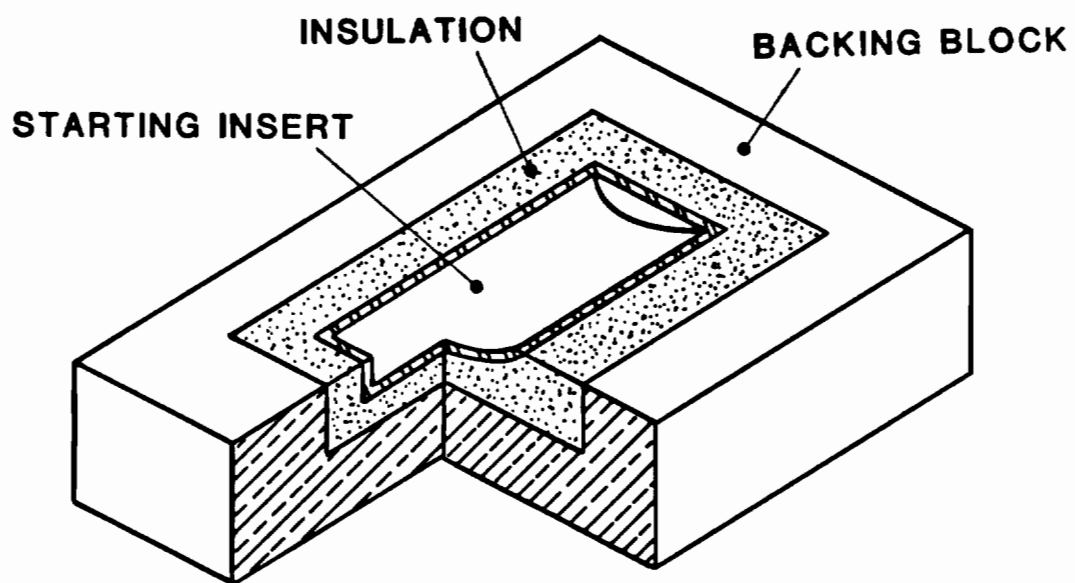
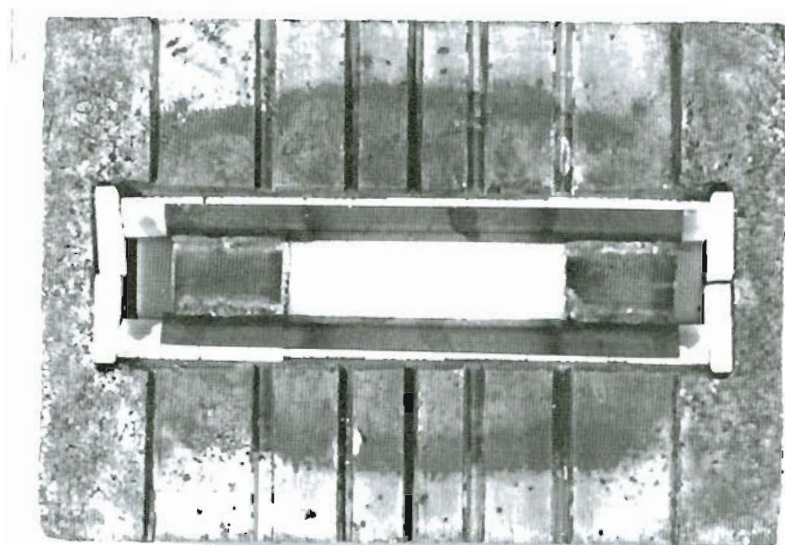
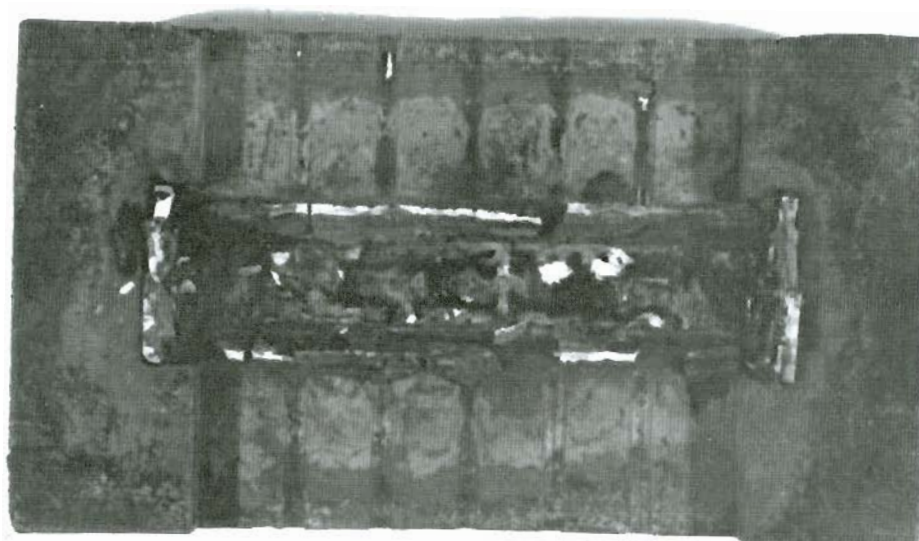


Figure 34. STARTING BLOCK DESIGN WITH PRELIMINARY INSERT AND INSULATION PATTERNS.



a.

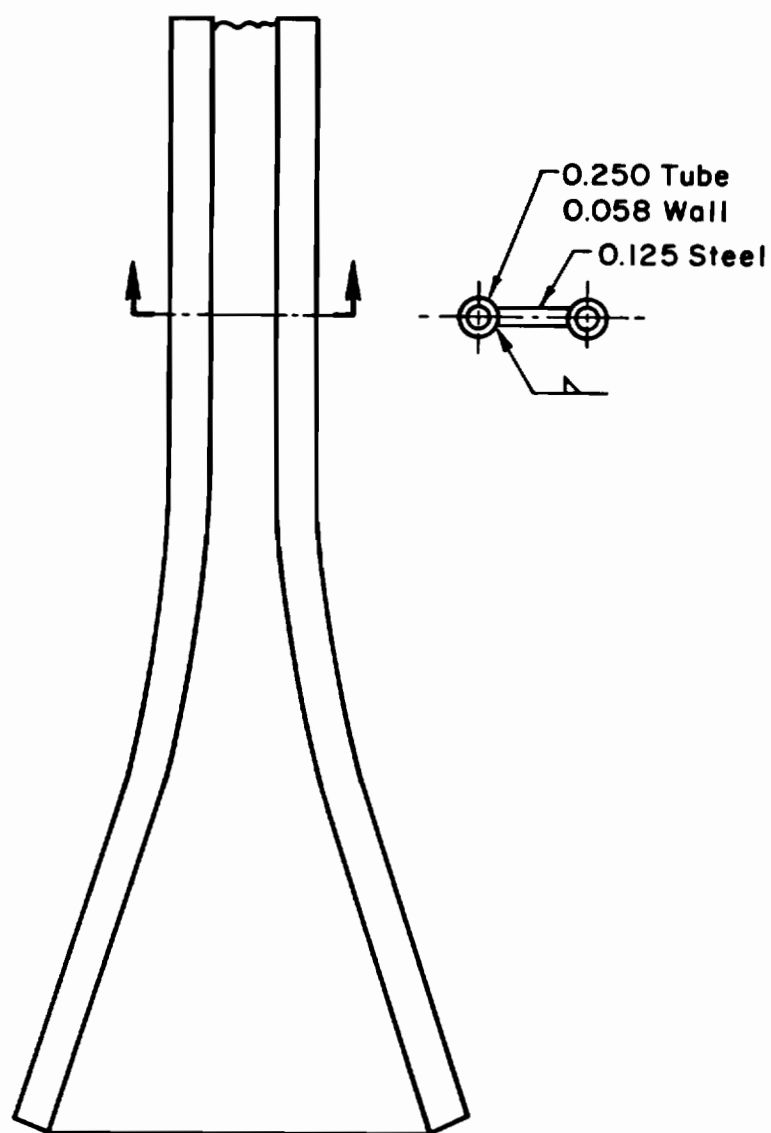


b.

Figure 35. CERAMIC STARTING BLOCK INSULATION BEFORE (a) AND AFTER (b) WELDING.



Figure 36. IMPROPER PENETRATION AND WELD SHAPE (CAVITY) IN THE WELD BENEATH THE RAIL BASE AS A RESULT OF GAS ENTRAPMENT.



PRELIMINARY RAIL GUIDE TUBE

Figure 37. INITIAL GUIDE TUBE DESIGN.

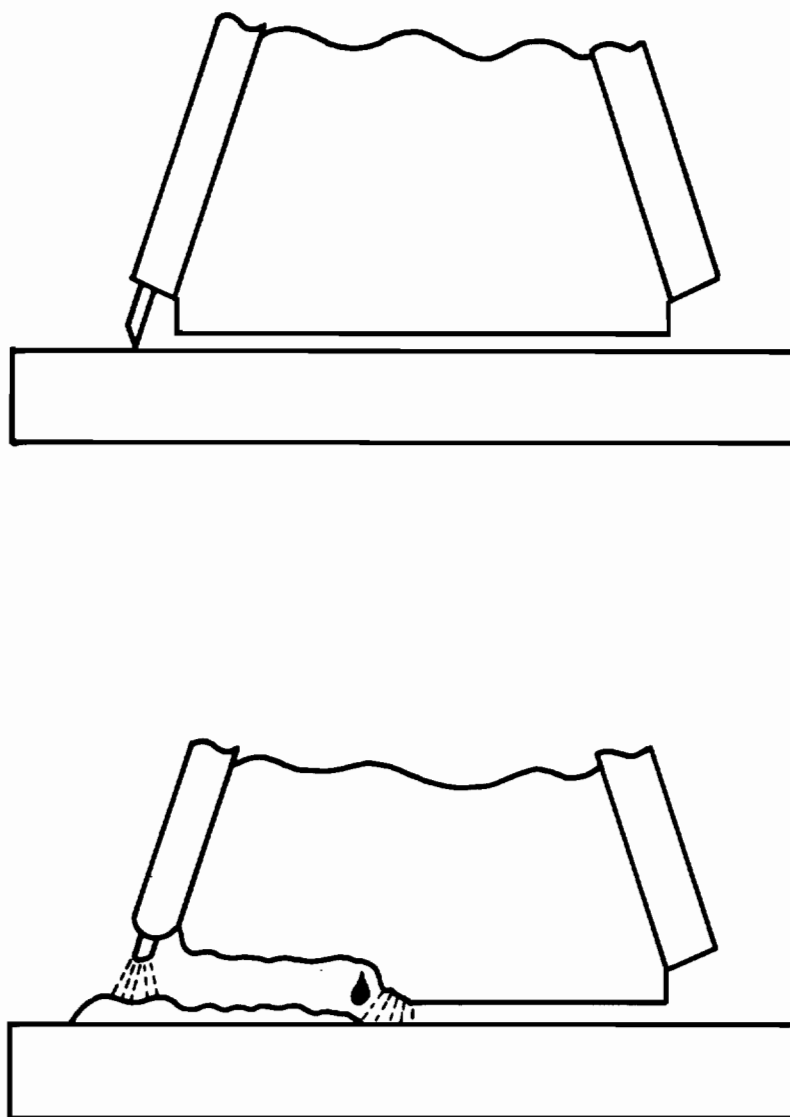


Figure 38. GUIDE TUBE INFLUENCE ON SLAG BATH FORMATION.

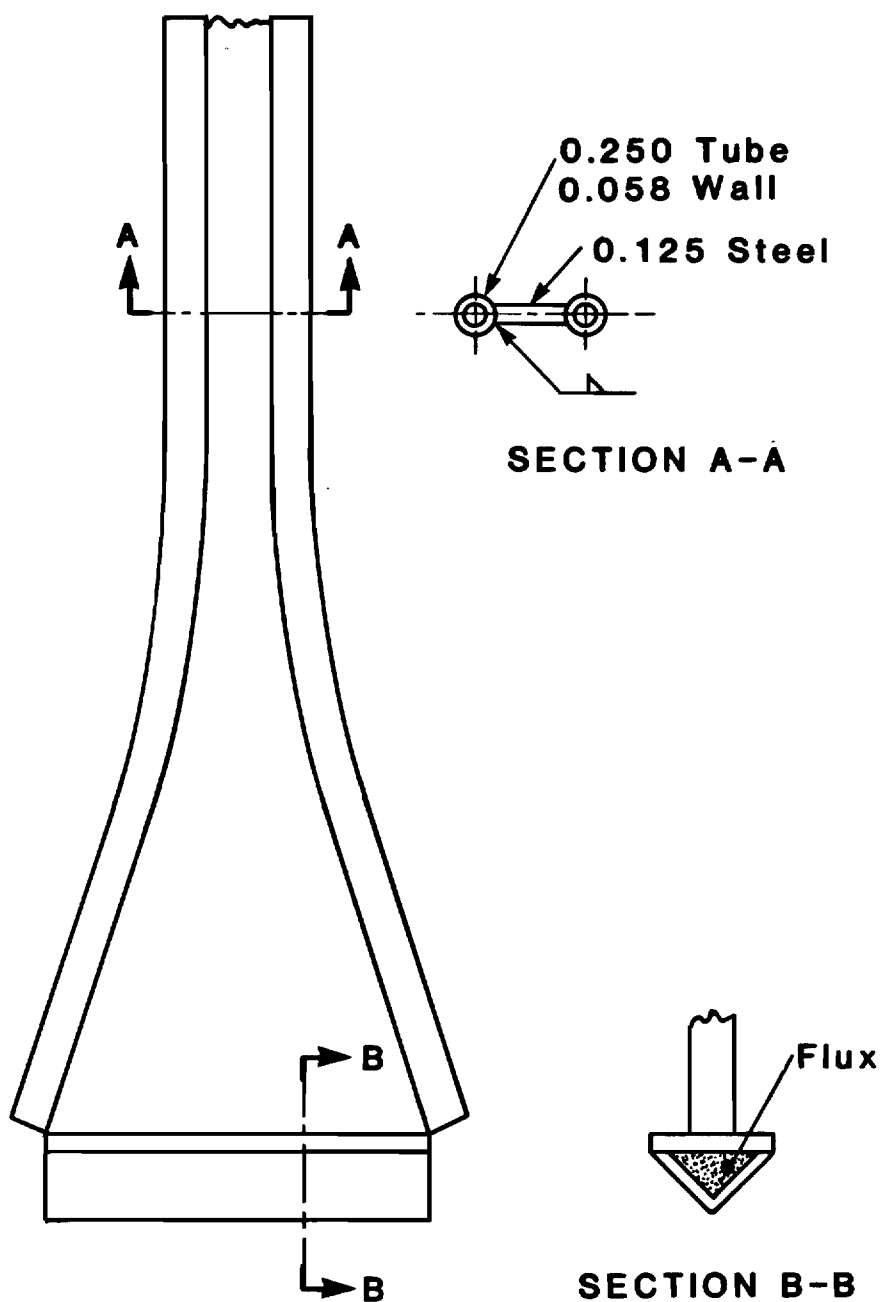


Figure 39. INITIAL GUIDE TUBE SPECIFICALLY DESIGNED TO IMPROVE SLAG BATH FORMATION.

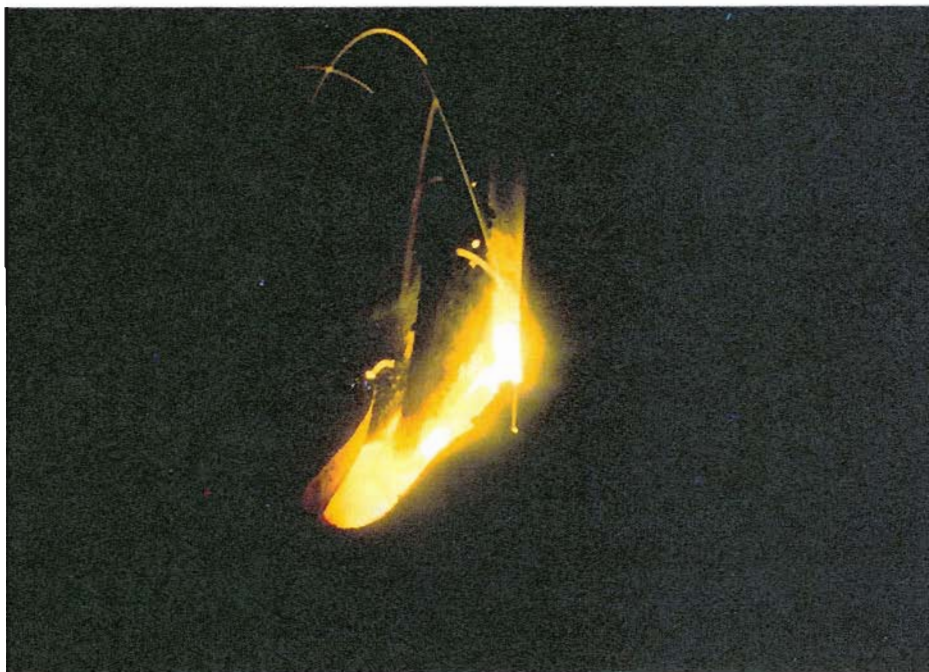
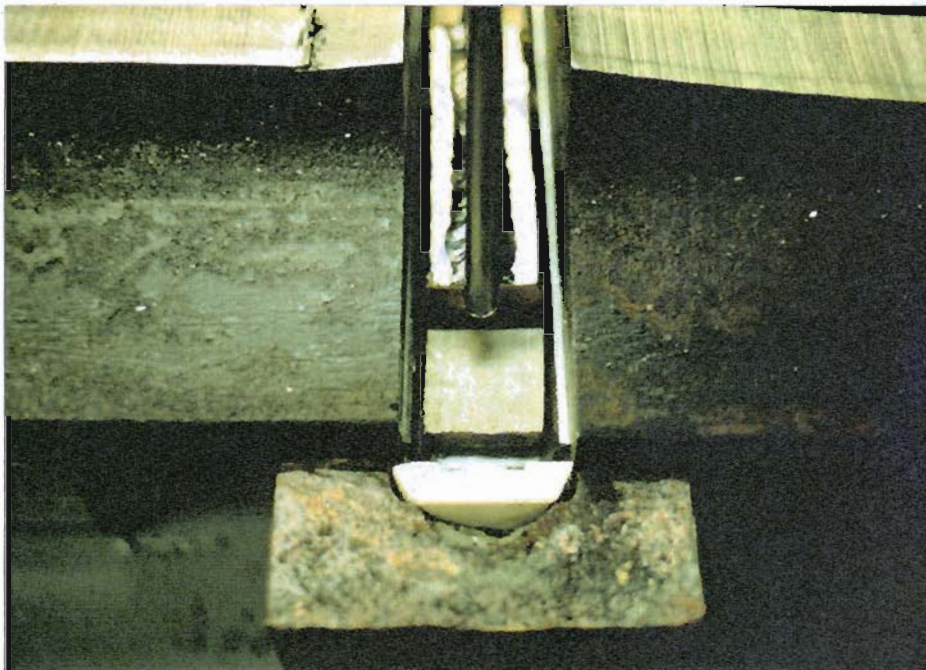


Figure 40. MOLD AND WELD SET-UP FOR EVALUATION OF THE GUIDE TUBE INFLUENCE UPON WELD STARTING.

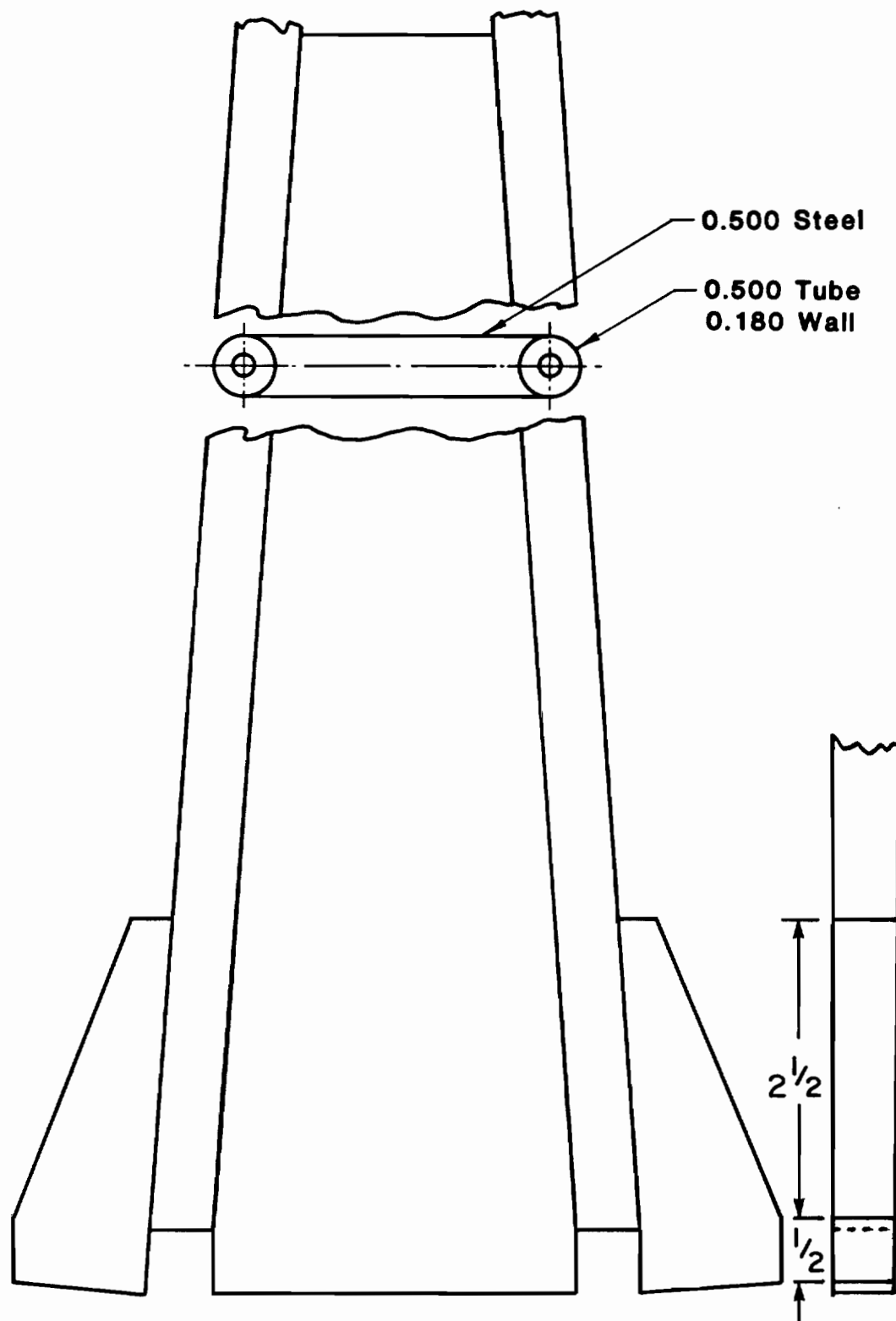


Figure 41. UNIFORM 1/2 INCH THICK GUIDE TUBE DESIGN.

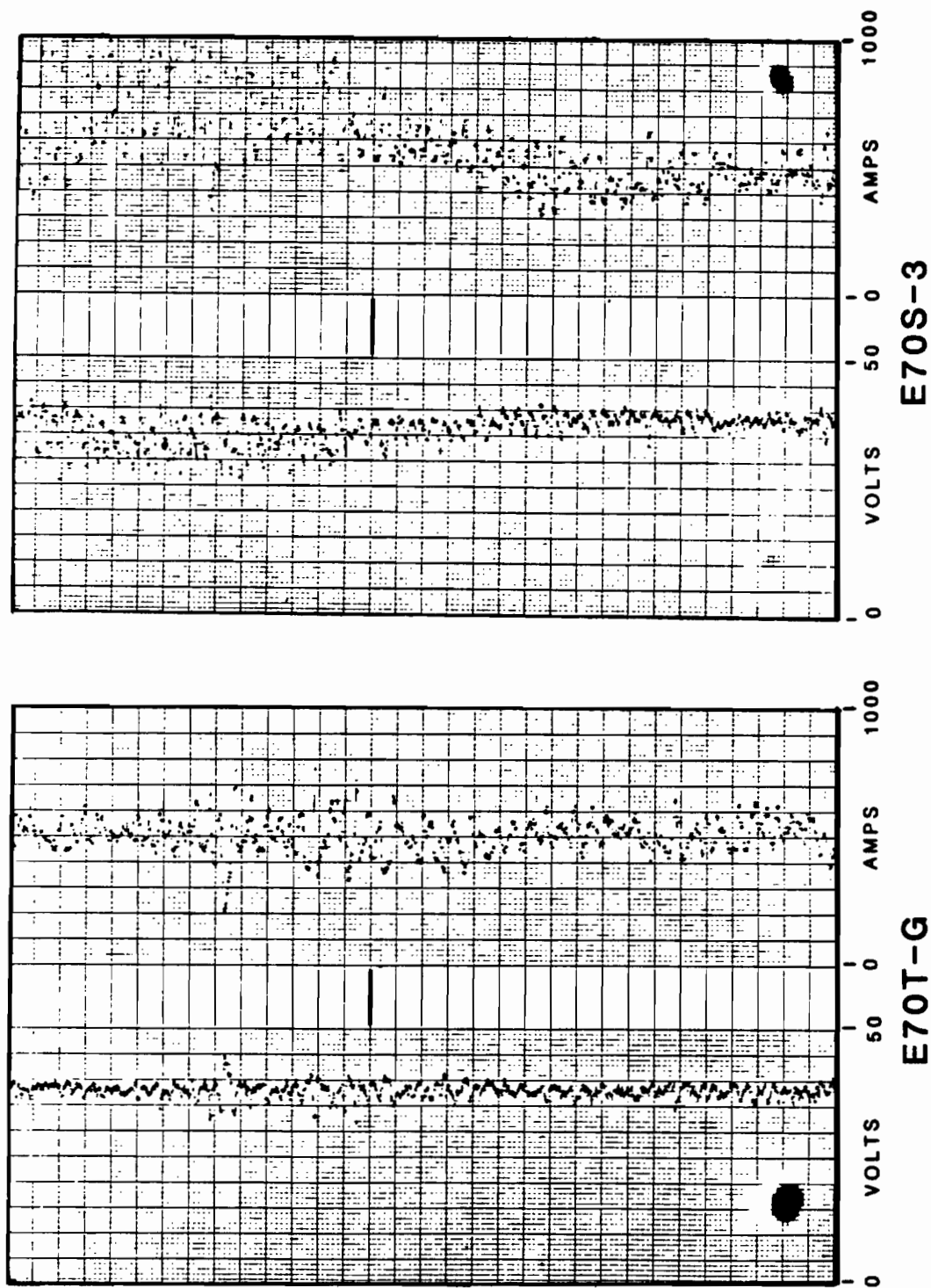


Figure 42. WELDING POWER CONTROL COMPARISON BY STRIP CHART RECORDINGS FOR SOLID (E70S-3) VS. TUBULAR ELECTRODE WIRE (E70T-G).

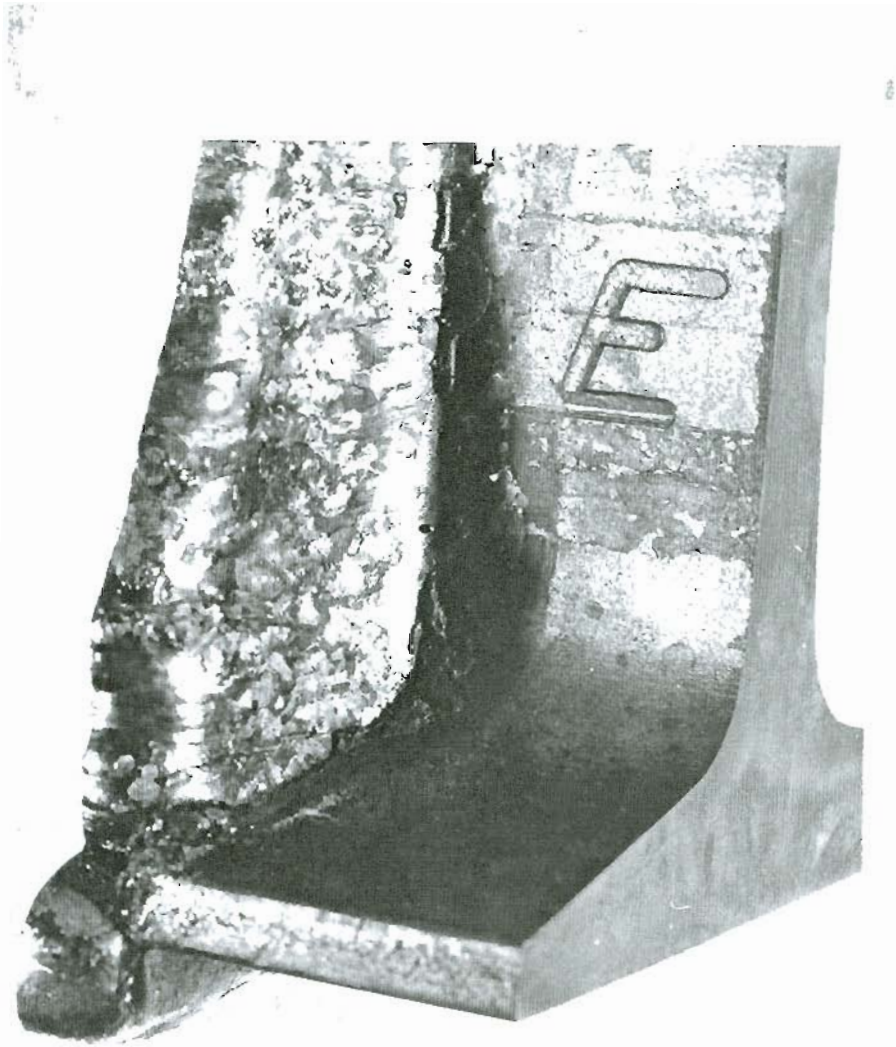


Figure 43. WELD REINFORCEMENT NOTCHING DUE TO OVER COOLING OF THE SLAG BATH.

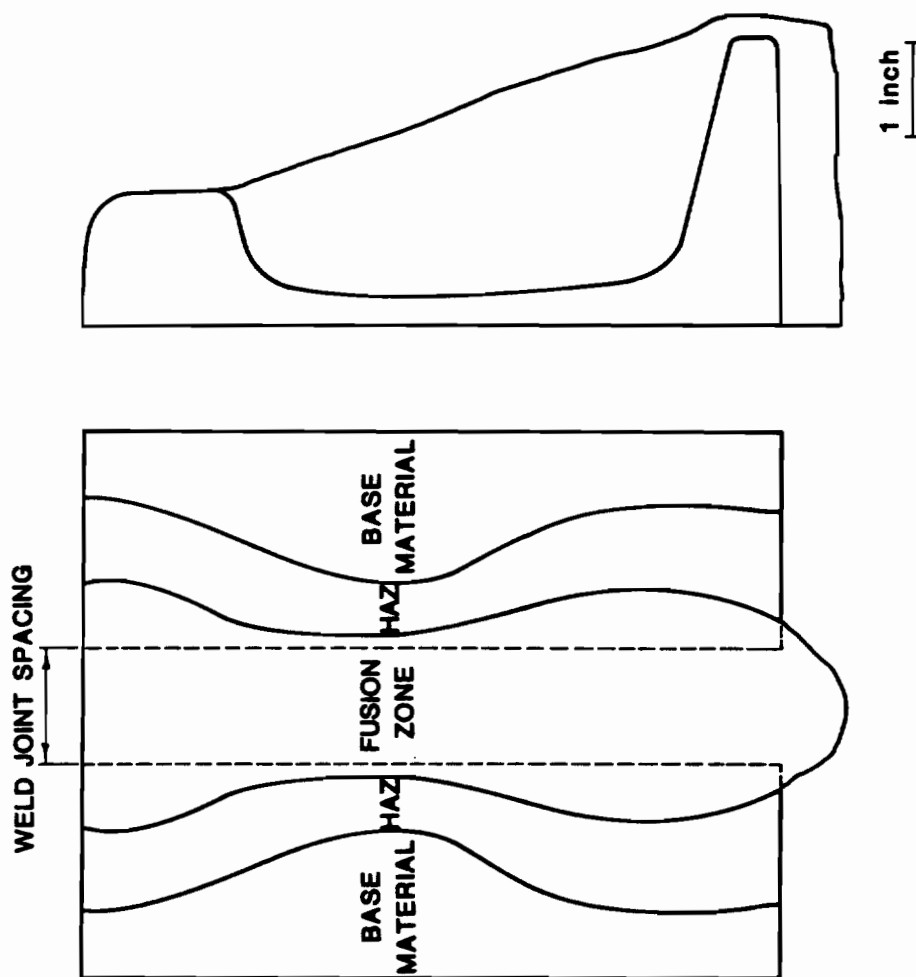


Figure 44. TYPICAL ESRW FUSION AND HEAT AFFECTED ZONE PATTERNS THROUGH THE LONGITUDINAL RAIL AND WELD CENTER SECTION.

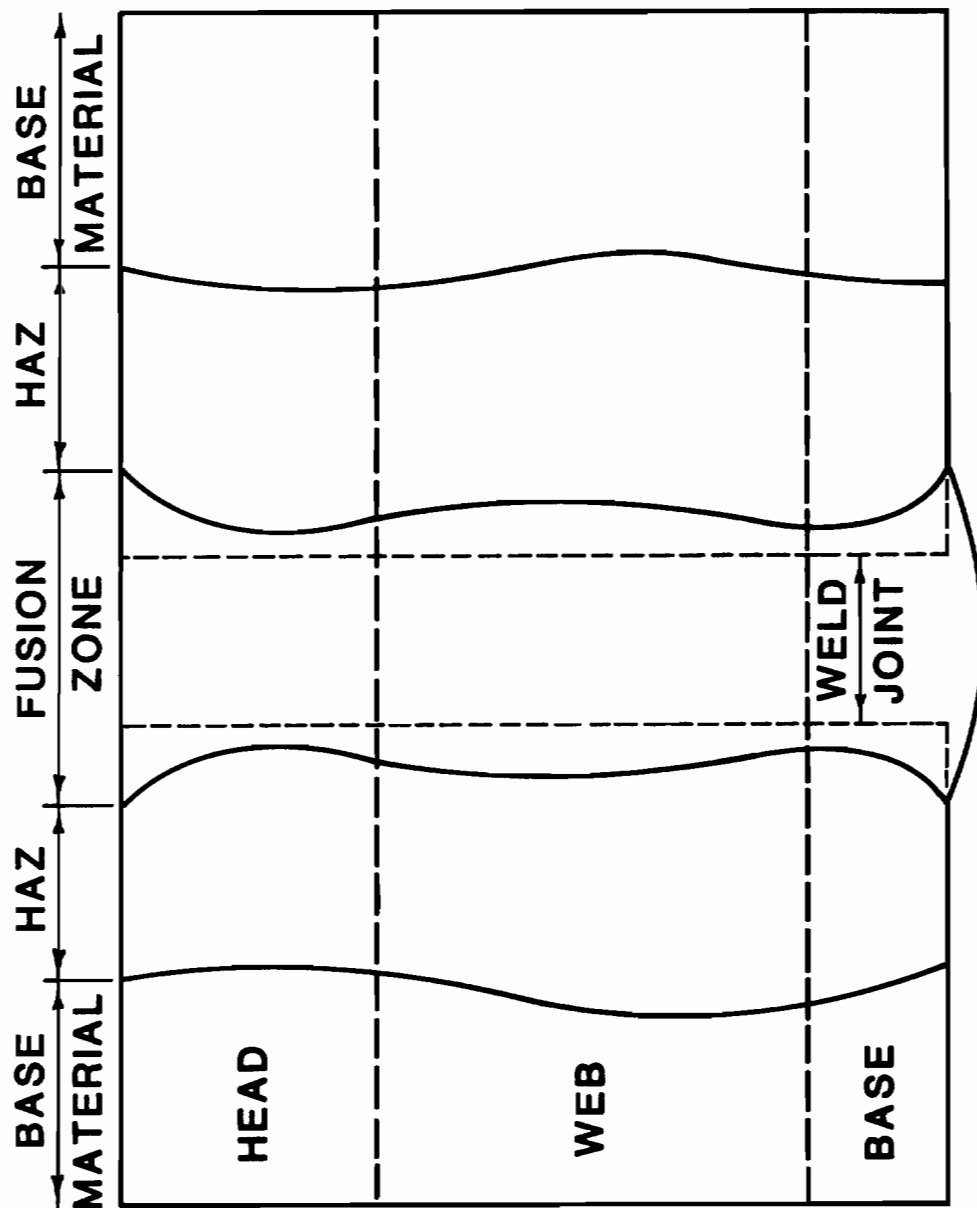


Figure 45. TYPICAL THERMIT WELD FUSION AND HEAT AFFECTED ZONE PATTERNS THROUGH THE LONGITUDINAL RAIL AND WELD CENTER SECTION (38).

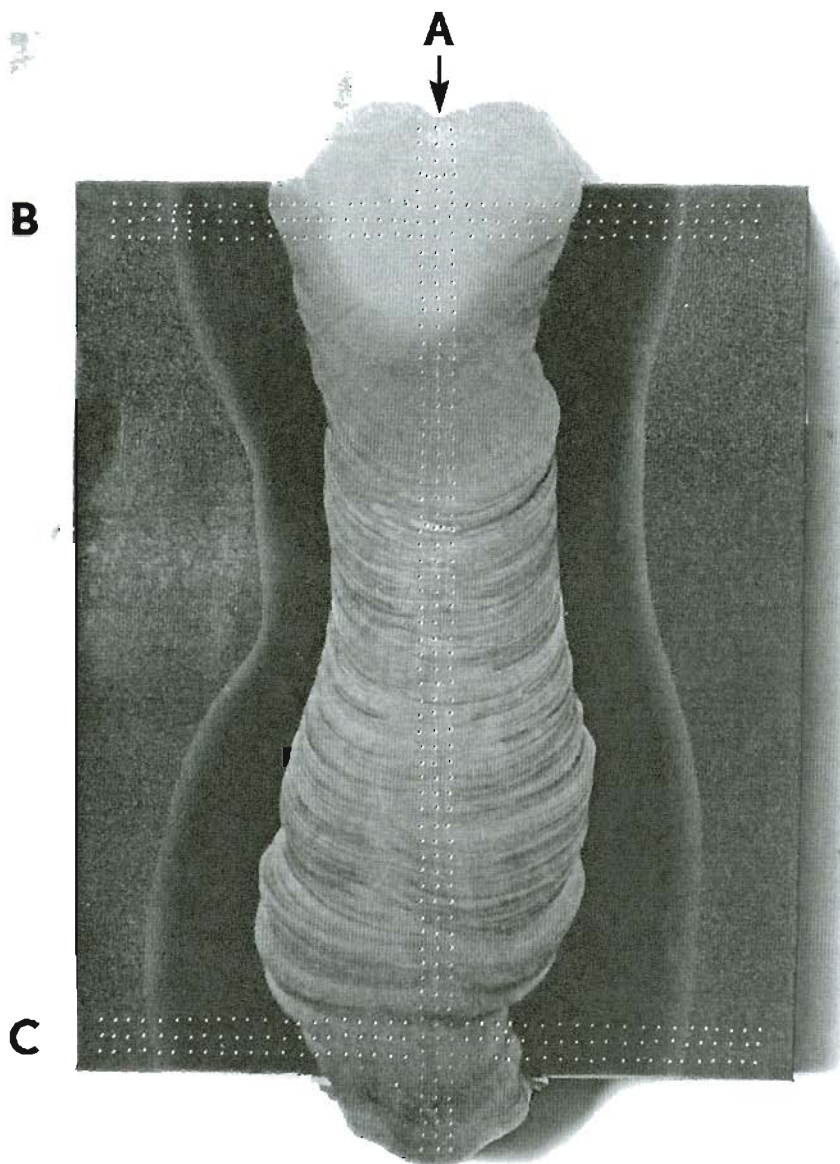


Figure 46. HARDNESS TRAVERSE LOCATIONS THROUGH THE LONGITUDINAL CENTER SECTION OF ESRW.

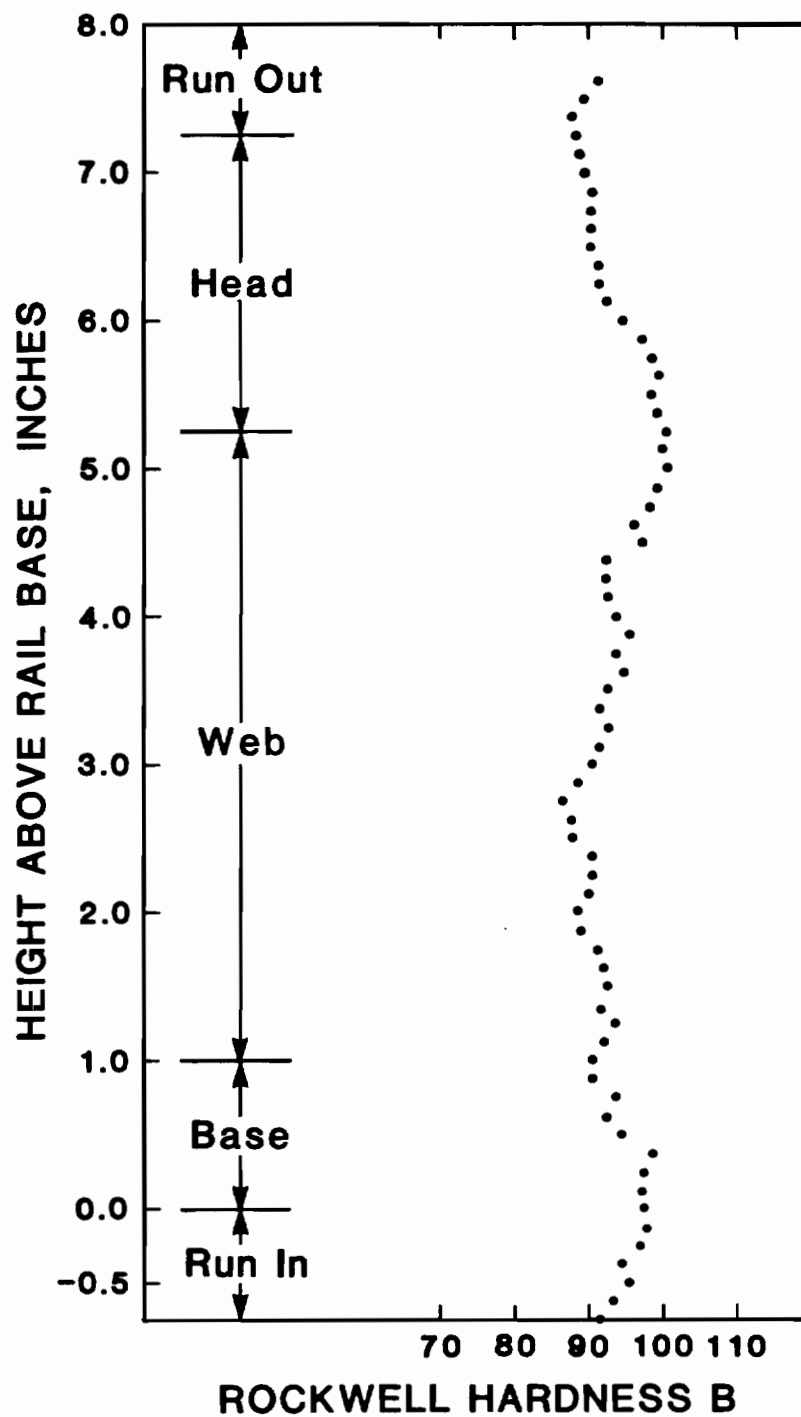


Figure 47. HARDNESS TRAVERSE PLOT OF THE WELD METAL ("A" FIGURE 46) FROM AN ESRW.

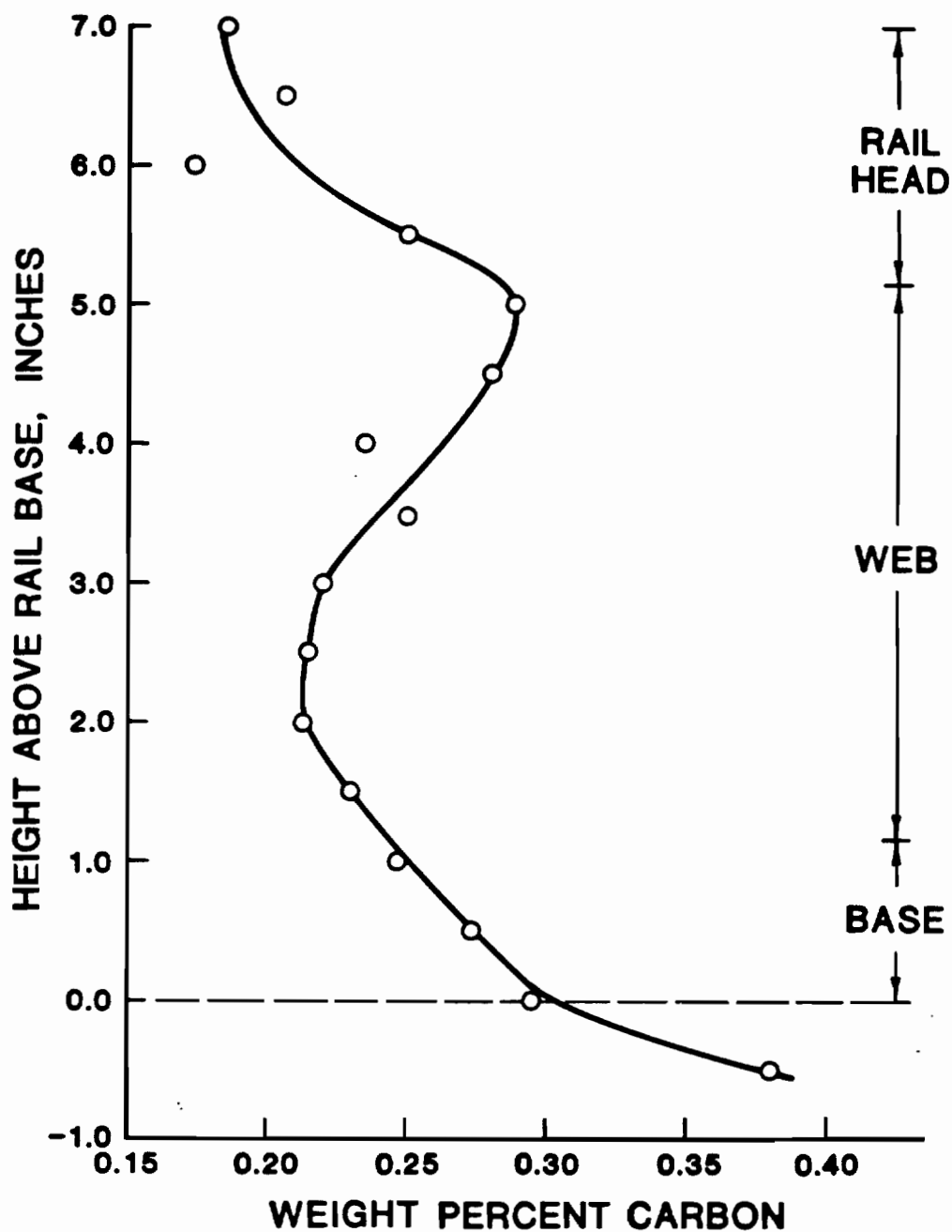


Figure 48. VARIATION OF CARBON CONTENT IN AN ESRW USING E70S-3 ELECTRODE WIRE (AS IN FIGURE 46).

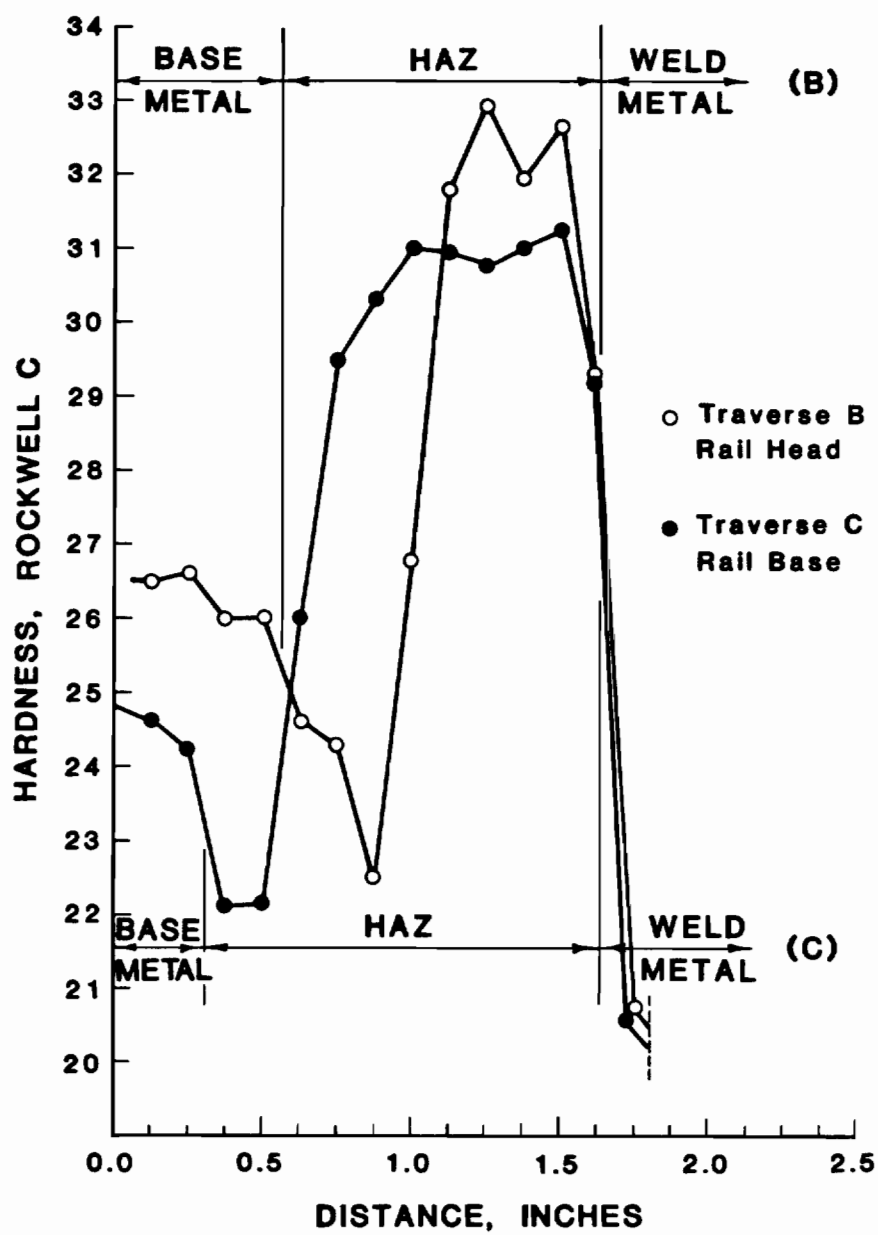


Figure 49. HARDNESS TRAVERSE PLOTS FROM B AND C OF FIGURE 46.

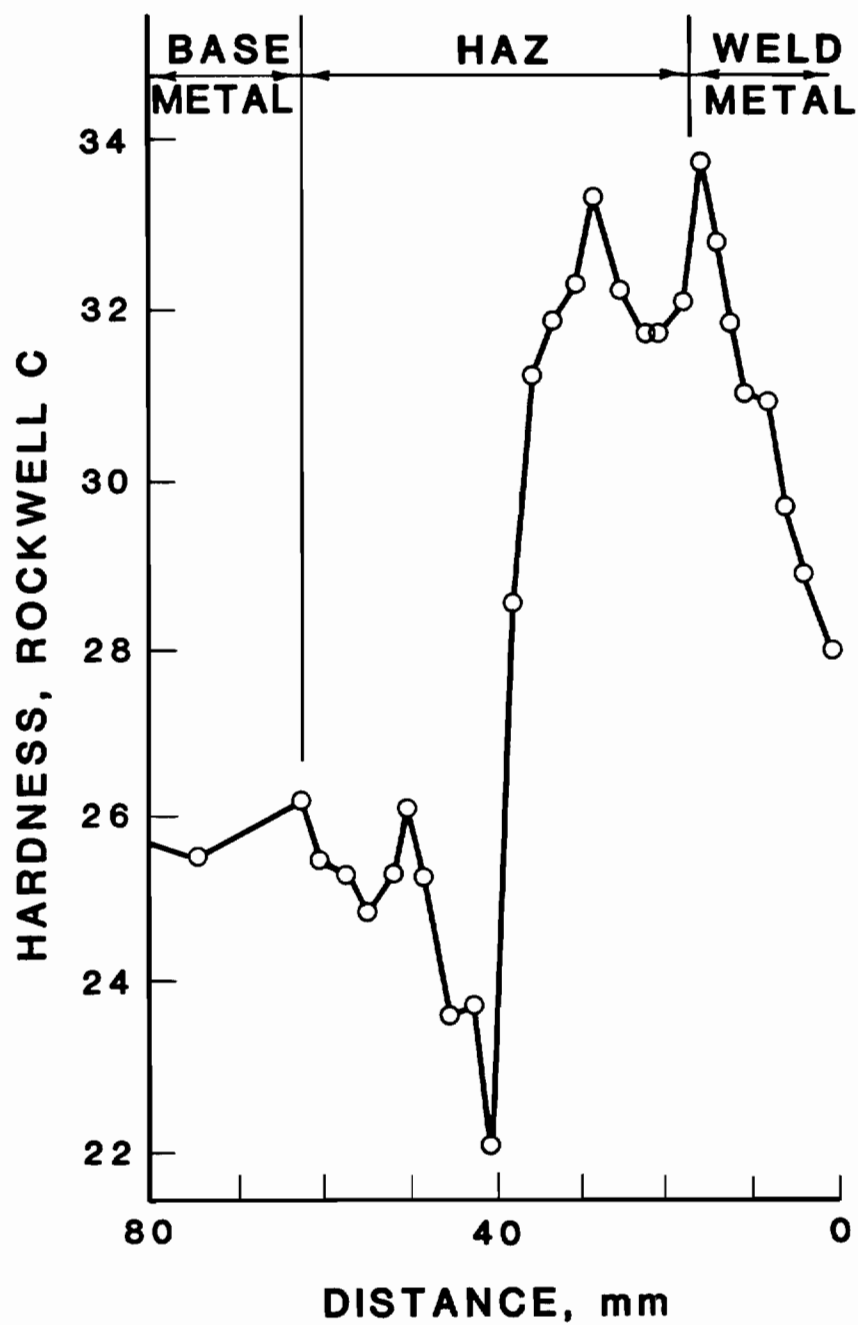


Figure 50. HARDNESS TRAVERSE OF A TYPICAL THERMIT WELD.

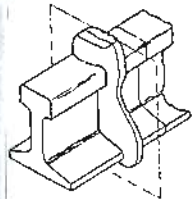
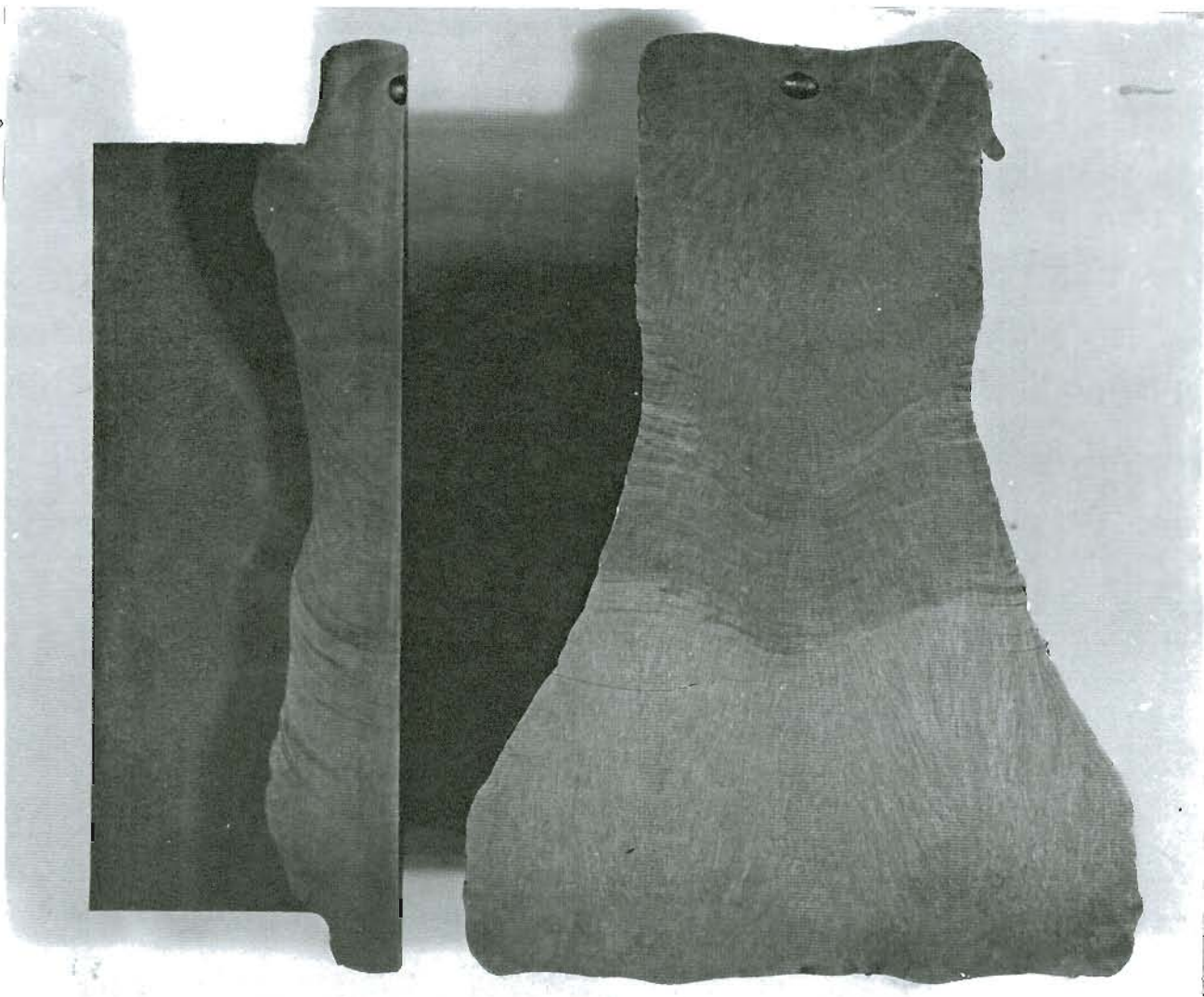
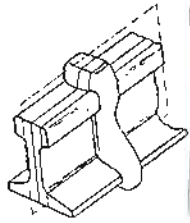


Figure 51. TRANSVERSE AND LONGITUDINAL SECTIONS OF AN ESRW MADE WITH ER90S-B3 ELECTRODE WIRE.

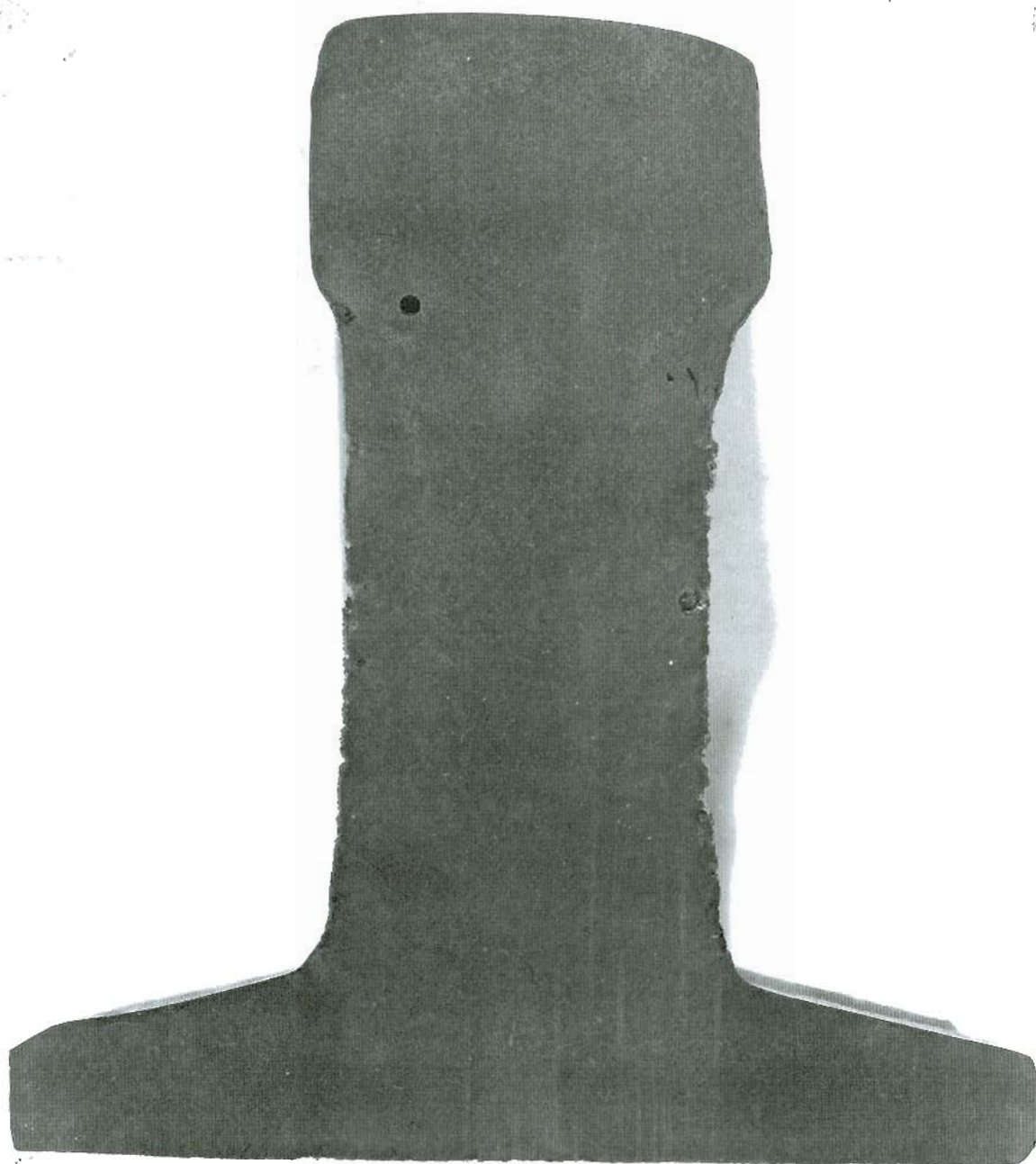
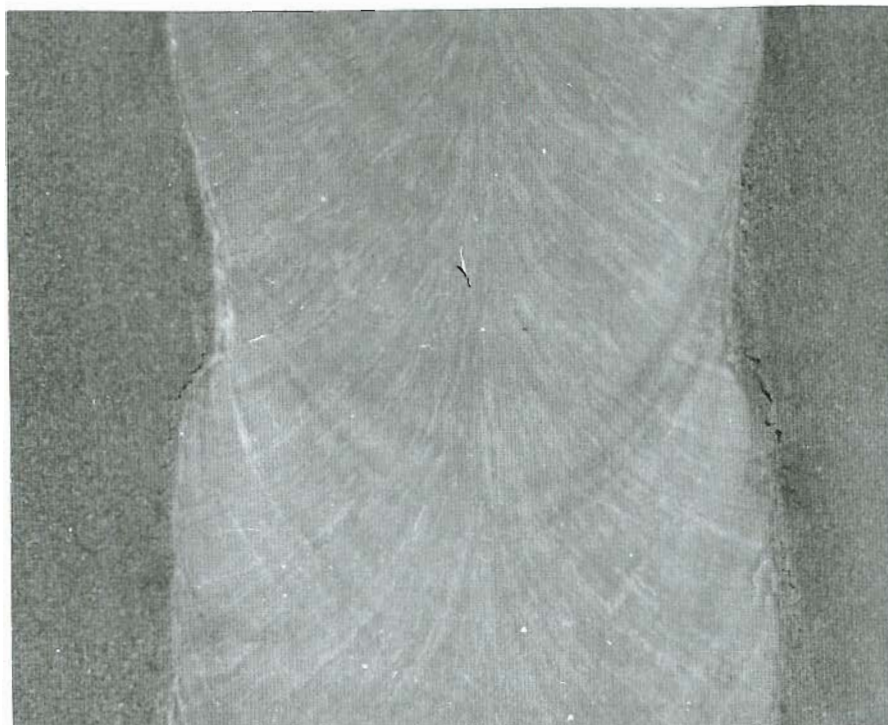


Figure 52. MACROSECTION OF A TYPICAL THERMIT WELD.



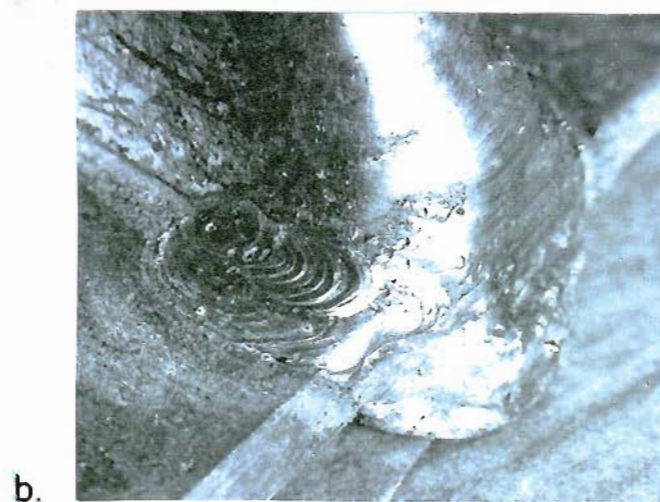
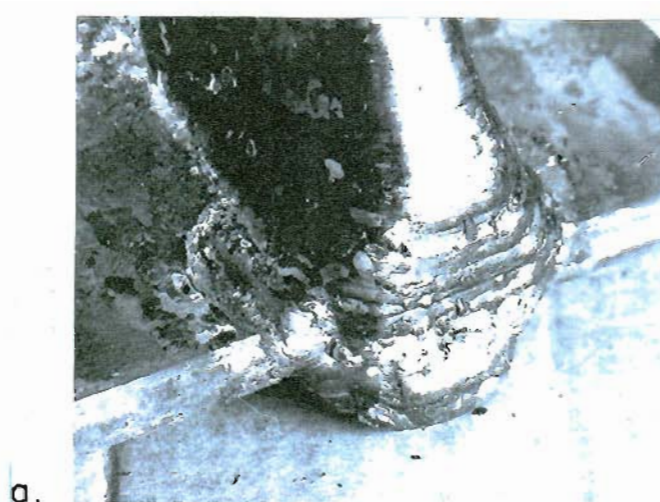
a.



b.

500x

Figure 53. HAZ CRACKS IN ESRW RESULTING FROM EXCESSIVE WELD SPEEDS.



c.

Figure 54. ESRW RAIL BASE UNDERCUT REPAIR USED IN THIS INVESTIGATION.

Appendix I.

GLOSSARY OF RAIL STEEL TERMINOLOGY

Brand--Rail identification rolled in raised characters on the side of the web of each rail a minimum of every 16 feet. The brand must include the data and order of arrangement as shown in the example below.

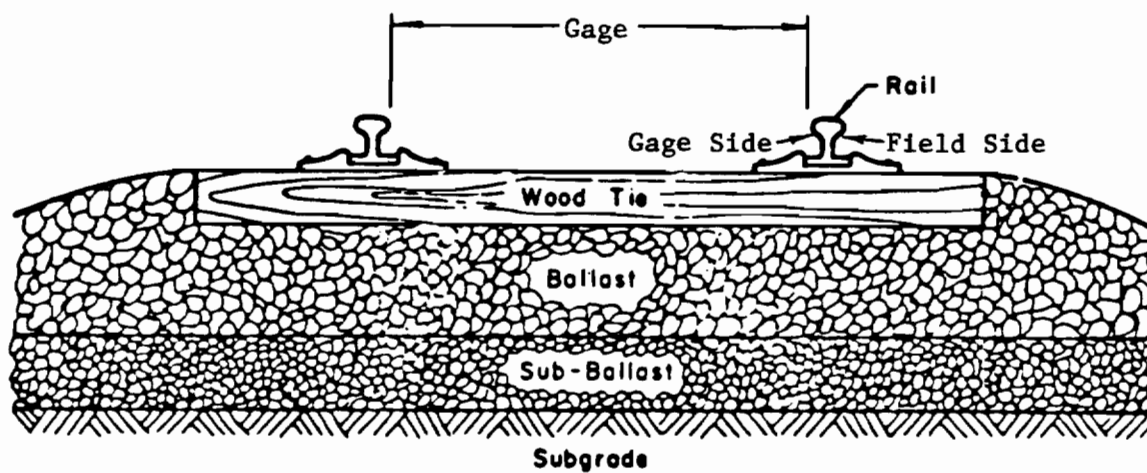
132	RE	CC	Manufacturer	1977	III
(Weight)	(Section)	(Method of Hydrogen Elimination, if Indicated in Brand)	(Mill Brand)	(Year Rolled)	(Month Rolled)

Stamping--The heat number, rail letter indicating the order the rail is taken from the heat, ingot number, and method of hydrogen elimination stamped into the web of each rail a minimum of every 16 feet on the side opposite the brand. The data and arrangement shall be as shown below in 5/8 inch figures.

287165	ABCDEFGH	12	BC
(Heat Number)	(Rail Letter)	(Ingot Number)	(Method of Hydrogen Elimination, if Indicated in Stamping)

Track System Description--(on next page)

Track System Description--(cont.)



Transverse Section

Appendix II.

RAIL CHEMISTRY

American Railway Engineering Association (AREA) and American Society for Testing of Materials (ASTM) Specifications for 136 pound per yard carbon steel rail.

	C	S	P	Mn	Si	Cr	Mo	Al
AREA	0.70- 0.82	0.04 Max	0.035 Max	0.75- 1.05	0.10- 0.35	--	--	--
ASTM	0.69- 0.82	0.05 Max	0.04 Max	0.70- 1.00	0.10- 0.25	--	--	--

Chemistry of rail heats and welds in this investigation as determined by spark spectro-analysis (in wt.%).

	C	S	P	Mn	Si	Cr	Mo	Al
Rail # 45400	0.73	0.043	0.033	0.93	0.225	0.09	0.005	0.006
Rail # 20304	0.72	0.022	0.033	0.85	0.196	0.04	0.005	0.009
Rail # 14192	0.73	0.040	0.025	0.89	0.213	0.04	0.005	0.007
ESRW Alloy ER90S-B3	0.14	0.028	0.016	0.587	0.175	1.827	0.755	0.006
Thermit Weld	0.49	0.021	0.033	1.093	0.366	0.031	0.091	0.369

Appendix III.

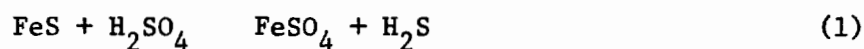
SULPHUR PRINTING

The surface of interest to be tested for distribution of sulphur should be reasonably smooth and free from foreign matter, such as dirt and grease. Grinding the surface on No. 00 or No. 000 emery paper and subsequent thorough washing will generally produce a surface satisfactory for the purpose.

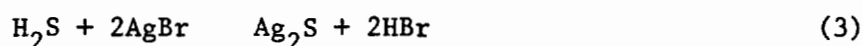
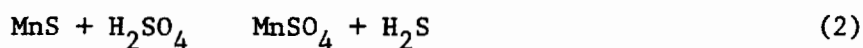
Photographic bromide paper is soaked in a 2% aqueous solution of sulphuric acid for approximately 3-4 minutes. This operation, as well as the entire process of sulphur printing, may be carried out in daylight; contrary to the usual requirements for the handling of photographic paper. Although in principle any surface finish on the paper will produce the desired results, it is recommended that a semi-matte paper be used, so as to minimize the danger of slippage when the paper is placed in contact with the specimen surface. The action of the dilute acid on the gelatin of the paper tends to make it soft and slimy, this condition being decidedly worse on glossy-finished paper than on semi-matte.

The paper is removed from the acid solution and allowed to drain free from excess solution. The emulsion side of the paper is then placed in direct contact with the prepared specimen surface and allowed to remain in contact under moderately applied pressure for 1 or 2 minutes. Care must be taken that all entrapped air bubbles between the paper and the specimen surface are eliminated. This may be assured by carefully pressing with a squeegee print roller.

The reaction of the sulphuric acid with the sulphide regions of the steel produces hydrogen sulphide gas, which reacts with the silver bromide in the paper emulsion, forming a characteristic brown to gray-black deposit of silver sulphide. These reactions may be expressed as follows:



or



When the reaction has proceeded for approximately the recommended length of time, the photographic paper is removed from the surface of the specimen, rinsed in clear running water, and then fixed permanently by placing it in a photographic fixing solution for about 15 minutes. When fixation is completed, the print is again washed in running water for approximately 30 minutes and subsequently dried in the usual manner.

The examination of a properly prepared sulphur print will disclose quite clearly, because of the presence of darkly colored areas of silver sulphide, the precise location of sulphur inclusions on the prepared surface of the metal. A grouping or agglomeration of such silver sulphide areas indicates the presence of sulphur segregation, whereas a random dispersion of the spots denotes a more uniform, and perhaps less harmful, distribution of the sulphur inclusions.

(Taken from Kehl, "The Principles of Metallographic Laboratory Practice", Third Edition.)

Appendix IV.

DYE-PENETRANT INSPECTION PROCEDURE

1. Preclean the area to be inspected by using a vapor degreaser or a residue-free volatile solvent, such as lacquer thinner, trichlorethylene, or chlorothene. Surfaces and flaws must be free of all soil. Improperly precleaned defects can lead to failure of the process. Power brushing or abrasive blasting should not be used as it may close the surface exposure of small cracks or holes.
2. After the cleaning solvent has completely evaporated from the surface and flaws, apply penetrant to the clean, dry surface. Allow a minimum of 5 minutes penetrant time. Increase penetration time if temperature is below 60°F or if unusually tight flaws, such as grinding cracks, fatigue cracks or laps, are suspected, or if thorough precleaning is not possible. Do not apply to surfaces over 140°F.
3. Remove excess penetrant from the surface as completely as possible, but avoid overcleaning. On smooth surfaces, wiping with clean, dry rags or paper toweling followed by wiping gently with clean rags or toweling moistened with commercial penetrant remover is recommended. Rough surfaces may require more severe wiping or a washdown with commercial emulsifier or water-washable remover.

4. Developer should be applied in a thin, even wet coating onto the dry surface. A thick coating can mask microscopic defects. Red marks in the white developer indicate presence of flaws. Flaws may appear the instant developer dries, but final inspection and interpretation should be made at least a few minutes later.
5. Interpretation of flaw indications may be made from the rate and extent of bleeding as well as from the richness of the red-colored flaw patterns on the white developer background. The rate of bleeding and color richness indicate the width and depth of the defect, while the extent of bleeding indicates the volume of the flaw. A wide, shallow defect shows up almost at once, while narrow, deeper flaws may not assume final pattern for some time.

(Dye-Penetrant Information from Met-L-Chek Co., Inc., Santa Monica, CA.)

Appendix V.

CONVERSION TABLE

1 inch (in) = 25.4 millimeters

1 foot (ft) = 0.3048 meters

1 yard (yd) = 0.9144 meters

1 mile = 1.609 kilometers

1 pound (lb) = 453.6 grams

1 ton = 907.185 kilograms

Degree C = $(\text{Degree F} - 32) \frac{5}{9}$

Degree F = $(\text{Degree C} \times 1.8) + 32$

BIOGRAPHICAL NOTE

Robert Turpin was born October 22, 1945, in Eugene, Oregon. He graduated from Roseburg Senior High School, Roseburg, Oregon, in 1963. He received an Associate of Applied Science degree of Welding Technology in 1969 from Oregon Technical Institute, Klamath Falls, Oregon, and his Bachelor of Science Degree of Trades and Technical Education in 1974 from Northern Arizona University, Flagstaff, Arizona. He was Assistant Professor of Industrial Processes Technology at Oregon Institute of Technology, Klamath Falls, Oregon, from 1975 through 1979. He joined the Oregon Graduate Center in the fall of 1979 and, while working as a Research Associate in the Materials Science and Engineering Department, completed requirements for the Masters degree in Materials Science and Engineering in December 1983.